

Reaching the boundary between stellar kinematic groups and very wide binaries

IV. The widest Washington Double Star systems with $\rho \geq 1000$ arcsec in *Gaia* DR3*

J. González-Payo¹, J. A. Caballero², M. Cortés-Contreras²

¹ Departamento de Física de la Tierra y Astrofísica, Facultad de Ciencias Físicas, Universidad Complutense de Madrid, E-28040 Madrid, Spain. e-mail: fcojgonz@ucm.es

² Centro de Astrobiología, CSIC-INTA, Camino Bajo del Castillo s/n, campus ESAC, E-28692 Villanueva de la Cañada, Spain

Received 16 November 2022 / Accepted 20 December 2022

ABSTRACT

Aims. With the latest *Gaia* DR3 data, we analyse the widest pairs in the Washington Double Star (WDS) catalogue with angular separations, ρ , greater than 1000 arcsec.

Methods. We confirmed the pairs' membership to stellar systems based on common proper motions, parallaxes, and (when available) radial velocities, together with the locii of the individual components in colour-magnitude diagrams. We also looked for additional closer companions to the ultrawide pairs, either reported by WDS or found by us with a new *Gaia* astrometric search. In addition, we determined masses for each star (and white dwarf) and, with the projected physical separation, computed the gravitational potential energy, $|U_g^*|$, of the systems.

Results. Of the 155 159 pairs currently catalogued by WDS, there are 504 with $\rho > 1000$ arcsec. Of these, only 2 ultrawide pairs have not been identified, 10 do not have any available astrometry, 339 have not passed a conservative filtering in proper motion or parallax, 59 are members of young stellar kinematic groups, associations or open clusters, and only 94 remain as bona fide ultrawide pairs in the galactic field. Accounting for the additional members at shorter separations identified in a complementary astrometric and bibliographic search, we found 79 new stars (39 reported, plus 40 not reported by WDS) in 94 ultrawide stellar systems. This sample is expanded when including new close binary candidates with large *Gaia* DR3 RUWE, σ_{Vr} , or a proper motion anomaly. Furthermore, the large fraction of subsystems and the non-hierarchical configurations of many wide systems with three or more stars is remarkable. In particular, we found 14 quadruple, 2 quintuple, 3 sextuple, and 2 septuple systems. The minimum computed binding energies, $|U_g^*| \sim 10^{33}$ J, are in line with theoretical predictions of tidal destruction by the Galactic gravitational potential. The most fragile and massive systems have huge projected physical separations of well over 1 pc. Therefore, they are either in the process of disruption or they are part of unidentified juvenile stellar kinematic groups.

Key words. surveys – virtual observatory tools – astrometry – stars: binaries: general, visual

1. Introduction

Multiple stars have been observed since ancient times, but it has been accepted for millenia that the proximity of two stars was mainly due to chance (Fracastoro 1988). In the 17th century, Galileo was the first to propose the association between stars when trying to measure stellar parallaxes, based on the recommendations of Tycho Brahe (Hirshfeld 2001). The first visual binary, Mizar A and B (ζ Ursae Majoris), was discovered by Benedetto Castelli, who asked Galileo for his observations of it in 1616, although the discovering was falsely attributed to Giovanni Battista Riccioli in 1650 (Allen 1899; Burnham 1978). The first catalogue of binary stars was published in 1781 by Christian Mayer, who speculated about the possibility of them being physical systems, as predicted by Isaac Newton (Niemela 2001). Nevertheless, in the following century, William F. Herschel questioned that idea, considering that multiple systems could have

a gravitational link only when their orbital motion were proven (Fracastoro 1988; Niemela 2001). Some years later, he published a work based on his observations (Herschel 1802), where he demonstrated that some real star systems were ruled by the universal gravitation laws (Niemela 2001). It was the first time that science confirmed that Newton's laws are also valid outside the Solar System, which sparked a new revolution.

A double or binary system contains two stars that describe closed orbits around their common centre of gravity (Batten 1973), while multiple systems contain three or more stars with different hierarchical levels (Tokovinin 1997, 2008; Eggleton & Tokovinin 2008; Duchêne & Kraus 2013). The components of wide multiple systems have large separations between them and, therefore, relatively low gravitational energies. The classical maximum separation between components in wide systems rarely exceeds 0.1 pc, driven by the dynamic processes of the stars formation and evolution (Tolbert 1964; Kraicheva et al. 1985; Abt 1988; Weinberg & Wasserman 1988; Close et al. 1990; Latham et al. 1991; Wasserman & Weinberg 1991; Garnavich 1993; Allen et al. 1998; Caballero 2009) and strongly

* Tables B.1, B.2, B.3, and B.4 are only available in electronic form at the CDS via anonymous ftp to cdsarc.cds.unistra.fr (130.79.128.5) or via <https://cdsarc.cds.unistra.fr/cgi-bin/qcat?J/A+A/>

depends on their mass (i.e. spectral type), age, and kinematics (Duquennoy & Mayor 1991; Jensen et al. 1993; Patience et al. 2002; Zapatero Osorio & Martín 2005; Kraus & Hillenbrand 2009). There are newer studies that increase this maximum separation up to 1 pc (Jiang & Tremaine 2010; Caballero 2010) or even to 1–8 pc (Shaya & Olling 2011; Kirkpatrick et al. 2016; González-Payo et al. 2021). At these separations, the pairs are less likely bound for extended lifetimes (Ritterer & King 1982; Weinberg et al. 1987; Dhital et al. 2010).

In this work, we perform a detailed characterisation of the widest pairs in the Washington Double Star (WDS) catalogue (Mason et al. 2001) by making use of the latest *Gaia* DR3 data (Gaia Collaboration et al. 2022). The WDS, which is maintained by the United States Naval Observatory, is the world’s principal database of astrometric double and multiple star information. For each system, we ascertain their actual gravitational binding and search for additional companions. Since we are investigating pairs with angular separations, ρ , greater than 1000 arcsec, this work can be understood as a *Gaia* update of that by Caballero (2009), who also used $\rho = 1000$ arcsec as the minimum separation between the widest WDS pairs at that time, but had only *Hipparcos* (Perryman et al. 1997) parallaxes for a few bright stars and relatively insufficient proper motions for the faintest components. Furthermore, this work is the fourth item in the series initiated by Caballero (2009), which aims to shed light from an observational perspective on the formation and evolution of the most separated and fragile multiple stellar systems in the Milky Way. Although young systems play an important role in our analysis, here, we focus on field systems that are relatively evolved, old, and at the brink of disruption by the galactic gravitational potential.

This paper is structured as follows: In Sect. 2, we describe the stellar sample. Section 3 shows the analysis that we followed to filter, classify, and characterise WDS pairs, as well as to carry out our search for other possible members of the multiple systems. We present our results, along with a discussion in Sect. 4. Finally, we summarise our work in Sect. 5.

2. Sample

We built our sample from the latest version of the WDS¹. For each of the 155 159 resolved pairs, WDS tabulates the WDS identifier (based on J2000 position), discoverer code and number, number of observations and of components (when there are more than two), date, position angle (θ , i.e. orientation on the celestial plane of the companion with respect to the primary), and ρ of the first and last observations, magnitudes, and proper motions of the two components, along with the equatorial coordinates of the primary of the pair and notes about the pair. In a few cases, WDS also tabulates the Durchmusterung number (Bonn, Córdoba, Cape – Schönfeld 1886; Argelander 1903) and the spectral type of the primary or companion (or both). There are numerous pairs that take part of multiple systems with, usually, the same primary star; in general, they share the same WDS identifier, but not always.

In Fig. 1, the cumulative number of WDS pair angular separations increases with a power law between $\rho \sim 0.4$ arcsec and $\rho \sim 100$ arcsec. This distribution follows Öpik’s law (Öpik 1924) for binaries with projected physical separations greater than 25 au (Allen et al. 1997). Outside the $\rho \sim 0.4$ –100 arcsec range, the distribution flattens at both sides. This flattening is an

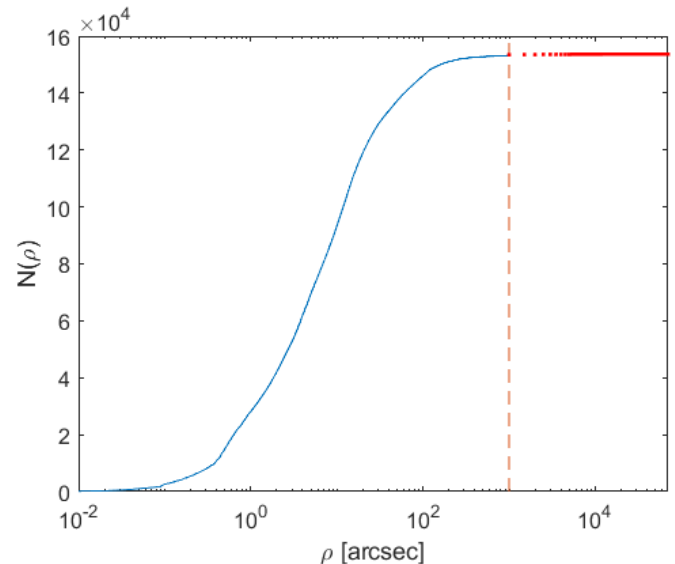


Fig. 1: Cumulative number of WDS pairs as a function of ρ . Red data points with $\rho > 1000$ arcsec (to the right of the orange vertical dashed line) mark the 504 WDS pair candidates investigated by us. This figure can be compared with Fig. 1 in Caballero (2009).

observational bias at short angular separations, as micrometer, speckle, lucky imaging, adaptive optics, and even imaging from space are limited by the atmospheric seeing, telescope size, or optical quality (but there seems to be a slight overabundance of close pairs of $\rho \sim 0.4$ –4.0 arcsec with respect to more separated ones).

The flattening of the ρ distribution at wide separations, especially at $\rho \sim 200$ arcsec, is mainly due to the actual formation and evolution of multiple stellar systems, although there may also be a contribution from another observational bias: until the advent of *Gaia* (Gaia Collaboration et al. 2016, 2018, 2021), accurate proper motion and parallax measurements were available only for a tiny fraction of stars, while most wide WDS pairs come from pre-*Gaia* common proper motion surveys (e.g. Allen et al. 2000; Chanamé & Gould 2004; Lépine & Bongiorno 2007; Dhital et al. 2010; Raghavan et al. 2010; Tokovinin & Lépine 2012; and references therein²). In spite of numerous common proper motion surveys, the observational bias remains at $\rho \gtrsim 200$ arcsec because most of them looked for companions at angular separations of up to a few arcminutes only, mostly due to past computational limitations. However, this difficulty is starting to be alleviated thanks to new *Gaia* surveys (e.g. Kervella et al. 2022; Sarro et al. 2022). Due to the observational bias or the actual difficulty in forming wide binaries (Kouwenhoven et al. 2010; Reipurth & Mikkola 2012; Lee et al. 2017; Tokovinin 2017), the distribution of ultrawide WDS pairs with $\rho \gtrsim 1000$ arcsec becomes extremely flat (Fig. 1).

At the time of our analysis, WDS contained 504 pairs separated by more than 1000 arcsec. For comparison, Caballero (2009) investigated about 105 000 WDS pairs, of which only 35 had $\rho > 1000$ arcsec. Together with the *Gaia* DR3 data, a sam-

² There are also relevant unpublished contributions to the WDS, such as that of the Observatori Astronòmic del Garraf (Caballero et al. 2013). See further details at <http://www.astro.gsu.edu/wds/wdstext.html#intro>.

¹ http://www.astro.gsu.edu/wds/Webtextfiles/wds_precise.txt, accessed on 12 November 2022.

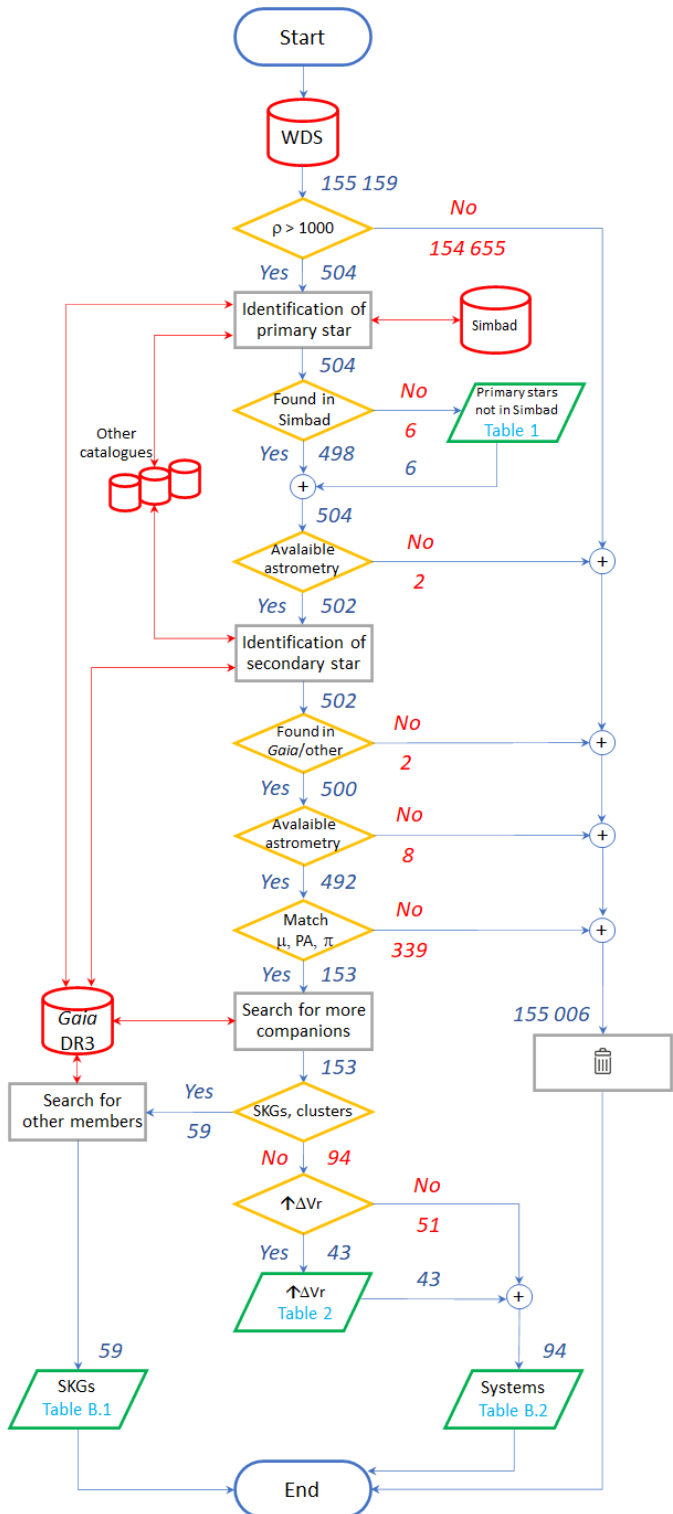


Fig. 2: Flowchart describing our analysis.

ple about 15 times larger represents a qualitative and quantitative leap with respect to the first item of this paper series.

3. Analysis

Our analysis procedure is illustrated by the flowchart in Fig. 2, with the following elements: ovals represent the initial and final status of the process, diamonds are Boolean questions for which only possible answers are ‘Yes’ or ‘No’, rectangles are

specific actions, trapezia are partial or final obtained results, and cylinders are databases (or catalogues) from where the data are collected or consulted. In Fig. 2, the incoming numbers in every block represent the number of processed WDS pairs in that block, and the outgoing numbers represent the number of pairs that match the condition or pass through to the next block of the flowchart.

3.1. Primary stars in *Gaia* DR3

For each primary star of the 504 WDS ultrawide pairs, we collected its main identifier in the Simbad astronomical database (Wenger et al. 2000). Of them, only six do not have a Simbad entry; they are shown in Table 1. Using TOPCAT (Taylor 2005) and the equatorial coordinates tabulated by WDS, we automatically cross-matched every primary with *Gaia* DR3. Next, we visually inspected all cross-matches with the help of the Aladin sky atlas (Bonnarel et al. 2000), and VizieR (Ochsenbein et al. 2000). When there were more than a single *Gaia* counterpart per primary within our ~ 5 arcsec cross-match radius, we chose the right star by comparing WDS and *Gaia* proper motions, magnitudes, and spectral types.

Of the 504 primaries, 44 are redundant (they belong to two or more pairs). Only 6 out of the 460 non-redundant primaries had no *Gaia* DR3 entry because of their extreme brightness (α Aur – Capella–, α Car –Canopus–, α PsA –Fomalhaut–, α Cen, γ Cen, and δ Vel), for which we took proper motions and parallaxes from *Hipparcos*. In addition, another 22 primaries are in *Gaia* DR3, but do not have a five-parameter astrometric solution. For 11 of them, namely, those of moderate brightness ($G = 2.3\text{--}9.5$ mag), we again took proper motions and parallaxes from *Hipparcos*, while for 9 of them, we took the data from *Gaia* DR2 (Gaia Collaboration et al. 2018)³. The 2 remaining stars are LSPM J2323+6559 and 2MASS J00202956–1535280, for which there are only proper motions available from Lépine & Shara (2005) and Cutri et al. (2014), respectively. Since the 2 later primaries do not have published parallaxes, we discarded the corresponding pairs from the analysis. Accounting for these two discards, we retained 502 pairs for the next step of the analysis.

3.2. Search for WDS companions

The WDS catalogue provides the relative positions of the companion stars of the pairs with respect to the primaries through ρ and θ . To manually locate the companions to the primaries, we used Aladin. We loaded different catalogues and services, namely *Gaia* DR3, 2MASS (Skrutskie et al. 2006), Simbad, and WDS, and we used the dist tool. For the correct identification of the companion, we proceeded to carry out a visual confirmation of the primary cross-match and we chose the *Gaia* DR3 candidate companion within 10 arcsec around the expected location that matched the WDS values of proper motion, magnitude, and spectral type. If the companion had not been identified, especially in the widest systems ($\rho > 10\,000$ arcsec), we enlarged the search radius in steps up to 120 arcsec. For these outliers, we used all the available information, namely, the WDS remarks and the original publications. There were only two cases where the companion star was not found by us with the ρ and θ provided

³ The nine primary stars with *Gaia* DR2 data are: LP 295–49, G 202–45, 36 And A, 4 Sex, HD 111456, HD 125354, HD 340345, BD-12 6174, and HD 213987.

Table 1: Primary stars without a Simbad entry.

WDS name	Discoverer code	Primary star	α (J2000)	δ (J2000)	G (mag)	d (pc)
00474–7345	OGL 84	Gaia DR3 4685766099704705280	00:47:25.09	-73:44:42.5	17.5	1700±200
00489–7434	OGL 87	Gaia DR3 4685482661910629248	00:48:55.94	-74:33:46.7	19.4	504±54
01121–7400	OGL 161	Gaia DR3 4686310976416294528	01:12:11.20	-73:59:42.9	16.6	1870±150
01235–7356	OGL 188	Gaia DR3 4686225867342046848	01:23:33.07	-73:55:34.7	14.3	468.0±3.1
03074–4655	TSN 110	Gaia DR3 4750712533547201920	03:07:26.03	-46:54:44.8	16.6	136.0±1.0
10181–0130	TSN 113	Gaia DR3 3830436797339858176	10:18:03.35	-01:30:11.6	17.8	397±21

by WDS, even after enlarging the search radius and scouring the literature⁴.

As for the primaries, we retrieved Simbad identifiers and *Gaia* DR3 for the corresponding companions. Only eight of the companions had not parallaxes (or even proper motions) available in any catalogue, and we also discarded them from the analysis⁵. We computed our own ρ and θ parameters for the 492 (502 – 2 – 8) remaining pairs using the standard equations of spherical trigonometry (e.g. Smolinski & Osborn 2006):

$$\rho = \arccos [\cos(\Delta\alpha \cos \delta_1) \cos(\Delta\delta)], \quad (1)$$

and

$$\theta = \frac{\pi}{2} - \arctan \left[\frac{\sin(\Delta\delta)}{\cos(\Delta\delta) \sin(\Delta\alpha \cos \delta_1)} \right], \quad (2)$$

where $\Delta\alpha = \alpha_2 - \alpha_1$, $\Delta\delta = \delta_2 - \delta_1$, and α_1, δ_1 and α_2, δ_2 are the equatorial coordinates of the primary and companion stars, respectively.

We compared the ρ and θ values we measured with those tabulated by WDS (in particular, with the latest measurements, i.e. sep2 and pa2). For the position angle, the standard deviation of the differences between our measurements and those from WDS is 0.84 deg. The distribution of the differences in θ is not Gaussian, with a narrow peak centred at 0 deg and wide, but shallow, wings at both sides. Of the 492 identified pairs with parallaxes, only 23 have absolute differences in θ greater than 1 deg (and up to 4.2 deg). Most of the kinds of differences ascribed to uncertainties propagated from inaccurate pre-*Gaia* coordinates, especially for the widest systems, such as WDS 23127+6317 (e.g. with Eq. 2 being highly non-linear). The distribution of the differences in ρ is similar to that of θ , with a narrow peak centred at 0 arcsec and a relatively large standard deviation of the differences of 21.0 arcsec. This large amount is originated by the difficulty in previous works to measure ρ or even to identify the companion of the widest systems, such as the ‘outliers’

⁴ The two WDS pairs with unidentified companion stars are WDS 03074–5655 (TSN 110) and WDS 03353–4020 (TSN 111). In a preliminary analysis, there was a third unidentified system, namely WDS 05463+5627 (LDS 3673), but it suffered from a typographical error in WDS that was corrected afterwards (Carro 2021; B. D. Mason, priv. comm.). We revise its relative astrometry to $\rho = 57.1$ arcsec, $\theta = 262.5$ deg, and epoch = J2016.0.

⁵ The eight companions without parallax are: LSPM J1536+2856, SCR J1900–3939, UCAC3 208–200112, 2MASS J13543510–0607333, 2MASS J14313545–0313117, Gaia DR3 276070675205077632, Gaia DR3 4655216993788228480, and Gaia DR3 601133385210548736.

described above and found at more than 10 arcsec from their expected locations⁶.

The distribution of our new values of ρ are plotted with red data points in Fig. 1. Of the 492 identified pairs with parallax, 298 have $\rho = 1000$ –2000 arcsec, 117 have $\rho = 2000$ –10 000 arcsec, and 77 have $\rho > 10 000$ arcsec. The latter ultrawide pairs come mostly from the works by Probst (1983) and Shaya & Olling (2011). The widest pair has $\rho = 66 094$ arcsec (WDS 02157+6740, SHY 10; Shaya & Olling 2011). As described below, not all of them are physically bound.

3.3. Pair validation

To validate the 492 pairs, we used the criteria established by Montes et al. (2018) to distinguish between physical (bound) and optical (unbound) systems. For that purpose, we computed two astrometric parameters that quantify the similarity of the proper motions of two stars:

$$\mu \text{ ratio} = \sqrt{\frac{(\mu_\alpha \cos \delta_1 - \mu_\alpha \cos \delta_2)^2 + (\mu_{\delta 1} - \mu_{\delta 2})^2}{(\mu_\alpha \cos \delta_1)^2 + (\mu_{\delta 1})^2}} < 0.15, \quad (3)$$

and

$$\Delta \text{PA} = |\text{PA}_1 - \text{PA}_2| < 15 \text{ deg}, \quad (4)$$

where PA_i are the angles of the proper motion vectors, with $i = 1$ for the primary star and $i = 2$ for the companion. We added an extra buffer in the μ ratio of up to 0.25 to account for projection effects on the celestial sphere of nearby ultrawide systems, as in the case of α Cen AB + Proxima (Innes 1915; Wertheimer & Laughlin 2006; Caballero 2009).

At the time of publication by Montes et al. (2018), *Gaia* parallaxes were not available except for the 2.5 million stars of the Tycho-*Gaia* Astrometric Solution (Michalik et al. 2015). With the advent of the third *Gaia* data release with precise parallaxes for ∼700 times more stars, we added one additional condition to our validation. Cifuentes et al. (2021) imposed parallactic distances to agree within 10%, while González-Payo et al. (2021) did it within 15%, which is the value we chose to impose. In short, our third astrometric criterion was:

$$\left| \frac{\pi_1^{-1} - \pi_2^{-1}}{\pi_1^{-1}} \right| < 0.15, \quad (5)$$

⁶ For example, Tokovinin & Lépine (2012) and we ourselves measured $\rho = 1684.2$ arcsec and 1684.49 arcsec, respectively, for the outlier system HD 45875 + Gaia DR3 1115649542191409664 (TOK 503, WDS 06387+7542 AD), but WDS instead tabulates 1898.64 arcsec collected in 2015.

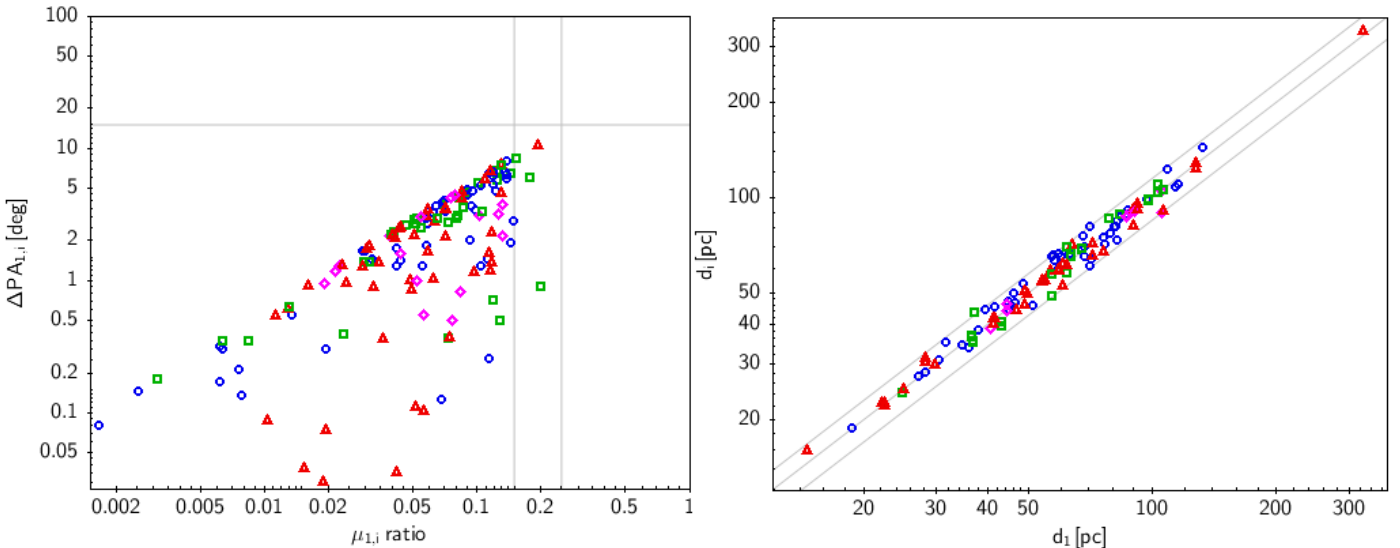


Fig. 3: Astrometric criteria for pair validation. In both diagrams, we plot pairs between primaries and secondaries with blue circles, tertiaries with red triangles, quaternaries with green squares, and higher order companions with purple diamonds. *Left:* $\Delta PA_{1,i}$ vs. $\mu_{1,i}$ ratio diagram. Vertical and horizontal grey lines mark the μ ratios of 0.15 and 0.25 μ and ΔPA of 15 deg, respectively. Compare with Fig. 2 in Montes et al. (2018). *Right:* Distance of companions vs. distance of primaries. Diagonal lines indicate the 1.15:1, 1:1, and 0.85:1 distance relationships. The α Cen AB + Proxima system, at $d \sim 1.3$ pc, is not shown.

with π_1 and π_2 as the parallaxes of both components of the pair (we did not apply any colour correction for computing distances – Bailer-Jones et al. 2018; Lindegren et al. 2021). In Fig. 3, we show the relations between μ ratio and ΔPA and between distances of the two components of the 153 pairs that satisfy the three imposed criteria simultaneously (and additionally, the multiple companions obtained in Sect. 3.4). Although we refer to them as pairs, in many cases they are actually part of hierarchical multiple (triple, quadruple, quintuple...) systems made of stars at very different angular separations to their primaries. This is described in detail below.

Except for 2 of them⁷, all the 153 pairs are located at heliocentric distances shorter than 150 pc, with a distribution peaking at 40–50 pc. The distribution of total proper motions is, however, flatter, with only one pair⁸ with a μ greater than 700 mas a^{-1} and none with a μ less than 25 mas a^{-1} .

We did not keep in our final list of validated pairs an ultrawide system candidate at about 2400 pc towards the Magellanic Clouds, namely OGL 54 (Poleski et al. 2012). It is made of OGLE SMC-SC1 161-162 and Gaia DR3 468574771724739328 (“SMC128.7.9551”), which are separated by about 12 pc. If truly linked, the pair would be much further and wider than any other system considered here. Last but not least, we revised the system ρ from 1017 arcsec to 977 arcsec, below our boundary at 1000 arcsec.

3.4. Additional companions and stellar kinematic groups in *Gaia* DR3

We looked for additional proper motion and parallax companions within 1 pc around both the primary and the companion of the 153 validated pairs. We followed the methodology described in Sect. 3 of González-Payo et al. (2021); however, in our work,

apart from TOPCAT and a customised code in astronomic data query language (Yasuda et al. 2004), we used *Gaia* DR3 and the criteria imposed by Eqs. 3–5. For a few cases of ultrawide WDS pairs with projected physical separations greater than 1 pc, we extended the search radius up to the maximum separation between known components.

In our *Gaia* search, we identified 349 additional common proper motion and parallax companions that satisfy the astrometric criteria of Eqs. 3, 4, and 5. Of these, 111 additional companions are catalogued by WDS and 239 are not. The large multiplicity order of some system candidates, made of over a dozen pairs each (i.e. higher than dodecuple), together with the presence of debris discs in some of the components (e.g. α^{01} Lib, AU Mic – Kalas et al. 2004; Chen et al. 2005; Mizusawa et al. 2012; Gáspár et al. 2013; Mittal et al. 2015; Plavchan et al. 2020), has led us to investigate the membership of all our targets in young stellar kinematic groups (SKGs – Eggen 1965; Montes et al. 2001; Zuckerman & Song 2004), stellar associations (Ambartsumian 1949; Blaauw 1991; de Zeeuw et al. 1999), and even open clusters.

Of the 153 validated pairs in Sect. 3.3, there are 59 with at least one component (primary, companion, or both) that had previously been considered part of young SKGs, associations, and clusters such as the Tucana-Horologium and Coma Berenices moving groups, the ϵ Chamaeleontis association, or the Hyades open cluster (e.g. Perryman et al. 1998; Murphy et al. 2013; Kraus et al. 2014; Pecaut & Mamajek 2016; Riedel et al. 2017; Gagné et al. 2018a; Tang et al. 2019). Furthermore, of the 239 additional astrometric companions not catalogued by WDS, a total of 199 share proper motion and parallax companions with these young pairs. Table B.1 shows the name, equatorial coordinates, and *G*-band magnitude of 349 young stars and candidates, together with the corresponding group (SKG, association, or cluster) when available (309 cases), and references. The full names and acronyms of the 22 considered groups, with ages ranging from 4–8 Ma (of the Chamaeleon-Scorpius-Centaurus-Crux complex) to 600–800 Ma (of the Hyades and

⁷ The two systems at $d > 150$ pc are γ Cas + HD 5408 (188 pc) and G 143–33 + G 143–27 (324 pc).

⁸ The high proper motion pair with $\mu > 700$ mas a^{-1} is α Cen AB + Proxima (3710 mas a^{-1}).

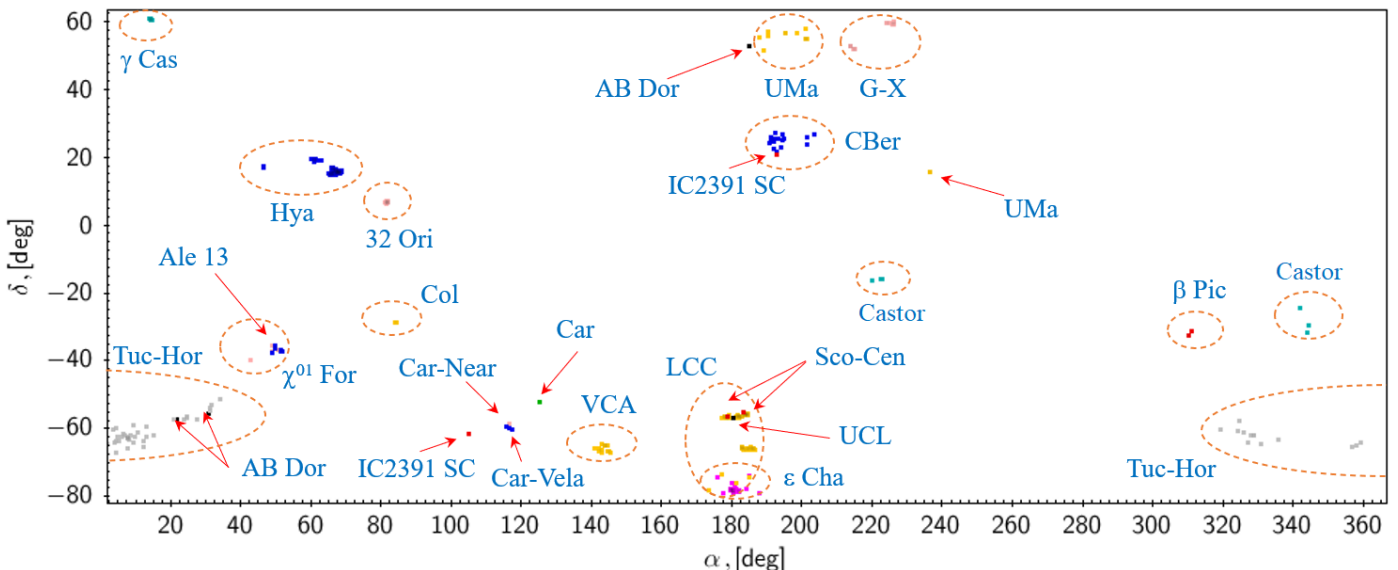


Fig. 4: Spatial distribution of the 309 identified young stars in SKGs, associations, and open clusters.

[TPY2019] Group-X), are provided in the table notes. Discoverer codes are given for all components tabulated by WDS (some stars that belong to different WDS systems can have different entries⁹), while the 199 additional companions have the string ‘...’ in the discoverer code column. The spatial distribution of the 309 young stars and candidates in SKGs, associations, and open clusters is shown in Fig. 4.

About 80% of the 199 additional companions had also been ascribed to young groups, but not all. We report 40 stars, marked with ‘...’ in the group column in Table B.1, that are new candidate members in young SKGs, associations, and clusters. Eight of them had actually been considered as previous members, but the most recent works have classified them as “improbable members” (e.g. HD 207377 AB in Tucana-Horologium; Zuckerman et al. 2001). In any case, some of the 40 stars, because of either their brightness (e.g. HD 71043, which is probably an A0 V, $G \approx 5.9$ mag, 200–300 Ma-old star in Carina) or faintness (e.g. 2MASS J12145318–5519494, which probably is a young brown dwarf in Lower Centaurus-Crux; Folkes et al. 2012), may be interesting to confirm in future works.

One more wide pair, composed by the bright stars γ Cas and HD 5408, resulted in a nonuple system after our initial astrometric analysis and bibliographic search. Since γ Cas is an extremely young classical Be star (Poeckert & Marlborough 1978; White et al. 1982; Henrichs et al. 1983; Stee et al. 1995), we also tabulated the resolved pair components in Table B.1, although it has never been ascribed to any group in particular (but see Majajek 2017). The γ Cas system is discussed in further detail in Appendix A.

Despite the far-reaching title of this series of papers, in this particular work, we focus on relatively evolved and old systems in the galactic field. Common proper motion (and parallax) surveys of resolved companions to bona fide SKG members is indeed a widely used and successful technique for discovering new young stars and brown dwarfs (Alonso-Floriano et al. 2015, and references therein). However, a dedicated work on disentangling actual very wide binaries from unbound components in SKGs with similar galactocentric space velocities is planned.

After removing the 59 pairs with stars in young SKGs, associations, and clusters, we kept 94 wide pairs in the galactic field. To them, we added the 40 additional astrometric companions found in our *Gaia* DR3 search and not catalogued by WDS plus 39 already reported by WDS and separated by less than 1000 arcsec. As a result, there were 266 stars¹⁰ in 243 resolved *Gaia* sources and in 94 systems that passed to the next step of our analysis. All the systems and resolved *Gaia* sources are listed in Tables B.2 and B.3.

3.5. New close binary candidates from *Gaia* data

We carried out a cross-matching with WDS and scoured the literature in search of additional companions not identified in our *Gaia* DR3 search. We did not find any additional WDS companion at $\rho < 1000$ arcsec that were resolvable by *Gaia* and that had not been recovered in our search. However, WDS also tabulates very close systems ($\rho \lesssim 1.3$ arcsec) that were discovered and characterised with micrometers, speckle, lucky imaging, or adaptive optics, and which are unresolvable by *Gaia* thanks to the close separation or relatively large magnitude difference between components (e.g. HD 6101, HD 102590, HD 186957). In addition, there is a number of pair components that are spectroscopic binaries (e.g. HD 120510; Pourbaix et al. 2004) or triples (e.g. δ Vel, which is also an eclipsing binary with a close astrometric companion; Kervella et al. 2013), or very close binaries from proper motion anomalies (e.g. HD 125354; Kervella et al. 2019). We further consider all this information in Sect. 4.

Three pairs in multiple systems are in the 0.15–0.25 μ ratio buffer interval in the ΔPA vs. μ ratio diagram (Fig. 3), namely WDS 09487–2625, WDS 16278–0822, and WDS 23309–5807. The origin of their large μ ratio lies on wide amplitude orbital (i.e. proper motion) variations induced by additional components in the systems at 1.83 arcsec (HD 85043, I 205), ~1.0 arcsec (ν Oph, RST 3949), and 1.27 arcsec (HD 221252, I 145) to the primaries or companions. As a result, we also validated the three

¹⁰ HD 79392 is catalogued by WDS as the primary of two different systems (WDS 09150+3837/TOK 525 and WDS 09150+3837/DAM1575).

⁹ For example, HD 1466 is SHY 113 G, SHY 114 G, and CVN 33 G.

systems (one triple and two quadruples) in spite of not satisfying our original μ ratio criterion.

Next, we cross-matched our 243 *Gaia* sources in 94 systems with the *Hipparcos-Gaia* catalogues of accelerations of Kervella et al. (2019) and Brandt (2021). Of them, 54 have a measurable proper motion anomaly (Boolean variable set to unit in *Gaia* DR2, proper motion anomaly binary flag BinG2 –Kervella et al. 2019–, or $\text{chi}^2 > 11.8$ –Brandt 2021–) that are probably induced by unseen companions. They are marked with a footnote in Tables B.2 and B.3.

In addition, we looked for new very close binary candidates among the 94 systems. First we used the *Gaia* re-normalised unit weight error (RUWE), which is a robust indicator of the goodness of a star's astrometric solution (Arenou et al. 2018; Lindegren et al. 2018). Large RUWE values correspond to stars with angular separations small enough not to be resolved by *Gaia*, but large enough to perturb the astrometric solution. *Gaia* DR3 provides RUWE values for 234 *Gaia* entries. The nine sources without RUWE values are either very bright stars (δ Vel, α Cen A and B, ν Oph) or known close binaries with angular separations $\rho \sim 0.2\text{--}0.9$ arcsec (e.g. HD 6101). There are 14 stars with $\text{RUWE} > 10$. They are also marked with a footnote in Tables B.2 and B.3. The five *Gaia* sources with the greatest RUWE, of about 20–40, are either already known close binaries below the *Gaia* resolution limit (e.g. G 210–44, $\rho \sim 0.1$ arcsec – HDS 2989 in the Hipparcos Double Stars catalogue) or strong, relatively faint, new binary candidates (e.g. 2MASS J02022892–3849021, UCAC3 109–11370, LSPM J0956+0441, and HD 59438 C). Of the other nine *Gaia* sources with moderate RUWE of about 10–20, some have also been tabulated as candidate binaries, such as HD 75514 and HD 139696, which were listed in the *Hipparcos-Gaia* catalogue of accelerations (Kervella et al. 2019), HD 210111, which is a λ Bootis-type spectroscopic binary (Paunzen et al. 2012), and HD 215243, which is subgiant spectroscopic binary (Gorynya & Tokovinin 2018). The rest of *Gaia* sources with $\text{RUWE} > 10$ would need an independent confirmation of binarity. Being less conservative, we could have extended our analysis down to $\text{RUWE} = 5$, which is about three times greater than the critical value of 1.41 of Arenou et al. (2018), Lindegren et al. (2018), or Cifuentes et al. (2020). There are only five *Gaia* sources (in double or multiple systems) with $5 \leq \text{RUWE} \leq 10$. However, as some careful studies of nearby stars indicate, RUWE values slightly larger than 1.4 do not necessarily translate into close binarity (Ramsay et al. 2022; Ribas et al. accepted). Since the confirmation of actual close binarity requires a radial-velocity or high-resolution imaging follow-up, we imposed a very conservative RUWE limit.

Next, we used the standard deviation of the radial velocities, V_r , measured with the *Gaia* Radial Velocity Spectrometer, which receives the misleading label `radial_velocity_error` (Gaia Collaboration et al. 2022; Katz et al. 2022). Of the 243 *Gaia* entries, 182 have V_r and its standard deviation, σ_{Vr} . The median formal precision of the velocities for the brightest, most stable *Gaia* stars lies at about 0.12 km s^{-1} to 0.15 m s^{-1} and smoothly increases for fainter stars (Katz et al. 2022). However, we identified at least six *Gaia* sources that have significantly greater σ_{Vr} than expected given their magnitudes. Being all stars of intermediate ages and spectral types in the main sequence (i.e. no pulsating giants or subgiants, nor very active T Tauri stars), we adscribed the large σ_{Vr} to spectroscopic binarity. Actually, two of them had already been reported as spectroscopic binaries, namely HD 2000077 (Konacki et al. 2010; Montes et al. 2018 and references therein) and HD 215243 (Gorynya & Tokovinin 2018, which also has a large RUWE).

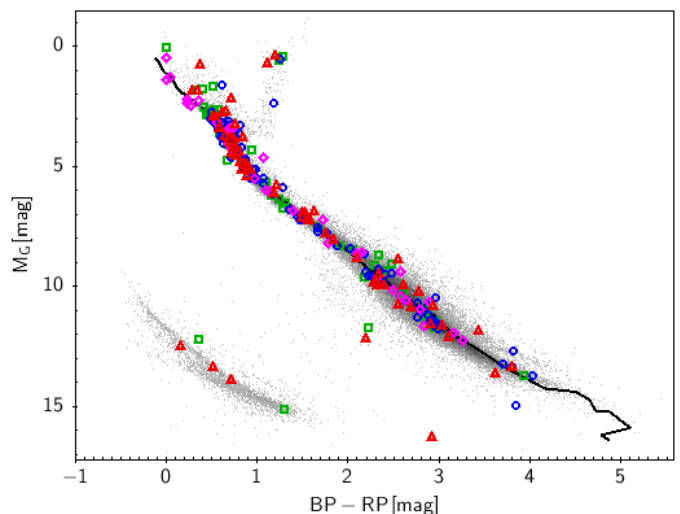


Fig. 5: HR diagram of all investigated stars. Coloured open symbols stand for stars in double (blue circles), triple (red triangles), quadruple (green squares), and higher-order multiple systems (purple diamonds). Grey dots represent selected field stars from *Gaia*. The black solid line is the updated main sequence of Pecaut & Mamajek (2013). The stars outside the main sequence are discussed in the text.

A third one, namely HD 75514 (Kervella et al. 2019; Brandt 2021), has a significant proper motion anomaly. The other three new spectroscopic binary candidates have a large RUWE (8.1; BD+32 2868), moderate RUWE and σ_{Vr} ($2.48, 2.86 \text{ km s}^{-1}$), or a small RUWE but a huge σ_{Vr} for a bright single star ($G \approx 7.7 \text{ mag}, 17.76 \text{ km s}^{-1}$; HD 201670).

At this stage, we may wonder why common parallax and proper motion criteria alone were used for system validation, instead of common radial velocities as well, at least for the 99 pairs with data for the two components. We note that a large difference in radial velocities may be a symptom of long-period spectroscopic binarity of one of the components (by “long period,” we mean longer than or of the same order of the 34 months of the *Gaia* DR3 radial-velocity coverage). Nevertheless, the above-mentioned properties of high RUWE, σ_{Vr} , or, especially, proper motion anomaly do not always indicate unknown close companions, but can also be produced by the already detected close companions. Some examples of known pairs with astrometric accelerations and orbital periods of tens to hundreds years are HD 6101, HD 59438, and HD 85043.

In Table 2, we list 43 pairs of primaries and companions with radial velocity differences larger than three times the quadratic sum of the respective σ_{Vr} . Among them, we can find known spectroscopic binaries, components with large RUWE values, proper motion anomalies, or a combination of them. Some of the pairs in Table 2 may be false positives, that is, two unrelated stars with very similar proper motions and parallaxes but very different radial velocities. However, with the data available to us, it is impossible to disentangle between them and true wide physical systems with one radial-velocity outlier component due to currently unknown long-period spectroscopic binarity.

3.6. Colour-magnitude diagram

Stellar masses are needed to compute gravitational binding energies, while luminosity classes are needed to estimate stellar

Table 2: Radial-velocity outlier candidates.

WDS	Discoverer code	Primary star	Companion star	$ \Delta V_r $ (km s $^{-1}$)
01066+1353	SHY 396	HD 6566	HD 5433 ^a	25.5±0.4
02022-4550	SHY 410	HD 12586	HD 12808	30.8±0.2
02310+0823	GIC 32	G 4-24	G 73-59 ^b	63.1±3.8
02315+0106	SHY 422	BD+00 415B	HD 17000	4.4±0.3
02462+0536	TOK 651	HD 17250	HD 17163	18.1±0.6
03503-0131	SHY 164	HD 24098A	HD 22584 ^a	5.9±0.2
04346-3539	TOK 488	HD 29231	L 447-2	25.5±0.4
05222+0524	TOK 497	HD 35066(A) ^a	TYC 109-530-1	0.8±0.3
08211+4021	TOK 516	BD+40 2030 ^a	G 111-70	36.9±0.3
08237-5519	SHY 526	HD 71257	HD 72143 ^a	4.9±0.3
08388-1315	SHY 201	HD 73583	BD-09 2535	18.6±0.3
08480-3115	SHY 529	HD 75269 ^a	HD 75514 ^{a,b}	8.5±1.5
09467+1632	TOK 531	BD+17 2130 ^a	LP 428-36	56.6±2.7
09487-2625	TOK 532	HD 85043A ^a	PM J09486-2644	1.8±0.3
09568+0415	TOK 533	HD 86147	LSPM J0956+0441 ^b	10.7±0.9
10289+3453	SHY 215	HD 90681	HD 92194	4.8±0.2
10532-3006	SHY 563	HD 94375 ^a	HD 94542 ^a	23.6±0.2
11214+0638	TOK 544	HD 98697	LP 552-34	19.4±3.5
11455+4740	LEP 45	HD 102158	G 122-46	19.6±0.6
13305+2231	SHY 626	HD 117528	BD+22 2587	93.2±0.2
13470+3833	SHY 633	HD 120164	HD 119767	21.6±0.2
15120+0245	WIS 281	LP 562-9	LP 562-10	24.5±3.7
15208+3129	LEP 74	HD 136654	AX CrB	0.8±0.2
15318-0204	SHY 677	HD 138370	HD 138159	17.3±0.3
15330-0111	SHY 678	11 Ser	HD 142011	12.0±0.2
15356+7726	WIS 288	LSPM J1535+7725	LP 22-358	24.3±0.3
15408-3252	SHY 278	HD 139696 ^{a,b}	CD-32 10820	42.8±2.9
15590+1820	SHY 691	HD 143292 ^a	HD 142899	42.7±0.3
16278-0822	SHY 287	ν Oph ^{a,c}	HD 144660	11.7±0.2
17166+0325	SHY 715	HD 156287 ^a	HD 159243	8.5±0.2
18143-4309	SHY 740	HD 166793	HD 166533	31.9±0.4
18496+1313	SHY 309	HD 229635	HD 229830	31.0±0.3
18571+5143	SHY 749	HD 176341	BD+49 2879	14.6±0.2
18597+1615	TOK 622	HD 176441 ^a	LSPM J1858+1613 ^b	19.3±0.5
19290-4952	SHY 319	HD 182857	HD 185112 ^a	14.0±0.3
20084+1503	LDS1033	G 143-33	G 143-27 ^c	66.3±1.7
20371+6122	SHY 780	HD 196903	HD 198662	12.4±0.2
20404-3251	SHY 781	HD 196746 ^a	HD 196189	26.2±0.2
20489-6847	SHY 782	HD 197569	HD 199760	7.6±0.2
21105+2227	SHY 793	HD 201670	HD 198759	54.4±17.8
22175+2335	GIC 179	G 127-13 ^b	G 127-14	21.7±0.9
22220-3431	SHY 802	HD 212035	HD 210111 ^c	11.4±0.5
23506+5412	SHY 840	HD 223582 ^a	HD 223788	1.7±0.2

Notes. ^(a) Stars with proper motion anomaly (Kervella et al. 2019; Brandt 2021). ^(b) Stars with RUWE > 10. ^(c) Known spectroscopic binaries.

masses. Estimated stellar ages are also needed to investigate the evolution of fragile multiple systems, while luminosity classes also shed light on stellar ages, especially outside the main sequence. The luminosity class of the stars in the 243 *Gaia* sources is illustrated by the Hertzsprung-Russell (H-R) diagram of Fig. 5. We took parallaxes and G , G_{BP} , and G_{RP} magnitudes from *Gaia* DR3, except for four very bright stars (δ Vel, α Cen A and B, ν Oph), for which we estimated their magnitudes from their well-determined spectral types, published Johnson B , V , R photometry, and the main-sequence colour-spectral type relation of Pecaut & Mamajek (2013). We also plot this relation in the diagram, although the main sequence, together with the loci of

white dwarfs and giants and subgiants beyond the turnoff point, is clearly marked by 57 345 field stars with good *Gaia* astrometry and photometry following the H-R example of Taylor (2021), but with the DR3 data set.

From their position in the H-R diagram, we identified eight giants and subgiants and five white dwarfs (listed in Table 3). We confirmed their classification with a comprehensive bibliographic study. Among the 13 stars, only one is part of a close pair unresolved by *Gaia*, namely δ Vel. Furthermore, all but one of the giants are so bright that were listed already by Bayer (1603) and Flamsteed (1725).

Four of the five white dwarfs have a spectral type determination, with only one presented as a white dwarf candidate by Gentile Fusillo et al. (2019). However, all of them are part of multiple systems (i.e. triple or higher). For example, WDS 01024+0504 is made of two spectroscopic binaries, namely the double, early K dwarf HD 6101 and the double, DA5.9 white dwarf EGGR 7 (Giclas et al. 1959; Maxted et al. 2000; Lajoie & Bergeron 2007; Caballero 2009; Gianninas et al. 2011; Toonen et al. 2017), while WDS 06536-3956 is made of the early M dwarf L 454-11 (Lépine & Gaidos 2011) and two white dwarfs, WT 201 (DA8.0) and WT 202 (DA7.0) (Subasavage et al. 2008). The system may also be quadruple because L 454-11 has a RUWE = 18.0. The other two white dwarfs are in triple and quadruple systems.

Apart from the 13 giants, subgiants, and white dwarfs in Table 3, there are still some objects lying outside the main sequence in the colour-magnitude diagram of Fig. 5. In particular, there are 4 sources apparently below the main sequence. The origin of this discrepancy lies in the four cases on wrong photometry: 2MASS J02004917-3848535 in the double system WDS 02025-3849 is an \sim M7-8 ultracool dwarf with G_{BP} fainter than the *Gaia* limit (Smart et al. 2019); Gaia DR3 749786356557791744 in the triple system WDS 10289+3453 is another ultracool dwarf with G_{BP} fainter than the *Gaia* limit, but with a spectral type at the M-L boundary; Gaia DR3 3923191426460144896 in the quadruple system WDS 11486+1417 is an \sim M4-5 late-type dwarf at $\rho \approx 10.1$ arcsec of the very bright ($G \approx 5.9$ mag) A8+G2 binary HD 102590; and Gaia DR3 1367008242580377216 in the triple system WDS 17415+4924 is an \sim M4-5 late-type dwarf with a relatively high value of G_{BP}/G_{RP} excess factor, E(BP/RP), which is an indicator of systematic errors in photometry (Riello et al. 2018). Remarkably, 2 of the 4 *Gaia* sources with the wrong photometry are the least massive stars in our sample (Sect. 3.7). The rest of the *Gaia* sources, which are especially redder than the subgiant turnoff point, are reasonably matched to the main sequence.

3.7. Masses and gravitational binding energies

For stars in the main sequence, we determined stellar masses, M , from the G -band absolute magnitude, *Gaia*, and 2MASS colours, spectral types, and the updated version of Table 4 in Pecaut & Mamajek (2013)¹¹. The match between spectral types derived by us from colours and absolute magnitudes and compiled from the bibliography is excellent (although we estimated spectral types for some *Gaia* sources that had previously gone unreported in the literature). In the case of unresolved (spectroscopic binaries and close WDS astrometric binaries), very bright stars (e.g. α Cen A and B), giants, subgiants, and white dwarfs (Table 3), we compiled M values from the bibliography (e.g. Lajoie & Bergeron 2007; Soubiran et al. 2008; Feuillet et al. 2016; Eker et al. 2018; Stock et al. 2018; Gentile Fusillo et al. 2019). If unavailable, we determined M from colours and absolute magnitudes by assuming either two equal-mass stars in double-lined spectroscopic binaries or that the mass of the companion, M_2 is much less than the mass of the primary, M_1 , in single-lined spectroscopic binaries (Latham et al. 2002). Because of this naïve approach, we established an uncertainty of 10% for our M values (Mann et al. 2019; Schweitzer et al. 1999), which may actually be larger in poorly investigated, single-lined spectroscopic binaries. In only two cases, namely, of white dwarfs without a public mass determination, we estimated their M as in Rebassa-Mansergas et al.

(2021). For the giants, subgiants, and white dwarfs we also compiled ages from the literature, as summarised in the last column of Table 3; such ages can be extrapolated to their wide companions. While the masses of the white dwarfs vary between about 0.5 and $0.8 M_\odot$ and of the giants between 1.0 and $3.2 M_\odot$, the masses of the stars on or near the main sequence vary from about 0.08 to $2.8 M_\odot$. The latter extremes correspond to the new ultracool dwarf Gaia DR3 749786356557791744 at the M-L boundary, which is at 13.7 arcsec to the solar-like HD 90681 star and the B9.5 IV HD 188162, which is the most massive star of a septuple system candidate (Sect. 4).

Next, we computed the projected physical separation, s , between every two *Gaia*-resolved components in each pair from the angular separation, ρ , and the distance, d , to the primary. Given the wide separations considered, instead of using the $s \approx d\rho$ approximation, we used instead the exact definition from the trigonometry:

$$s = d \sin \rho. \quad (6)$$

We considered the distance to the primary star (which usually has the smallest parallax uncertainty) as the distance to the whole system. The determined s vary from \sim 11 au in the case of nearby, close astrometric binaries (e.g. HD 6101), to $\sim 2.3 \cdot 10^6$ au (about 11 pc) in the case of the very widest companions (see below). The uncertainty in s is underestimated for primaries whose parallaxes may be affected by close binarity.

Finally, we determined reduced binding energies of the wide systems as in Caballero (2009):

$$|U_g^*| = G \frac{M_1 M_2}{s}, \quad (7)$$

They are “reduced” because we used the projected physical separation for computing $|U_g^*|$ instead of the actual separation or the semi-major axis, a , which is unknown. We did not apply a most probable conversion factor between a and s for easier computation and, especially, comparisons with previous works (Close et al. 2003; Burgasser et al. 2007; Radigan et al. 2009; Caballero 2010; Faherty et al. 2010). This conversion factor, resulting from a uniform distribution of tridimensional vectors projected on a bidimensional plane (Abt & Levy 1976; Fischer & Marcy 1992), would lead to about 26% larger actual separations and, therefore, 26% smaller (non-reduced) binding energies¹² (Dhital et al. 2010; Oelkers et al. 2017).

The resulting M_1 , M_2 , ρ , θ , s , and $|U_g^*|$ are listed in Table B.3. We computed $|U_g^*|$ only for systems with double-like hierarchy, that is, actual doubles and multiple systems with $\rho_{1,\text{wide}} \gg \rho_{1,i}$. Here, ‘wide’ indicates resolved companions at $\rho_{1,\text{wide}} > 1000$ arcsec and ‘ i ’ other components. As a result, we did not compute $|U_g^*|$ of 14 multiple systems with $\rho_{\text{wide}} \sim \rho_{1,i}$, which we called trapezoidal systems or trapezia.

4. Results and discussion

Among the 155 159 pairs contained in the WDS catalogue at the time of our analysis, 153 pairs with common-parallax, common-proper motion, ultrawide components at $\rho > 1000$ arcsec passed our astrometric criteria in Sect. 3.3, of which 59 ($38.6 \pm 9.8\%$) are part of young SKGs, associations, or open clusters (Table B.1), and 95 ($61.4 \pm 12.4\%$) are ultrawide pairs in 94 galactic systems

¹¹ https://www.pas.rochester.edu/~emamajek/EEM_dwarf_UBVIJHK_colors_Teff.txt

¹² Fischer & Marcy (1992) determined the statistical correction $\bar{a} \approx 1.26 \bar{s}$ between projected separation (s) and true separation (a) from Monte Carlo simulations over a full suite of binary parameters.

Table 3: Giants and white dwarfs in wide double and multiple systems.

Star	Spectral type	WDS	Discoverer code	α (J2000) (hh:mm:ss.ss)	δ (J2000) (dd:mm:ss.s)	M (M _⊙)	Age (Ga)
<i>Giants</i>							
δ Vel Aa	A2 IV	08447–5443	SHY 49	08:44:42.23	–54:42:31.7	3.19 ± 0.03^a	$\sim 0.431^a$
HD 120164	K0 III	13470+3833	SHY 633	13:46:59.77	+38:32:33.7	2.42 ± 0.24^b	$\sim 0.7^b$
ι Vir	F7 III	14190–0636	SHY 71	14:16:00.87	–06:00:02.0	$\sim 1.81^c$	1.809 ± 0.001^d
11 Ser	K0 III	15330–0111	SHY 678	15:32:57.94	–01:11:11.0	1.27 ± 0.35^e	$2.75^{+0.88}_{-0.66}^e$
64 Aql	K1 III–IV	20080–0041	SHY 325	20:08:01.82	–00:40:41.5	1.00 ± 0.27^e	9.33 ± 4.17^e
ν Aqr	K0 III	21096–1122	TOK 633	21:09:35.64	–11:22:18.1	$2.01^{+0.04}_{-0.11}^f$	$1.26^{+0.22}_{-0.19}^f$
κ Aqr	K1.5 III	22378–0414	TOK 640	22:37:45.38	–04:13:41.0	2.55 ± 0.13^g	2.79 ± 1.16^h
ι Cep	K1 III	22497+6612	SHY 359	22:49:40.81	+66:12:01.4	$1.55^{+0.05}_{-0.20}^f$	$2.57^{+0.18}_{-0.38}^f$
<i>White dwarfs</i>							
EGGR 7	DA5.9	01024+0504	WNO 50	01:03:49.92	+05:04:30.6	$\sim 0.77^i$...
WT 202	DA7.0	06536–3956	SUB 2	06:53:35.44	–39:55:34.8	0.64 ± 0.02^j	$2.4^{+1.0}_{-0.11}^j$
WT 201	DA8.0	06536–3956	SUB 2	06:53:30.21	–39:54:29.1	0.64 ± 0.02^j	$3.2^{+1.1}_{-0.1}^j$
Gaia DR3 812109085097488768 ... ^k	...	09150+3837	DAM1575	09:14:58.95	+38:36:58.3	0.5 ± 0.1^l	...
SDSS J230056.41+640815.5	DC	22497+6612	...	23:00:56.46	+64:08:16.0	0.5 ± 0.1^l	...

Notes. ^(a) David & Hillenbrand (2015); ^(b) da Silva et al. (2015); ^(c) Gontcharov & Kiyaeva (2010); ^(d) Eker et al. (2018); ^(e) Feuillet et al. (2016); ^(f) Stock et al. (2018); ^(g) Kervella et al. (2019); ^(h) Soubiran et al. (2008); ⁽ⁱ⁾ Lajoie & Bergeron (2007); ^(j) Rebassa-Mansergas (priv. comm.); ^(k) Gentile Fusillo et al. (2019); ^(l) This work.

Table 4: Multiplicity order rates of ultrawide galactic systems.

System type	Minimum rate ^a (%)	Estimated rate ^b (%)
Double	51.6 ± 14.6	32.3 ± 11.5
Triple	25.8 ± 10.3	23.7 ± 9.9
Quadruple	15.1 ± 7.9	21.5 ± 9.4
Quintuple or higher	7.5 ± 5.6	22.6 ± 9.7

Notes. ^(a) Multiplicity order rate including only systems resolved by *Gaia* or tabulated by WDS. ^(b) Multiplicity order rate including also close binary candidates with large RUWE, σ_{Vr} , or proper motion anomaly.

—one triple is made of two pairs with $\rho > 1000$ arcsec and different WDS entries (see Sect. 3.4), which makes 95 WDS pairs. Because of the small sample size, we used the Wald interval (Agresti & Coull 1998) with a 95% of confidence to calculate the ratio uncertainties¹³. To the galactic systems, we added 39 companions from the literature and separated by $\rho < 1000$ arcsec. In our *Gaia* DR3 search, we also found 39 additional astrometric companions not catalogued by WDS; that is, we found new companions in about a quarter of the investigated systems. In contrast, WDS tabulated a number of additional companion candidates with accurate *Gaia* DR3 data that did not pass our conservative astrometric criteria (Sect. 3.3). Most, but not all, of them are flagged by WDS with ‘U’ (‘proper motion or other technique indicates that this pair is non-physical’).

The 94 galactic field systems and their components are listed in Tables B.2 (basic astrometry and photometry) and B.3 (stellar masses, angular and projected physical separations, position angles, and binding energies). We remark that we reclassified the

stars in Tables B.2 and B.3 as primaries, secondaries, tertiaries, and so on, according to their *G*-band magnitudes. As a result, the WDS nomenclature “A”, “B”, “C” (etc.) does not always match our re-ordering.

Among the 94 galactic field systems, there are 48 double, 24 triple, 14 quadruple, 2 quintuple, 3 sextuples, and 2 septuples. The corresponding minimum multiplicity order rates are displayed in Table 4. The estimated multiplicity order rates and, therefore, the number of multiple systems increase significantly at the expense of the number of doubles if the new candidate companions with large RUWE, σ_{Vr} , or proper motion anomaly are included (Sect. 3.5). When these close binary candidates are taken into account, most of the ultrawide systems (67.8%) become multiple: 23.7% are triple, 21.5% are quadruple, and 22.6% have a higher multiplicity order. These rates are far greater than what is found in less separated multiple systems in the field (Chanamé & Gould 2004; Duchêne & Kraus 2013; Tokovinin 1997). Such a higher-than-usual multiplicity order implies a larger total mass, which, in turn, implies a larger binding energy.

In the left panel of Fig. 6, we display the minimum reduced gravitational binding energy of the 80 systems for which we were able to compute their $|U_g^*|$ as a function of the total mass in the system, $M_{\text{total}} = \sum M_i, i = 1 : 7$ (i.e. all except for the 14 trapezia). This diagram would be complete only by adding systems with angular separations $\rho < 1000$ arcsec but with very low masses (e.g. Caballero 2007b,a; Artigau et al. 2007; Rica & Caballero 2012). It is complete, however, at the highest total masses and lowest binding energies. Actual total masses and binding energies, when close binary candidates are taken into account, are larger.

There are three systems with $|U_g^*| < 10^{33}$ J, significantly lower than those of the other 77 systems. They are listed at the top of Table 5 with their WDS identifiers, discoverer codes (i.e. Wide-field Infrared Survey Explorer, WIS, Kirkpatrick et al. 2016), Simbad names, stellar masses, distances, projected phys-

¹³ Wald 95% confidence interval is $(\lambda - 1.96 \sqrt{\lambda/n}, \lambda + 1.96 \sqrt{\lambda/n})$, where λ is the number of successes in n trials.

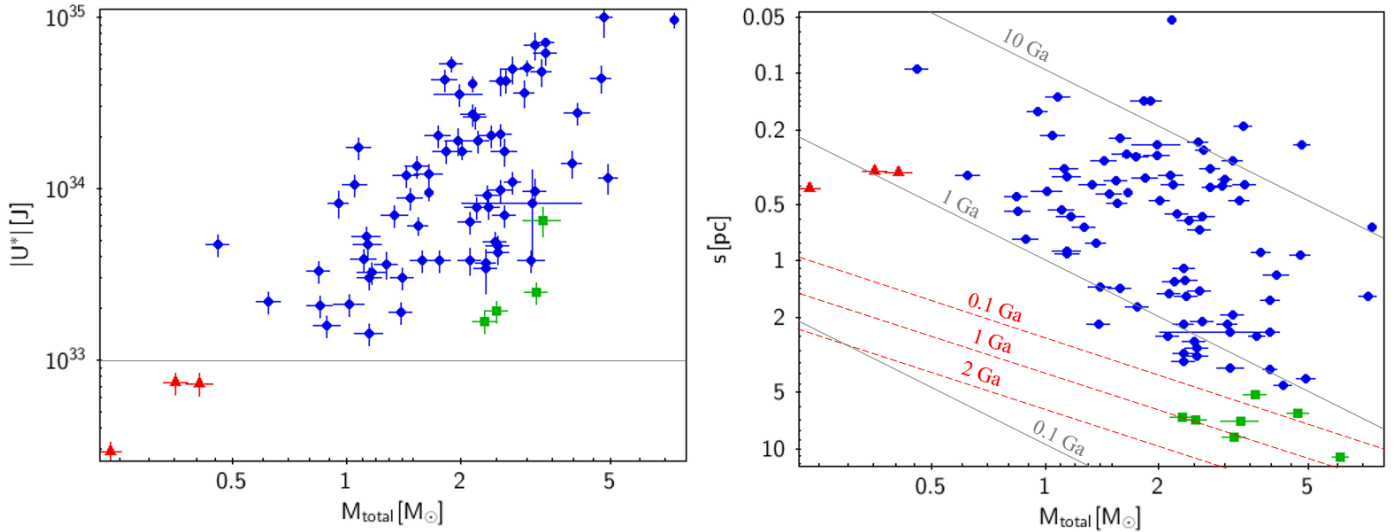


Fig. 6: Reduced binding energy (*left*) and projected physical separation (*right*) as functions of ultrawide system total mass. In both panels, the three most fragile systems (top of Table 5) and the most separated systems (bottom of Table 5) are plotted in red triangles and green squares, respectively, while the rest of investigated ultrawide systems are plotted in blue circles. The error bars in s are smaller than the used symbols. In the *left* panel, the horizontal line marks the limit of $|U_g^*|$ at 10^{33} J. In the *right* panel, the grey solid diagonal lines mark the statistical maximum ages of 0.1, 1, and 10 Ga at which the systems are likely bound (computed with Eq. 9), while the red dashed diagonal lines mark the corresponding orbital periods of 0.1, 1, and 2 Ga (computed with Kepler's third law). In both cases we used the correction $a \approx 1.26$ s (Fischer & Marcy 1992).

ical separations, and gravitational binding energies. The three systems are doubles composed of M3–6 V primaries and M5–9 V secondaries. These spectral types were estimated by us from M_G from the relations of Pecaut & Mamajek (2013) and Cifuentes et al. (2020), except for the secondary star in WDS 15488+4929, namely, LSPM J1550+4921, whose spectral type M7.0 V was determined by West et al. (2011) from low-resolution spectroscopy. With a mass of about $0.09 M_\odot$, the secondary in the system WDS 02025–3849, namely, 2MASS J02004917–3848535 (~M7–8 V), is the second-least massive star in our whole sample. The low masses of the system components and the wide separations, of about $68\text{--}85\,10^3$ au (six to eight times wider than α Cen + Proxima), explain the very low $|U_g^*|$. Actual binding energies may be larger, as the primary in WDS 02025–3849 has a RUWE = 40.7; assuming an equal-mass binary, the corrected binding energy would double. None of the three systems have radial-velocity determinations (from Gaia DR3 and West et al. 2011) for the two resolved components. Given their relatively large μ ratios and ΔPA (but within our boundary conditions), a dedicated radial-velocity follow-up would be necessary to ascertain whether the three fragile binaries are actually triples.

Even if each of the three systems had an additional component and, therefore, higher total masses and binding energies than estimated above, there seems to be a lower boundary of $|U_g^*|$ for the most fragile systems at about 10^{33} J (first mentioned by Caballero 2010). This lower limit may be a consequence of the tidal disruption of wide systems by the galactic gravitational potential, via energy and momentum exchange in encounters with other stars or even the interstellar medium (Heggie 1975; Draine 1980; Bahcall & Soneira 1981; Dhital et al. 2010; Jiang & Tremaine 2010). Actually, during the lifetime of a stellar system, the continuous small and dissipative encounters with other stars are much more disruptive than occasional single catastrophic encounters (Ritterer & King 1982; Weinberg et al. 1987). As a result of these interactions, the initial distribution of

separations of stellar systems change (increase) over time until eventual disruption. Using the Fokker–Planck coefficients to describe the effects produced on the orbital binding energies due to those small encounters over time, Weinberg et al. (1987) estimated the average lifetime of a binary as:

$$t_*(a) \simeq 18 \text{ Ga} \left(\frac{n_*}{0.05 \text{ pc}^{-3}} \right)^{-1} \left(\frac{M_*}{M_\odot} \right)^{-2} \left(\frac{M_{\text{tot}}}{M_\odot} \right) \left(\frac{V_{\text{rel}}}{20 \text{ km s}^{-1}} \right) \left(\frac{a}{0.1 \text{ pc}} \right)^{-1} \ln^{-1} \Lambda, \quad (8)$$

where n_* and M_* are the number density and average mass of the perturber objects, V_{rel} is the relative velocity between the binary system and the perturber, M_{tot} and a are the total mass and semi-major axis of the binary system, and $\ln \Lambda$ is the Coulomb logarithm. The calculation was simplified by Dhital et al. (2010) by setting the values $n_* = 0.1 M_\odot \text{ pc}^{-3}$, $M_* = 0.7 M_\odot$, $V_{\text{rel}} = 20 \text{ km s}^{-1}$, and $\ln \Lambda = 1$ (Close et al. 2007), and produced an equation that describes in a statistical way the maximum separation of a surviving stellar system at a given age:

$$a \simeq 1.212 \frac{M_{\text{total}}}{t_*}, \quad (9)$$

where the total mass is in M_\odot , the average lifetime in Ga, and the semi-major axis in pc.

We plot the projected physical separation s as a function of the total mass M_\odot of the 94 ultrawide systems in the right panel of Fig. 6. Overplotted on them, we display the physical separations corresponding to 0.1, 1.0, and 10 Ga and the orbital periods for 0.1, 1.0, and 2 Ga. The three most fragile systems may have survived in their current configuration by about 1 Ga or slightly less in the case of WDS 15488+4929. However, there are other systems that are less fragile (i.e. have higher reduced binding energies, comparable to those of well-recognised systems) but

Table 5: Most fragile ($|U_g^*| < 10^{33}$ J) and the most separated ($s \geq 5$ pc) systems.

WDS	Discoverer code	Star	M (M_\odot)	d^a (pc)	s^b (10^3 au)	$ U_g^* $ (10^{33} J)
<i>The most fragile systems</i>						
00016–0102	WIS 1	2MASS J00013688–0101441	0.22±0.02			
		SIPS J0000-0112	0.13±0.01	60.33±0.13	68.5±0.2	0.74±0.10
02025–3849	WIS 248	2MASS J02022892–3849021 ^c	0.32±0.03			
		2MASS J02004917–3848535	0.09±0.01	59.46±2.29	69.3±2.7	0.72±0.11
15488+4929	WIS 295	LSPM J1548+4928	0.12±0.01			
		LSPM J1550+4921	0.11±0.01	76.81±0.63	85.0±0.7	0.29±0.04
<i>The most separated systems</i>						
02315+0106		HD 15695	1.75±0.18			
		BD+00 415B	1.63±0.16			
		SHY 422	1.14±0.11			
		...	1.07±0.11	105.52±0.33	2284.7±7.2	...
		...	0.30±0.03			
		...	0.20±0.02			
07166–2319	SHY 508	HD 56578 ^e	2.42±0.24			
		HD 57527 ^e	1.92±0.19	106.32±0.47	1340.9±6.0	...
		...	0.35±0.03			
10532–3006	SHY 563	HD 94375 ^e	1.32±0.13			
		HD 94542 ^e	1.19±0.12	82.17±0.16	1439.6±2.8	1.91±0.27
15330–0111	SHY 678	11 Ser	1.27±0.35			
		HD 142011	1.21±0.12			
		...	0.43±0.04	83.61±0.42	1483.0±7.4	3.08±0.62
		...	0.40±0.04			
17166+0325	SHY 715	HD 156287 ^e	1.24±0.12			
		HD 159243	1.08±0.11	82.15±0.17	1407.6±2.8	1.68±0.24
21105+2227	SHY 793	HD 201670 ^d	1.74±0.17			
		HD 198759	1.45±0.15	113.81±0.97	1783.3±15.2	2.49±0.35
22497+6612	SHY 359	ι Cep	1.55±0.20			
		HD 215588	1.23±0.12			
		...	0.35±0.03	36.65±0.18	1061.3±5.1	...
		UCAC3 297-187960	0.50±0.10			

Notes. ^(a) Distance of the primary star. ^(b) Maximum separation between stars inside the system. ^(c) RUWE> 10. ^(d) Large σ_{V_r} for its G magnitude. ^(e) Proper motion anomaly measured by [Kervella et al. \(2019\)](#), [Brandt \(2021\)](#) or both.

that can be disrupted in a few hundred million years. As we may expect, they are among the most separated systems.

There are seven system candidates with $s = 1.1\text{--}2.3 \cdot 10^6$ au (5.1–11.1 pc), listed at the bottom of Table 5. These refer to the kinds of systems that lend their name to the topic of this work (Reaching the boundary between stellar kinematic groups and very wide binaries). In the spherical volume of radius 10 pc centred on the Sun, according to the exhaustive compendium by [Reylé et al. \(2021\)](#), there are 339 systems containing stars, brown dwarfs, and exoplanets. As a result, regardless of their (unknown) age, the ultrawide binary and multiple systems may be at the last stages of disruption and follow the formation-evolution-dissolution sequence described by [Close et al. \(2003\)](#), who predicted an overabundance of very low-mass binaries far from the centre of the original ‘minicluster.’ This is the case of the most separated components in the systems WDS 02315+0106 and WDS 15330–0111, which have low masses and large σ_{V_r} for their G magnitudes. The seven system candidates, all of them identified by [Shaya & Olling \(2011\)](#), may be the rem-

nants of previous SKGs that are being dissolved in the Milky Way and that are older than the ones identified in Sect. 3.4. Three system candidates, including the sextuple (perhaps septuple) WDS 02315+0106 system, are trapezia and, therefore, their reduced binding energies were not computed. The other four systems consist of three very wide binaries made of two bright Henry Draper stars ([Cannon & Pickering 1918](#)) and one double-like hierarchical quadruple (perhaps quintuple) system. The latter, namely WDS 15330–01110, is made of the K0 giant 11 Ser (Table 3), the G1 dwarf HD 142011, and two anonymous early M dwarfs, one of which has a large σ_{V_r} for their G magnitude. These two (or three) M dwarfs are very close to each other ($s \sim 92$ au) and to the Sun-like star ($s \sim 630\text{--}690$ au), which allowed us to compute $|U_g^*|$. However, the K0 giant and the G1+M+M triple are separated by about $1.5 \cdot 10^6$ au (7.2 pc). Between them, dozens of unrelated stars with similar parallaxes must exist, but with very different proper motions that exert smooth ‘continuous small and dissipative’ gravitational thrusts.

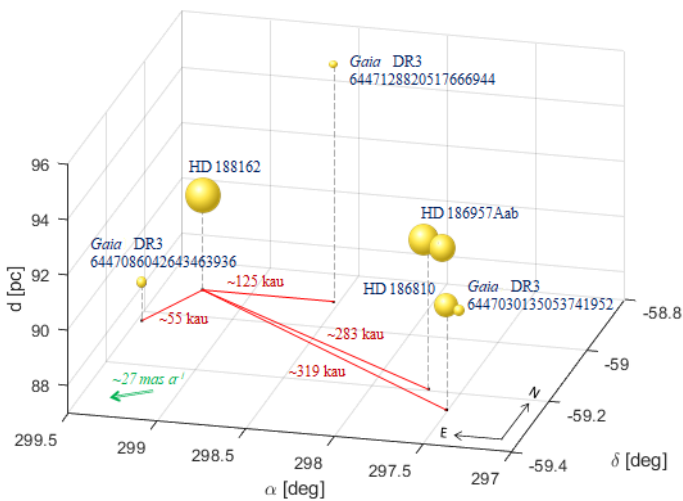


Fig. 7: Spatial distribution of the septuple system WDS 19507–5912. The size of the spheres representing every star, labelled in blue, are proportional to their brightness. The projected physical separations from the primary star, HD 188162, in red, are in 10^3 au. The overall proper motion, in green, is in mas a^{-1} .

Something similar may occur in the case of the 14 ultrawide trapezia, which tend to have a high multiplicity hierarchy: 1 of the 2 septuple systems, the 3 sextuples, 7 of the 15 quadruples, and 3 of the 25 triples are trapezia. In particular, the trapezoidal septuple system WDS 19507–5912 is sketched in Fig. 7. It consists of three late-B-to-early-A stars (one is a spectroscopic binary) and three intermediate-to-late M dwarfs (one is close to an A star). Given the early spectral types of the most massive stars, this system may approximately be the age of the Hyades (600–700 Ma; Perryman et al. 1998; Gossage et al. 2018; Martín et al. 2018) and, therefore, stand as an unidentified sparse young SKG¹⁴. All these results are in accordance with the suggestions by Basri & Reiners (2006) and Caballero (2007b), who proposed a major prevalence of wide triples over wide binaries. We also confirm that the individual components of systems at very wide separations are often multiple systems themselves, as stated by Cifuentes et al. (2021).

Five of the seven ultrawidest systems have orbital periods of the order of 1 Ga, even older than the Hyades. Such long orbital periods stand as a challenge to the ‘binary’ definition itself, namely: a system of two stars that are gravitationally bound to and in orbit around each other. As a result, the ultrawidest pairs may have not completed one revolution either because of their young age or because they were recently disrupted by passing stars and, therefore, should not be called ‘binaries’. This statement should also be extrapolated to the system candidates in young stellar kinematic groups (Section 3.4), including less separated but also less massive, pairs. Furthermore, Caballero (2009) already claimed that the AU Mic+AT Mic system in the β Pictoris moving group has only completed at most two orbital periods since its formation. All of this makes the boundary between stellar kinematic groups and very wide binaries blurrier and blurrier.

Finally, we used the accurate *Gaia* astrometry to measure the relative transverse velocity, ΔV , as a function of the projected physical separation of the 48 widest systems with $s > 0.1$ pc,

and compared it with the maximum velocity allowed for a bound binary, as done by some other authors (e.g. El-Badry 2019; El-Badry et al. 2021). This comparison may interpret several observational studies that have reported that the difference in the proper motions or radial velocities of the components of nearby wide binaries appear larger than predicted by Kepler’s laws, indicating a potential breakdown of general relativity at low accelerations. However, our data, which are relatively scarce compared to extensive simulations (cf. El-Badry 2019), do not even show projection effects. Furthermore, inner subsystems, which are frequent, disturb our ΔV estimates. As a result, the actual bound nature of our most fragile system is hardly verifiable.

To sum up, wide pairs with very low-mass components and $|U_g^*| \sim 10^{33}$ J (e.g. ultracool dwarf binaries with late-M and early-L spectral types and projected physical separations of a few thousand astronomical units – Caballero 2007b,a; Artigau et al. 2007) are perhaps more relevant for investigating the disruption of fragile systems by the galactic gravitational potential rather than ultrawide systems of gargantuan projected physical separations (much larger than those proposed by Tolbert 1964, Bahcall & Soneira 1981, or Ritterer & King 1982) caught in the act of destruction and, that probably are the leftover of past SKGs.

5. Summary

Thanks to the *Gaia* DR3 (Gaia Collaboration et al. 2022) and a number of parallax and proper motion searches in the previous decade (e.g. Caballero 2010; Shaya & Olling 2011; Tokovinin & Lépine 2012; Kirkpatrick et al. 2016), we present a leap forward with respect to the first item of this series of papers, on the Washington double stars with the widest angular separations (Caballero 2009). Accordingly, we increase by over an order of magnitude the sample size and the astrometric precision of systems with angular separations $\rho > 1000$ arcsec. Among other results of our analysis, we present: (i) 40 additional astrometric companions not catalogued yet by WDS, including several ultracool dwarfs at the M-L boundary and one hot white dwarf, not counting several dozens close binary candidates from large *Gaia* DR3 RUWE and σ_{RV} ; (ii) a general confusion in the literature between actual, physically bound, ultrawide pairs and components in young SKGs, associations, and even clusters with identical galactocentric space velocities; (iii) three very fragile systems discovered by Kirkpatrick et al. (2016) that are made of intermediate and late M dwarfs with large projected physical separations of 0.33–0.41 pc and small reduced binding energies $|U_g^*| \lesssim 10^{33}$ J, which is probably the smallest value found among gravitationally bound systems; (iv) the individual components of systems at very wide separations are often multiple systems themselves (Cifuentes et al. 2021), which implies an overabundance of high-order multiples (triples, quadruples, quintuples, and more) among the widest systems, and larger binding energies and total masses than systems with comparable separations but lower multiplicity order; and (v) an additional observational confirmation of classical theoretical predictions (e.g. Weinberg et al. 1987) of disruption of binary systems by the galactic gravitational potential, which destroys the ultrawidest systems with total masses below $10 M_\odot$ in less than 600–700 Ma (the age of the Hyades cluster). As incidental results, we report 40 new candidate stars in known young SKGs and at least one new young stellar association around the bright star γ Cas, although some of our highest-order multiple systems, such as the septuple around the B9.5 IV star HD 188162, may also be association remnants.

¹⁴ If confirmed in the future, we propose naming the SKG following the discovery name of the brightest, earliest star: HD 188162.

In conclusion, the total mass, binding energy, and probability that an ultrawide system is actually bound increase as the stellar multiplicity order also increases. Many systems reported here have overwhelmingly large projected physical separations, but have instead total masses large enough for the binding energies being comparable to those of less separated, less massive systems that are widely accepted as physical. However, none of the ultrawide systems will survive for another few hundred million years. In a sense, the widest multiple systems of today, which are now being torn apart by the Galaxy, will be the single stars of tomorrow.

Acknowledgements. We thank the anonymous reviewer for their constructive suggestions and comments, Jesús Maíz Apellániz for discussion on the γ Cas system, Alberto Rebassa-Mansergas for estimating masses of two white dwarfs, Brian D. Mason for help with five unidentified wide WDS companions, and Andrei Tokovinin for providing us the ρ of a wide pair and very useful discussion on hierarchical multiplicity. We acknowledge financial support from the Agencia Estatal de Investigación 10.13039/501100011033 of the Ministerio de Ciencia e Innovación and the ERDF “A way of making Europe” through projects PID2019-109522GB-C51 and PID2020-112949GB-I00, and the Centre of Excellence “María de Maeztu” award to the Centro de Astrobiología (MDM-2017-0737), and from the European Commission Framework Programme Horizon 2020 Research and Innovation through the ESCAPE project under grant agreement no. 824064. This research made use of the Washington Double Star Catalog maintained at the U.S. Naval Observatory, NASA’s Astrophysics Data System Bibliographic Services, the Simbad database, VizieR catalogue access tool, and Aladin sky atlas at the CDS, Strasbourg (France), and the TOPCAT tool.

References

- Abt, H. A. 1988, *ApJ*, 331, 922
 Abt, H. A. & Levy, S. G. 1976, *ApJS*, 30, 273
 Agresti, A. & Coull, B. 1998, *Am. Stat.*, 52, 119
 Allen, C., Herrera, M. A., & Poveda, A. 1998, in IX Latin American Regional IAU Meeting, “Focal Points in Latin American Astronomy”, ed. A. Aguilar & A. Carraminana, 21
 Allen, C., Poveda, A., & Herrera, M. A. 1997, The Distribution of Separations of Wide Binaries, Vol. 223 (Springer), 133
 Allen, C., Poveda, A., & Herrera, M. A. 2000, *A&A*, 356, 529
 Allen, R. H. 1899, Star-names and their meanings
 Alonso-Floriano, F. J., Caballero, J. A., Cortés-Contreras, M., Solano, E., & Montes, D. 2015, *A&A*, 583, A85
 Ambartsumian, V. A. 1949, *Sov. Astron.*, 26, 3
 Arenou, F., Luri, X., Babusiaux, C., et al. 2018, *A&A*, 616, A17
 Argelander, F. W. A. 1903, *Eds Marcus and Weber’s Verlag*, 0
 Artigau, É., Lafrenière, D., Doyon, R., et al. 2007, *ApJ*, 659, L49
 Bahcall, J. N. & Soneira, R. M. 1981, *ApJ*, 246, 122
 Bailer-Jones, C. A. L., Rybizki, J., Fouesneau, M., Mantelet, G., & Andrae, R. 2018, *AJ*, 156, 58
 Basri, G. & Reiners, A. 2006, *AJ*, 132, 663
 Batten, A. H. 1973, Binary and multiple systems of stars: International Series of Monographs in Natural Philosophy (Pergamon)
 Bayer, J. 1603, *Uranometria omnium asterismorum continens schemata, nova methodo delineata aereis laminis expressa*
 Bell, C. P. M., Murphy, S. J., & Mamajek, E. E. 2017, *MNRAS*, 468, 1198
 Blaauw, A. 1991, in NATO Advanced Study Institute (ASI) Series C, Vol. 342, The Physics of Star Formation and Early Stellar Evolution, ed. C. J. Lada & N. D. Kylafis, 125
 Bohn, A. J., Ginski, C., Kenworthy, M. A., et al. 2022, *A&A*, 657, A53
 Bonnarel, F., Fernique, P., Bienaymé, O., et al. 2000, *A&AS*, 143, 33
 Bouvier, J., Kendall, T., Meeus, G., et al. 2008, *A&A*, 481, 661
 Brandt, T. D. 2021, *ApJS*, 254, 42
 Bressan, A., Marigo, P., Girardi, L., et al. 2012, *MNRAS*, 427, 127
 Burgasser, A. J., Reid, I. N., Siegler, N., et al. 2007, in Protostars and Planets V, ed. B. Reipurth, D. Jewitt, & K. Keil, 427
 Burnham, Robert, J. 1978, *Burnham’s Celestial Handbook: An Observer’s Guide to the Universe Beyond the Solar System*, in three volumes.
 Caballero, J. A. 2007a, *ApJ*, 667, 520
 Caballero, J. A. 2007b, *A&A*, 462, L61
 Caballero, J. A. 2008, *MNRAS*, 383, 375
 Caballero, J. A. 2009, *A&A*, 507, 251
 Caballero, J. A. 2010, *A&A*, 514, A98
 Caballero, J. A., Genebriera, J., Tobal, T., et al. 2013, in Highlights of Spanish Astrophysics VII, ed. J. C. Guirado, L. M. Lara, V. Quilis, & J. Gorgas, 971–976
 Cannon, A. J. & Pickering, E. C. 1918, *Annals of Harvard College Observatory*, 91, 1
 Cantat-Gaudin, T., Jordi, C., Vallenari, A., et al. 2018, *A&A*, 618, A93
 Carro, J. M. 2021, *Il Bollettino delle Stelle Doppie*, 33, 12
 Chabrier, G. 2003, *PASP*, 115, 763
 Chanamé, J. & Gould, A. 2004, *ApJ*, 601, 289
 Chen, C. H., Patten, B. M., Werner, M. W., et al. 2005, *ApJ*, 634, 1372
 Christy, J. W. & Walker, R. L. J. 1969, *PASP*, 81, 643
 Cifuentes, C., Caballero, J. A., & Agustí, S. 2021, *RNAAS*, 5, 129
 Cifuentes, C., Caballero, J. A., Cortés-Contreras, M., et al. 2020, *A&A*, 642, A115
 Close, L. M., Richer, H. B., & Crabtree, D. R. 1990, *AJ*, 100, 1968
 Close, L. M., Siegler, N., & Freed, M. 2003, in Brown Dwarfs, ed. E. Martín, Vol. 211, 249
 Close, L. M., Zuckerman, B., Song, I., et al. 2007, *ApJ*, 660, 1492
 Cutri, R. M., Wright, E. L., Conrow, T., et al. 2014, *VizieR Online Data Catalog*, 2328, 0
 da Silva, R., Milone, A. d. C., & Rocha-Pinto, H. J. 2015, *A&A*, 580, A24
 David, T. J. & Hillenbrand, L. A. 2015, *ApJ*, 804, 146
 de Zeeuw, P. T., Hoogerwerf, R., de Bruijne, J. H. J., Brown, A. G. A., & Blaauw, A. 1999, *AJ*, 117, 354
 Dhital, S., West, A. A., Stassun, K. G., & Bochanski, J. J. 2010, *AJ*, 139, 2566
 Dopcke, G., Porto de Mello, G. F., & Sneden, C. 2019, *MNRAS*, 485, 4375
 Draine, B. T. 1980, *ApJ*, 241, 1021
 Duchêne, G. & Kraus, A. 2013, *ARA&A*, 51, 269
 Duquennoy, A. & Mayor, M. 1991, *A&A*, 248, 485
 Dzib, S. A., Loinard, L., Ortiz-León, G. N., Rodríguez, L. F., & Galli, P. A. B. 2018, *ApJ*, 867, 151
 Eggen, O. J. 1965, in Galactic structure. Edited by Adriaan Blaauw and Maarten Schmidt. Published by the University of Chicago Press, 111
 Eggleton, P. P. & Tokovinin, A. A. 2008, *MNRAS*, 389, 869
 Eker, Z., Bakış, V., Bilir, S., et al. 2018, *MNRAS*, 479, 5491
 El-Badry, K. 2019, *MNRAS*, 482, 5018
 El-Badry, K., Rix, H.-W., & Heintz, T. M. 2021, *MNRAS*, 506, 2269
 Faherty, J. K., Burgasser, A. J., West, A. A., et al. 2010, *AJ*, 139, 176
 Fekel, F. C. J. 1979, PhD thesis, University of Texas, Austin
 Feuillet, D. K., Bovy, J., Holtzman, J., et al. 2016, *VizieR Online Data Catalog*, J/ApJ/817/40
 Fischer, D. A. & Marcy, G. W. 1992, *ApJ*, 396, 178
 Flamsteed, J. 1725, *Historia Coelestis Britannicae, tribus Voluminibus contenta (1675–1689)*, (1689–1720), vol. 1, 2, 3
 Folkes, S. L., Pinfield, D. J., Jones, H. R. A., et al. 2012, *MNRAS*, 427, 3280
 Fracastoro, M. G. 1988, *Ap&SS*, 142, 11
 Freund, S., Robrade, J., Schneider, P. C., & Schmitt, J. H. M. M. 2020, *A&A*, 640, A66
 Fürnkranz, V., Meingast, S., & Alves, J. 2019, *A&A*, 624, L11
 Gagné, J. & Faherty, J. K. 2018, *ApJ*, 862, 138
 Gagné, J., Lafrenière, D., Doyon, R., Malo, L., & Artigau, É. 2015, *ApJ*, 798, 73
 Gagné, J., Mamajek, E. E., Malo, L., et al. 2018a, *ApJ*, 856, 23
 Gagné, J., Roy-Loubier, O., Faherty, J. K., Doyon, R., & Malo, L. 2018b, *ApJ*, 860, 43
 Gaia Collaboration, Brown, A. G. A., Vallenari, A., et al. 2018, *A&A*, 616, A1
 Gaia Collaboration, Brown, A. G. A., Vallenari, A., et al. 2021, *A&A*, 649, A1
 Gaia Collaboration, Brown, A. G. A., Vallenari, A., et al. 2016, *A&A*, 595, A2
 Gaia Collaboration, Vallenari, A., Brown, A.G.A., Prusti, T., & et al. 2022, *A&A*, 650, A1
 Garnavich, P. M. 1993, *PASP*, 105, 321
 Gáspár, A., Rieke, G. H., & Balog, Z. 2013, *ApJ*, 768, 25
 Gentile Fusillo, N. P., Tremblay, P.-E., Gänsicke, B. T., et al. 2019, *MNRAS*, 482, 4570
 Gianninas, A., Bergeron, P., & Ruiz, M. T. 2011, *ApJ*, 743, 138
 Giclas, H. L., Slaughter, C. D., & Burnham, R. 1959, *Lowell Observatory Bulletin*, 4, 136
 Goldman, B., Röser, S., Schilbach, E., Moór, A. C., & Henning, T. 2018, *ApJ*, 868, 32
 Gontcharov, G. A. & Kiyaeva, O. V. 2010, *New Astron.*, 15, 324
 González-Payo, J., Cortés-Contreras, M., Lodieu, N., et al. 2021, *A&A*, 650, A190
 Gorynya, N. A. & Tokovinin, A. 2018, *MNRAS*, 475, 1375
 Gossage, S., Conroy, C., Dotter, A., et al. 2018, *ApJ*, 863, 67
 Guenther, E. W., Paulson, D. B., Cochran, W. D., et al. 2005, *A&A*, 442, 1031
 Heggie, D. C. 1975, *MNRAS*, 173, 729
 Henrichs, H. F., Hammerschlag-Hensberge, G., Howarth, I. D., & Barr, P. 1983, *ApJ*, 268, 807
 Herschel, W. 1802, *Philos. T. R. Soc. Lond.*, 92, 213
 Hirshfeld, A. W. 2001, Parallax: The Race to Measure the Cosmos
 Hoogerwerf, R. 2000, *MNRAS*, 313, 43
 Hubble, E. P. 1922, *ApJ*, 56, 162
 Hutter, D. J., Tycner, C., Zavala, R. T., et al. 2021, *ApJS*, 257, 69
 Innes, R. T. A. 1915, Circular of the Union Observatory Johannesburg, 30, 235
 Jansen, D. J., van Dishoeck, E. F., & Black, J. H. 1994, *A&A*, 282, 605

- Jensen, E. L., Mathieu, R. D., & Fuller, G. A. 1993, in American Astronomical Society Meeting Abstracts, Vol. 182, American Astronomical Society Meeting Abstracts #182, 62.21
- Jiang, Y.-F. & Tremaine, S. 2010, MNRAS, 401, 977
- Kalas, P., Liu, M. C., & Matthews, B. C. 2004, Science, 303, 1990
- Karr, J. L., Noriega-Crespo, A., & Martin, P. G. 2005, AJ, 129, 954
- Katz, D., Sartoretti, P., Guerrier, A., et al. 2022, arXiv e-prints, arXiv:2206.05902
- Kervella, P., Arenou, F., Mignard, F., & Thévenin, F. 2019, A&A, 623, A72
- Kervella, P., Arenou, F., & Thévenin, F. 2022, A&A, 657, A7
- Kervella, P., Mérand, A., Petr-Gotzens, M. G., Pribulla, T., & Thévenin, F. 2013, A&A, 552, A18
- Kirkpatrick, J. D., Kellogg, K., Schneider, A. C., et al. 2016, ApJS, 224, 36
- Konacki, M., Mutterspaugh, M. W., Kulkarni, S. R., & Helminiak, K. G. 2010, ApJ, 719, 1293
- Kopytova, T. G., Brandner, W., Tognelli, E., et al. 2016, A&A, 585, A7
- Kouwenhoven, M. B. N., Goodwin, S. P., Parker, R. J., et al. 2010, MNRAS, 404, 1835
- Kraicheva, Z. T., Popova, E. I., Tutukov, A. V., & Iungelson, L. R. 1985, Astrofizika, 22, 105
- Kraus, A. L. & Hillenbrand, L. A. 2009, ApJ, 703, 1511
- Kraus, A. L., Shkolnik, E. L., Allers, K. N., & Liu, M. C. 2014, AJ, 147, 146
- Kroupa, P. 2001, MNRAS, 322, 231
- Lajoie, C. P. & Bergeron, P. 2007, ApJ, 667, 1126
- Latham, D. W., Mazeh, T., Davis, R. J., Stefanik, R. P., & Abt, H. A. 1991, AJ, 101, 625
- Latham, D. W., Stefanik, R. P., Torres, G., et al. 2002, AJ, 124, 1144
- Lee, J.-E., Lee, S., Dunham, M. M., et al. 2017, Nature Astronomy, 1, 0172
- Lépine, S. & Bongiorno, B. 2007, AJ, 133, 889
- Lépine, S. & Gaidos, E. 2011, AJ, 142, 138
- Lépine, S. & Shara, M. M. 2005, AJ, 129, 1483
- Lindgren, L., Bastian, U., Biermann, M., et al. 2021, A&A, 649, A4
- Lindgren, L., Hernández, J., Bombrun, A., et al. 2018, A&A, 616, A2
- Malkov, O. Y., Tamazian, V. S., Docobo, J. A., & Chulkov, D. A. 2012, A&A, 546, A69
- Mamajek, E. 2017, JDSO, 13, 264
- Mann, A. W., Dupuy, T., Kraus, A. L., et al. 2019, ApJ, 871, 63
- Martín, E. L., Lodieu, N., Pavlenko, Y., & Béjar, V. J. S. 2018, ApJ, 856, 40
- Mason, B. D., Wycoff, G. L., Hartkopf, W. I., Douglass, G. G., & Worley, C. E. 2001, AJ, 122, 3466
- Maxted, P. F. L., Marsh, T. R., & Moran, C. K. J. 2000, MNRAS, 319, 305
- Michalik, D., Lindgren, L., & Hobbs, D. 2015, A&A, 574, A115
- Mitrofanova, A., Dyachenko, V., Beskakotov, A., et al. 2021, AJ, 162, 156
- Mittal, T., Chen, C. H., Jang-Condell, H., et al. 2015, ApJ, 798, 87
- Mizusawa, T. F., Rebull, L. M., Stauffer, J. R., et al. 2012, AJ, 144, 135
- Montes, D., González-Peinado, R., Tabernero, H. M., et al. 2018, MNRAS, 479, 1332
- Montes, D., López-Santiago, J., Gálvez, M. C., et al. 2001, MNRAS, 328, 45
- Morgan, W. W., Keenan, P. C., & Kellman, E. 1943, An atlas of stellar spectra, with an outline of spectral classification (Chicago, Ill., The University of Chicago press)
- Murphy, S. J., Lawson, W. A., & Bessell, M. S. 2013, MNRAS, 435, 1325
- Nazé, Y., Rauw, G., Czesla, S., Smith, M. A., & Robrade, J. 2022, MNRAS, 510, 2286
- Nemravová, J., Harmanec, P., Koubský, P., et al. 2012, A&A, 537, A59
- Nesci, R., Tuvikene, T., Rossi, C., et al. 2018, Rev. Mexicana Astron. Astrofis., 54, 341
- Niemela, V. 2001, in Rev. Mex. Astron. Astrofis. Conf. Ser., Vol. 11, Rev. Mex. Astron. Astrofis. Conf. Ser., 23–26
- Ochsenbein, F., Bauer, P., & Marcout, J. 2000, A&AS, 143, 23
- Oelkers, R. J., Stassun, K. G., & Dhital, S. 2017, AJ, 153, 259
- Öpik, E. 1924, Tartu Obs. Publ., 25
- Osterbrock, D. E. 1957, ApJ, 125, 622
- Patience, J., Ghez, A. M., Reid, I. N., & Matthews, K. 2002, AJ, 123, 1570
- Paunzen, E., Heiter, U., Fraga, L., & Pintado, O. 2012, MNRAS, 419, 3604
- Peña Ramírez, K., Béjar, V. J. S., Zapatero Osorio, M. R., Petr-Gotzens, M. G., & Martín, E. L. 2012, ApJ, 754, 30
- Pecaut, M. J. & Mamajek, E. E. 2013, ApJS, 208, 9
- Pecaut, M. J. & Mamajek, E. E. 2016, MNRAS, 461, 794
- Perryman, M. A. C., Brown, A. G. A., Lebreton, Y., et al. 1998, A&A, 331, 81
- Perryman, M. A. C., Lindegren, L., Kovalevsky, J., et al. 1997, A&A, 300, 501
- Plavchan, P., Barclay, T., Gagné, J., et al. 2020, Nature, 582, 497
- Poeckert, R. & Marlborough, J. M. 1978, ApJ, 220, 940
- Poleski, R., Soszyński, I., Udalski, A., et al. 2012, Acta Astron., 62, 1
- Pourbaix, D. & Boffin, H. M. J. 2016, A&A, 586, A90
- Pourbaix, D., Tokovinin, A. A., Batten, A. H., et al. 2004, A&A, 424, 727
- Probst, R. G. 1983, ApJS, 53, 335
- Radigan, J., Lafrenière, D., Jayawardhana, R., & Doyon, R. 2009, ApJ, 698, 405
- Raghavan, D., McAlister, H. A., Henry, T. J., et al. 2010, ApJS, 190, 1
- Ramsay, G., Hakala, P., Doyle, J. G., Doyle, L., & Bagnulo, S. 2022, MNRAS, 511, 2755
- Rebassa-Mansergas, A., Maldonado, J., Raddi, R., et al. 2021, MNRAS, 505, 3165
- Reid, N. 1993, MNRAS, 265, 785
- Reino, S., de Bruijne, J., Zari, E., d'Antona, F., & Ventura, P. 2018, MNRAS, 477, 3197
- Reipurth, B. & Mikkola, S. 2012, Nature, 492, 221
- Retterer, J. M. & King, I. R. 1982, ApJ, 254, 214
- Reylé, C., Jardine, K., Fouqué, P., et al. 2021, A&A, 650, A201
- Rica, F. M. & Caballero, J. A. 2012, The Observatory, 132, 305
- Riedel, A. R., Blunt, S. C., Lambrides, E. L., et al. 2017, AJ, 153, 95
- Riello, M., De Angeli, F., Evans, D. W., et al. 2018, A&A, 616, A3
- Rizzuto, A. C., Ireland, M. J., & Robertson, J. G. 2011, MNRAS, 416, 3108
- Röser, S., Schilbach, E., Piskunov, A. E., Kharchenko, N. V., & Scholz, R. D. 2011, A&A, 531, A92
- Sarro, L. M., Berihuete, A., Smart, R. L., et al. 2022, arXiv e-prints, arXiv:2211.03641
- Schönfeld, E. 1886, Eds Marcus and Weber's Verlag, 0
- Schweitzer, A., Scholz, R.-D., Stauffer, J., Irwin, M., & McCaughrean, M. J. 1999, A&A, 350, L62
- Sharpless, S. 1959, ApJS, 4, 257
- Shaya, E. J. & Olling, R. P. 2011, ApJS, 192, 2
- Skrutskie, M. F., Cutri, R. M., Stiening, R., et al. 2006, AJ, 131, 1163
- Smart, R. L., Marocco, F., Sarro, L. M., et al. 2019, MNRAS, 485, 4423
- Smolinski, J. & Osborn, W. 2006, in Rev. Mex. Astron. Astrofis. Conf. Ser., Vol. 25, Rev. Mex. Astron. Astrofis. Conf. Ser., ed. C. Abad, A. Bongiovanni, & Y. Guillen, 65–68
- Soubiran, C., Bienaymé, O., Mishenina, T. V., & Kovtyukh, V. V. 2008, A&A, 480, 91
- Stauffer, J., Rebull, L. M., Jardine, M., et al. 2021, AJ, 161, 60
- Stee, P., de Araujo, F. X., Vakili, F., et al. 1995, A&A, 300, 219
- Stock, S., Reffert, S., & Quirrenbach, A. 2018, A&A, 616, A33
- Subasavage, J. P., Henry, T. J., Bergeron, P., Dufour, P., & Hambly, N. C. 2008, AJ, 136, 899
- Tang, S.-Y., Pang, X., Yuan, Z., et al. 2019, ApJ, 877, 12
- Taylor, M. B. 2005, in ASPCS, Vol. 347, Astronomical Data Analysis Software and Systems XIV, ed. P. Shopbell, M. Britton, & R. Ebert, 29
- Taylor, M. B. 2021, Tutorial: Exploring Gaia data with TOPCAT and STILTS, University of Bristol, Bristol UK
- Tokovinin, A. 2008, MNRAS, 389, 925
- Tokovinin, A. 2014, AJ, 147, 87
- Tokovinin, A. 2017, MNRAS, 468, 3461
- Tokovinin, A. 2018, ApJS, 235, 6
- Tokovinin, A. 2021, AJ, 161, 144
- Tokovinin, A. & Lépine, S. 2012, AJ, 144, 102
- Tokovinin, A. A. 1997, A&AS, 124, 75
- Tolbert, C. R. 1964, ApJ, 139, 1105
- Toonen, S., Hollands, M., Gänsicke, B. T., & Boekholt, T. 2017, A&A, 602, A16
- Wasserman, I. & Weinberg, M. D. 1991, ApJ, 382, 149
- Weinberg, M. D., Shapiro, S. L., & Wasserman, I. 1987, ApJ, 312, 367
- Weinberg, M. D. & Wasserman, I. 1988, ApJ, 329, 253
- Wenger, M., Ochsenbein, F., Egret, D., et al. 2000, A&AS, 143, 9
- Wertheimer, J. G. & Laughlin, G. 2006, AJ, 132, 1995
- West, A. A., Morgan, D. P., Bochanski, J. J., et al. 2011, AJ, 141, 97
- White, N. E., Swank, J. H., Holt, S. S., & Parmar, A. N. 1982, ApJ, 263, 277
- Yasuda, N., Mizumoto, Y., Ohishi, M., et al. 2004, in ASPCS, Vol. 314, Astronomical Data Analysis Software and Systems (ADASS) XIII, ed. F. Ochsenbein, M. G. Allen, & D. Egret, 293
- Zapatero Osorio, M. R. & Martín, E. L. 2005, in Rev. Mex. Astron. Astrofis. Conf. Ser., Vol. 24, Rev. Mex. Astron. Astrofis. Conf. Ser., ed. A. M. Hidalgo-Gámez, J. J. González, J. M. Rodríguez Espinosa, & S. Torres-Peimbert, 192–197
- Zorec, J., Frémant, Y., & Cidale, L. 2005, A&A, 441, 235
- Zuckerman, B. & Song, I. 2004, ARA&A, 42, 685
- Zuckerman, B., Song, I., & Webb, R. A. 2001, ApJ, 559, 388

Appendix A: The γ Cas association

Figure A.1 shows the spatial distribution around γ Cas in two panels. The left panel shows the 145 stars in Table B.4 forming a circle area with a radius of 6 degrees. The right panel reduce the radius to about 2 degrees to have only 30 stars including γ Cas. The IC 63 nebula emission, also named the ‘Phantom nebula’, is easily observed in the right panel.

The stars γ Cas and HD 5408, separated by 1274.5 arcsec, constitute the wide pair MAM 20 AD (Mamajek 2017). They actually form a quintuple system, as they are reported to be close double (B0.5 IV + F6 V)¹⁵ and triple (B7 V + B9 V + A1 V) stars, respectively (Morgan et al. 1943; Osterbrock 1957; Christy & Walker 1969; Fekel 1979; Nemravová et al. 2012; Hutter et al. 2021).

With such an early spectral type and an age of only about 8 Ma (Zorec et al. 2005), γ Cas is the ionising source of the nearby ($\rho \sim 1200$ arcsec) reflection nebulae IC 63 (The Ghost of Cassiopeia) and IC 59 (Hubble 1922; Sharpless 1959; Jansen et al. 1994), as well as of an irregular, ~ 3 deg-diameter, H II region (Karr et al. 2005). With a mass of about $19 M_\odot$ and a surrounding disc, it is also the prototype of the γ Cas type of stars (Poeckert & Marlborough 1978; Stee et al. 1995; Nazé et al. 2022).

Our astrometric search for common proper motion and parallax with the criteria in Sect. 3.3 resulted in four additional stars not tabulated by WDS. Of them, only one, namely UCAC4 752–011208 (M4 Ve), had been catalogued in the literature (Nesci et al. 2018). Together with the five components of the γ Cas+HD 5408 system, they made an agglomerate of nine stars of 8 Ma at about 188 pc. Since $19 M_\odot$ -mass stars do not form in isolation (Kroupa 2001; Chabrier 2003; Peña Ramírez et al. 2012), we extended our astrometric search and found additional stars that satisfy our criteria. In particular, we enlarged our search radius centred on γ Cas in consecutive steps and, besides γ Cas and HD 5408, we found 10, 30, 51, 85, 115, and 143 *Gaia* DR3 stars with a 2MASS counterpart, and that satisfy our astrometric criteria, up to 1, 2, 3, 4, 5, and 6 deg, respectively (Fig. A.1). Some of these stars are in turn spectroscopic binaries, so their total number is larger. Most selected stars follow the 10 Ma theoretical isochrones of PARSEC¹⁶ (Bressan et al. 2012, version 1.2S with the default values) at 188 pc in *Gaia*-2MASS colour-magnitude diagrams. Besides, the mass function computed from masses derived from the *J*-band absolute magnitude and PARSEC models do not deviate too much from Salpeter’s. However, we did not find a clustering of stars towards the most massive stars, as it is usually observed in open clusters of similar age (e.g. Caballero 2008). The hypothetical stars of an open cluster or, more likely, a stellar association around γ Cas (Mamajek 2017) overlaps with the extended and also young population of the Cas-Tau OB1 association (Blaauw 1991; de Zeeuw et al. 1999). As a result, additional work is necessary to disentangle the stars that were born together with γ Cas and HD 5408.

¹⁵ BU 499 AC is an optical pair, with “ADS 782 C” at 53 arcsec to γ Cas being a background star.

¹⁶ <http://stev.oapd.inaf.it/cgi-bin/cmd>

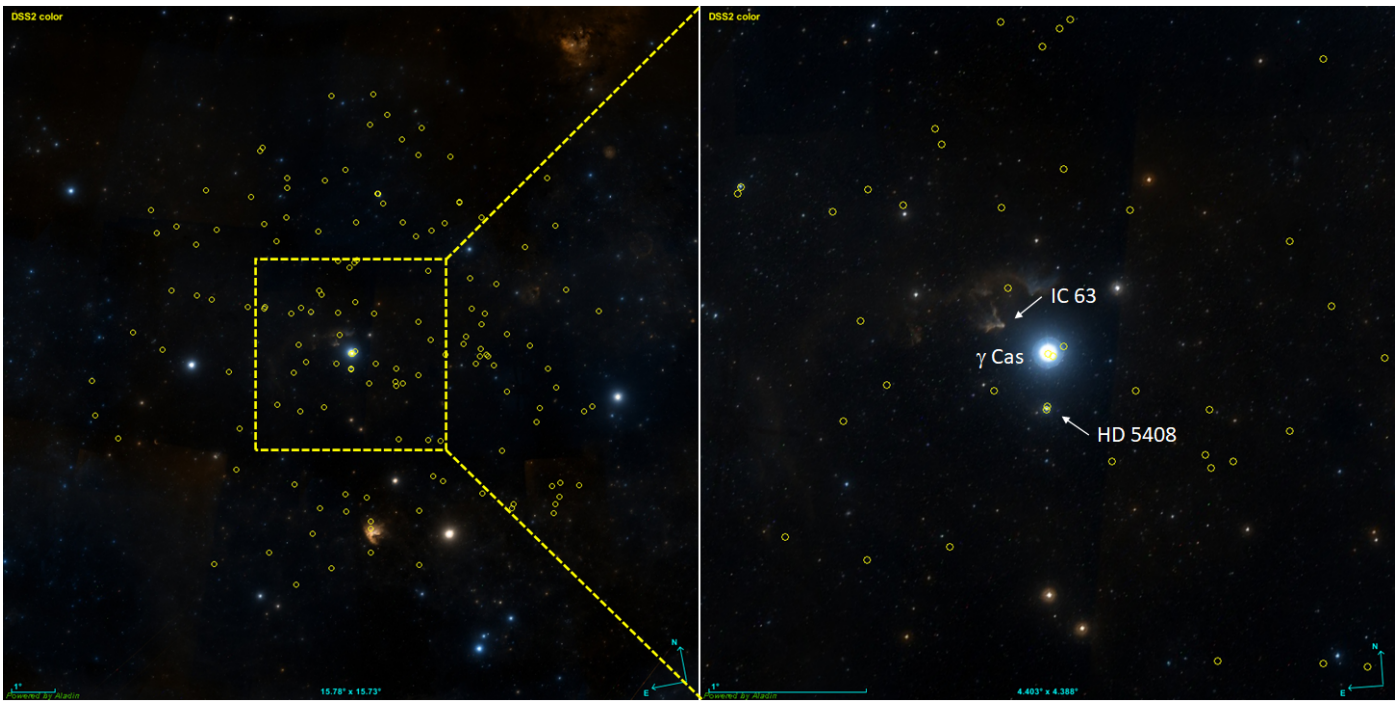


Fig. A.1: Spatial distribution of candidate young stars (open yellow circles) at less than 6 deg (left) and 2 deg (right) to γ Cas. In the right panel we also highlight HD 5408 (the most massive star after γ Cas) and the IC 63 emission nebula. The images were created with the Aladin sky atlas and blue, red, and infrared Digitised Sky Survey data.

Appendix B: Additional tables

Table B.1: Stars in young stellar kinematic groups.

Star	Discoverer code ^a	α (J2000) (hh:mm:ss.ss)	δ (J2000) (dd:mm:ss.s)	G (mag)	Group ^b	Refs. ^c
DENIS J000657.9-643654	...	00:06:57.93	-64:36:54.2	18.2	Tuc-Hor	1, 2
UPM J0014-6003	...	00:14:47.68	-60:03:47.8	12.7	Tuc-Hor	1, 3
UCAC3 52-533	...	00:15:27.52	-64:14:54.8	11.9	Tuc-Hor	1, 3
CD-60 31	...	00:17:30.50	-59:57:04.4	10.6	Tuc-Hor	3
HD 1466	SHY 113 G, SHY 114 G, CVN 33 G	00:18:26.12	-63:28:39.0	7.3	Tuc-Hor	1, 4
2MASS J00182834-6703130	...	00:18:28.33	-67:03:13.0	20.6	Tuc-Hor	2
2MASS J00191296-6226005	...	00:19:12.92	-62:26:00.4	21.0	Tuc-Hor	2
UCAC3 53-724	...	00:21:27.71	-63:51:08.2	14.7	Tuc-Hor	2
Smethells 165	SHY 117 I, CVN 1 A	00:24:08.98	-62:11:04.4	10.7	Tuc-Hor	1, 3
CT Tuc	SHY 113 H, SHY 116 H, SHY 117 H	00:25:14.66	-61:30:48.3	10.7	Tuc-Hor	1, 3, 4
UPM J0027-6157	...	00:27:33.30	-61:57:16.9	13.4	Tuc-Hor	1, 3
UCAC4 137-000438	DAM1269 B	00:30:25.14	-62:36:03.9	13.2	Tuc-Hor	1, 3
UCAC4 137-000439	JNN 296 Aa, DAM1269 A	00:30:25.71	-62:36:01.6	11.1
UPM J0030-6550	...	00:30:57.86	-65:50:06.0	12.9	Tuc-Hor	1, 2, 3
β^{01} Tuc	SHY 114 A, LCL 119 A	00:31:32.67	-62:57:29.6	4.3	Tuc-Hor	1
β^{02} Tuc A	SHY 114 C, LCL 119 C	00:31:33.47	-62:57:56.0	4.6	Tuc-Hor	1
β^{02} Tuc B	...	00:31:33.36	-62:57:55.7	...	Tuc-Hor	1
β^{03} Tuc (AB)	SHY 114 E, SHY 116 E, B 8 Ea-Eb	00:32:43.91	-63:01:53.4	5.1	Tuc-Hor	1
HD 3221	SHY 113 F, SHY 114 F, SHY 116 F, SHY 117 F	00:34:51.20	-61:54:58.1	9.1	Tuc-Hor	1, 3
2MASS J00374306-5846229	...	00:37:43.06	-58:46:22.8	20.5	Tuc-Hor	1, 2
2MASS J00381489-6403529	...	00:38:14.90	-64:03:52.9	19.5	Tuc-Hor	2
2MASS J00394063-6224125	...	00:39:40.63	-62:24:12.5	14.7	Tuc-Hor	1, 2, 3
2MASS J00425349-6117384	...	00:42:53.50	-61:17:38.5	14.6	Tuc-Hor	1, 2, 3
2MASS J00485254-6526330	...	00:48:52.55	-65:26:33.1	13.3	Tuc-Hor	1, 2, 3
UCAC3 53-1665	...	00:49:35.68	-63:47:41.6	11.9	Tuc-Hor	1, 3
2MASS J00514081-5913320	JNN 330 A	00:51:40.82	-59:13:32.1	14.5	Tuc-Hor	1, 2, 3
2MASS J00514561-6227073	...	00:51:45.63	-62:27:07.4	16.4	Tuc-Hor	2
Gaia DR3 426559693524626816	...	00:55:55.21	+60:45:44.5	18.8	γ Cas	5
Gaia DR3 426558563962119808	...	00:56:26.00	+60:41:55.5	12.3	γ Cas	5
γ Cas (AB)	BU 1028 Aa-Ab, MAM 20 A	00:56:42.53	+60:43:00.3	2.1	γ Cas	5
UCAC4 752-011208	...	00:56:44.80	+60:22:46.3	15.4	γ Cas	5
HD 5408(AabB)	MAM 20 D	00:56:46.97	+60:21:46.2	5.5	γ Cas	5
Gaia DR3 426494169508443520	...	00:59:29.60	+60:28:43.0	19.4	γ Cas	5
2MASS J01000219-6156270	...	01:00:02.20	-61:56:27.1	16.9	Tuc-Hor	2
HD 8558	SHY 130 F, CVN 35 A	01:23:21.25	-57:28:50.7	8.4	Tuc-Hor	1, 4
PM J01272-5717	...	01:27:12.13	-57:17:36.6	12.1	AB Dor	2, 6
2MASS J01344601-5707564	...	01:34:46.03	-57:07:56.4	15.6	Tuc-Hor	1, 2, 3
2MASS J01375879-5645447	...	01:37:58.79	-56:45:44.7	13.5	Tuc-Hor	1, 3
HD 10269	SHY 137 D, SHY 130 D,	01:39:07.62	-56:25:45.8	7.0	Tuc-Hor	7

Table B.1: Stars in young stellar kinematic groups (continued).

Star	Discoverer code ^a	α (J2000) (hh:mm:ss.ss)	δ (J2000) (dd:mm:ss.s)	G (mag)	Group ^b	Refs. ^c
	SHY 133 D					
2MASS J01504543-5716488	...	01:50:45.44	-57:16:48.8	15.8	Tuc-Hor	1, 2, 3
2MASS J02030658-5545420	...	02:03:06.59	-55:45:42.0	14.6	AB Dor/Tuc-Hor	1 / 2
HD 12894	SHY 133 C, SHY 143 C, SHY 137 C	02:04:35.11	-54:52:54.0	6.4	Tuc-Hor	1
[FS2003] 0075	...	02:04:53.17	-53:46:16.4	13.6	Tuc-Hor	1, 3
HD 13183	CAB 5 A	02:07:18.06	-53:11:56.5	8.5	Tuc-Hor	1, 4
ϕ Eri	SHY 137 A, DUN 6 A	02:16:30.59	-51:30:43.8	3.6	Tuc-Hor	1, 4
HD 17864	SHY 427 A, HDS 386 Aa	02:50:47.81	-39:55:56.0	6.4	χ^{01} For	1, 4
Gaia DR3 4949158198924393600	...	02:50:50.45	-39:56:10.8	15.7
HD 18184	SHY 427 B	02:53:51.82	-40:11:38.6	8.2
Gaia DR3 4949081507988380800	...	02:53:52.95	-40:11:48.5	15.0
LSPM J0305+1658	WIS 80 B	03:05:38.77	+16:58:34.0	16.5	Hya	8
LP 411-54	WIS 80 A	03:06:26.21	+17:13:29.3	14.0	Hya	9, 10
HD 20379	SHY 439 C, SHY 441 C	03:15:17.11	-37:02:30.1	8.5	χ^{01} For	1, 4
Gaia DR3 4854307557043632768	...	03:16:00.49	-37:29:05.9	16.1	Ale13	11
CD-37 1224	...	03:16:03.07	-37:25:22.3	9.8	χ^{01} For	1, 4
1RXS J031632.0-354142	...	03:16:32.00	-35:41:42.5
HD 20484	SHY 439 Aa, SHY 439 A	03:16:32.70	-35:41:28.3	7.0	χ^{01} For	1, 4
Gaia DR3 5047072423797247488	...	03:18:42.86	-35:38:35.7	16.2	Ale13	11
HD 20707	SHY 441 B, SHY 439 B	03:18:52.95	-36:07:37.5	8.1	χ^{01} For/Ale13	1, 4 / 11
Gaia DR3 5047006006423045376	...	03:18:53.12	-36:07:49.0	15.4	Ale13	11
Gaia DR3 5046898769679409152	...	03:19:01.63	-36:17:15.2	17.3	Ale13	11
CD-37 1263	...	03:22:20.01	-36:38:13.8	9.8	χ^{01} For/Ale13	1, 4 / 11
Gaia DR3 4854797629990991232	...	03:23:06.25	-36:24:13.2	19.2
Gaia DR3 4854562884259914240	...	03:23:48.43	-36:52:38.9	15.1	χ^{01} For	2, 6
HD 21341	SHY 439 D	03:25:12.81	-37:09:09.7	7.2	χ^{01} For/Ale13	1, 4 / 11
Gaia DR3 4854540344270707200	...	03:25:13.21	-37:09:08.5	15.1	Ale13	11
Gaia DR3 4854563983771572736	...	03:25:24.02	-37:06:06.0	14.8	χ^{01} For	2, 6
Gaia DR3 4860585901581589632	...	03:26:18.76	-36:37:06.4	17.6	Ale13	11
Gaia DR3 4854506946605939712	...	03:26:59.81	-37:12:17.5	16.8	Ale13	11
LP 414-30	...	04:00:15.58	+19:24:36.5	14.7	Hya	9, 10
HG 7-80	...	04:02:53.11	+18:24:26.3	13.8	Hya	9, 10
HD 285348B	...	04:03:38.84	+19:27:21.4	14.8	Hya	12
HD 285348(A)	...	04:03:39.04	+19:27:18.0	9.8	Hya	10, 12
LP 414-51	...	04:04:12.81	+18:59:44.6	18.5	Hya	9, 10
HG 7-88	TOK 481 A	04:05:25.67	+19:26:31.7	10.8	Hya	4, 9, 10, 12
LP 414-1100	TOK 481 B	04:06:20.63	+19:01:38.9	14.5	Hya	9, 10
HG 7-120	...	04:11:06.13	+18:55:44.7	14.2	Hya	10, 13
58 Tau	...	04:20:36.31	+15:05:43.6	5.2	Hya	4, 9, 10, 12
LP 475-9	...	04:20:56.07	+14:51:34.5	15.1	Hya	14
Melotte 25 LH 197	...	04:21:35.09	+14:41:42.9	14.3	Hya	9, 10
2MASS J04223052+1513128	...	04:22:30.54	+15:13:12.9	13.4	Hya	9, 10
HD 27691A(Aa-Ab)	STT 82 A, LDS1166 A	04:22:44.17	+15:03:22.0	7.1	Hya	4, 10, 12
HD 27691B	...	04:22:44.15	+15:03:23.2	8.4	Hya	4, 10, 12
LP 415-367	...	04:23:01.51	+15:13:41.6	15.1	Hya	10, 14
LP 415-35	TOK 246 E	04:23:12.48	+15:42:46.4	14.3	Hya	9, 10, 14
63 Tau	...	04:23:25.06	+16:46:38.2	5.6	Hya	4, 9, 10, 12
HD 27771	...	04:23:32.33	+14:40:13.7	8.9	Hya	4, 10, 12
Melotte 25 VR 8	...	04:23:59.14	+16:43:17.7	11.7	Hya	9, 10

Table B.1: Stars in young stellar kinematic groups (continued).

Star	Discoverer code ^a	α (J2000) (hh:mm:ss.ss)	δ (J2000) (dd:mm:ss.s)	G (mag)	Group ^b	Refs. ^c
V895 Tau	HDS 564 A	04:24:12.47	+14:45:29.5	7.5	Hya	4, 10
HD 27848	OCC 615 A	04:24:22.27	+17:04:44.2	6.9	Hya	4, 9, 10, 12
HG 7-200A	TOK 246 A, HDS 566 Aa, GWP 582 A	04:24:48.06	+15:52:29.0	11.3	Hya	10, 12
HG 7-200B	HDS 566 Ab	04:24:48.06	+15:52:29.4	... ^d	Hya	10, 12
HD 285742	...	04:25:00.25	+16:59:05.6	10.0	Hya	9, 10
70 Tau (AB)	FIN 342 Aa-Ab, BUP 57 A	04:25:37.32	+15:56:27.7	6.3	Hya	4, 10, 12
Melotte 25 LH 131	...	04:25:50.45	+15:00:09.2	14.7	Hya	10
HG 7-212	KPP3569 B	04:26:04.71	+15:02:29.0	11.5	Hya	12
LP 475-68 B	KPP3569 A	04:26:04.78	+15:02:27.3	14.8	Hya	7, 12
LDS 2240	LDS2240 A	04:27:06.43	+16:25:47.7	16.5	Hya	10, 14
V993 Tau	...	04:27:35.89	+15:35:21.1	7.3	Hya	4, 9, 10, 12
LP 415-113	...	04:27:40.75	+16:14:55.3	14.3	Hya	10
76 Tau	...	04:28:23.41	+14:44:27.4	5.8	Hya	9, 10, 12
θ^1 Tau (AB)	STFA 10 B	04:28:34.50	+15:57:43.8	3.5	Hya	4, 10, 12
θ^2 Tau (AB)	MKT 13 Aa-Ab, STFA 10 A	04:28:39.74	+15:52:15.1	3.4	Hya	4, 9, 10, 12
V994 Tau B	RAO 547 Aa, BPMA 8 A, RAO 547 A	04:28:50.82	+16:17:18.4	14.8	Hya	10
Melotte 25 VR 19	...	04:29:12.35	+15:16:26.1	11.6	Hya	9, 10
HD 285805	...	04:29:30.98	+16:14:41.2	9.9	Hya	9, 10
80 Tau A	STF 554 A	04:30:08.60	+15:38:16.2	5.6	Hya	4, 10, 12
80 Tau B	STF 554 B	04:30:08.63	+15:38:17.8	7.9	Hya	4, 10, 12
81 Tau (AB)	BUP 62 C, ARN 36 C	04:30:38.89	+15:41:30.8	5.4	Hya	4, 10, 12
2MASS J04311634+1500122	...	04:31:16.37	+15:00:11.9	16.1	Hya	14
Melotte 25 VR 24	GUE 6 A	04:31:43.72	+15:02:27.7	11.5	Hya	15
LP 415-175	WOR 16 M	04:31:44.66	+15:37:49.1	13.4	Hya	13
HG 7-252	WOR 16 F, LDS1174 F	04:31:44.84	+15:37:45.7	11.3	Hya	15
85 Tau	OCC9093 A	04:31:51.76	+15:51:05.8	5.9	Hya	4, 10, 12
HD 285876	TOK 486 K	04:31:52.47	+15:29:58.1	10.5	Hya	4, 9, 10, 12
V996 Tau	CHR 152 A	04:32:50.12	+16:00:21.0	8.7	Hya	10
V997 Tau	TOK 486 F	04:32:59.45	+15:49:08.3	8.5	Hya	7, 10, 12
HD 285931 (AB)	CHR 17 A-B	04:33:58.53	+15:09:49.3	8.3	Hya	4, 10, 12
HD 28977	...	04:34:32.18	+15:49:39.2	9.4	Hya	7, 9, 10, 12
HD 28992	...	04:34:35.31	+15:30:16.6	7.8	Hya	4, 10, 12
Gaia DR3 3237866752286153088	...	05:24:26.32	+06:03:25.8	20.0
2MASS J05243009+0640349	...	05:24:30.10	+06:40:35.0	15.5	32 Ori	4
1RXS J052532.3+062534	...	05:25:32.54	+06:25:33.7	13.4	32 Ori	1, 4, 16
HD 35656	SHY 478 A	05:26:38.83	+06:52:07.2	6.4	32 Ori	4, 16
2MASS J05264073+0712255	...	05:26:40.73	+07:12:25.6	14.8	32 Ori	4
Gaia DR3 3238067069561233920	...	05:26:41.39	+06:53:31.2	18.6
HD 35695	...	05:26:52.03	+06:28:22.8	9.1	32 Ori	1, 16
HD 35714	SHY 478 B	05:27:00.00	+07:10:13.0	7.0	32 Ori	16
2MASS J05270634+0650377	...	05:27:06.35	+06:50:37.7	15.9	32 Ori	4
Gaia DR3 3237987943378820736	...	05:27:28.05	+06:26:43.8	17.8	32 Ori	2, 6
HD 37286	SHY 484 A	05:36:10.30	-28:42:28.8	6.2	Col	1, 4
HD 37484	SHY 484 B	05:37:39.63	-28:37:34.7	7.2	Col	1, 4
2MASS J06595620-6145001	TOK 507 B	06:59:56.18	-61:44:59.8	14.5
HD 53143	TOK 507 A	06:59:59.66	-61:20:10.3	6.6	IC2391	1
HD 62850	SHY 194 C, SHY 197 D	07:42:36.06	-59:17:50.7	7.0	Car-Vela	1
HD 63581	SHY 194 A,	07:46:14.84	-59:48:50.8	7.9	Car-Near	1

Table B.1: Stars in young stellar kinematic groups (continued).

Star	Discoverer code ^a	α (J2000) (hh:mm:ss.ss)	δ (J2000) (dd:mm:ss.s)	G (mag)	Group ^b	Refs. ^c
HD 63608	SHY 197 C, COO 58 A SHY 194 B, COO 58 B	07:46:16.96	-59:48:34.2	8.1	Car-Vela	1
SIPS J0746-5841	...	07:46:41.91	-58:41:03.4	13.6	Car-Near	6
HD 64185 (Aa,Ab)	SHY 197 A, RMU 3 Aa-Ab, HJ 4012 A	07:49:12.94	-60:17:01.4	5.7	Car-Vela	1
HD 70703	SHY 525 B	08:21:00.46	-52:13:40.7	6.6	Car	7
HD 71043	SHY 525 A	08:22:55.16	-52:07:25.4	5.9
UCAC4 121-021394	...	09:23:42.00	-65:56:51.3	14.6	VCA	6
2MASS J09280826-6553589	...	09:28:08.24	-65:53:58.9	16.8	VCA	6
Gaia DR3 5247542633683950208	...	09:28:20.20	-67:02:46.6	15.8
HD 82406	SHY 550 F	09:28:30.54	-66:42:06.7	5.9	VCA	6
2MASS J09312193-6419239	...	09:31:21.92	-64:19:24.0	16.5	VCA	6
2MASS J09313619-6659363	...	09:31:36.20	-66:59:36.3	20.0	VCA	6
UCAC4 120-021739	...	09:31:44.04	-66:00:53.9	15.5	VCA	6
UCAC4 125-022457	SHY 550 B	09:34:55.78	-65:00:07.7	12.3	VCA	6
HD 83359	SHY 550 A, SHY 548 A, SHY 546 A	09:34:56.46	-64:59:58.0	7.9	VCA	6
HD 83523	SHY 548 C, SHY 543 C	09:36:05.18	-64:57:00.9	6.6	VCA	6
HD 83948	SHY 550 E, SHY 548 E	09:38:45.22	-66:51:32.7	7.3	VCA	6
HD 83946	SHY 548 D	09:38:54.10	-64:59:26.7	8.7	VCA	6
TYC 8953-1289-1	...	09:39:10.46	-66:46:15.5	10.7	VCA	6
UCAC4 116-024312	...	09:41:06.83	-66:58:58.4	15.7	VCA	6
UCAC4 060-011194	...	11:34:09.73	-78:00:05.2	13.1	LCC	17
2MASS J11432968-7418377	...	11:43:29.66	-74:18:37.8	14.1	ϵ Cha	2, 6
Gaia DR3 5226681359053691648	...	11:48:42.62	-73:37:23.4	15.0	LCC	17
Gaia DR3 5342275627839946752	...	11:49:02.75	-57:00:13.8	14.3	LCC	17
DZ Cha	...	11:49:31.85	-78:51:01.1	12.0	ϵ Cha	1, 4, 18
Gaia DR3 5342302050480208512	...	11:51:09.22	-56:36:28.6	16.7	LCC	17
Gaia DR3 5343805185945764224	...	11:51:57.24	-56:28:26.8	15.1	LCC	17
UCAC4 168-076644	...	11:52:06.33	-56:30:45.5	13.8	LCC	17
HD 103234	SHY 582 D	11:53:08.01	-56:43:38.1	8.2	LCC	19, 20, 21
Gaia DR3 5343610327564797952	...	11:53:08.58	-56:43:32.4	12.8	LCC	17
Gaia DR3 5343631531836865280	...	11:54:48.68	-56:28:19.6	15.2	LCC	17
Gaia DR3 5343603288130858112	...	11:55:42.91	-56:37:31.1	13.0	Sco-Cen	22
PM J11557-5637	ELP 28 A	11:55:42.99	-56:37:31.6	11.2	Sco-Cen	22
Gaia DR3 5343603180734334592	...	11:55:44.33	-56:38:38.9	11.5	LCC	17
Gaia DR3 5343692279848232832	...	11:57:09.84	-56:01:23.6	14.2	LCC	17
UCAC4 166-080432	...	11:57:30.85	-56:55:15.6	13.9	LCC	17
[FLG2003] ϵ Cha 20	...	11:58:26.81	-77:54:45.3	13.2	ϵ Cha	1, 18
DW Cha	KOH 91 A	11:58:28.16	-77:54:29.5	10.0	ϵ Cha	1, 4, 18
EE Cha	BRC 7 A	11:58:35.24	-77:49:31.5	6.7	ϵ Cha	1, 4, 18
2MASS J11590798-7812322	...	11:59:07.98	-78:12:32.0	15.2	ϵ Cha	1, 18
RX J1159.7-7601	SHY 592 B	11:59:42.27	-76:01:26.2	10.8	ϵ Cha	1, 4, 18
Gaia DR3 5226472073881424384	...	11:59:51.73	-74:41:24.4	17.3
UCAC4 056-012157	...	12:00:01.12	-78:48:29.0	13.7
DX Cha	FGL 2 A, GRY 1 A	12:00:05.09	-78:11:34.6	6.6	ϵ Cha	1, 4, 18
[FLG2003] ϵ Cha 6	FLG 2 D	12:00:08.26	-78:11:39.4	13.0	ϵ Cha	1, 4, 18
[FLG2003] ϵ Cha 7	FGL 2 E	12:00:09.31	-78:11:42.3	12.1	ϵ Cha	1, 4, 18
WISEA J120037.79-784508.3	...	12:00:37.94	-78:45:08.3	16.4
[FLG2003] ϵ Cha 10	...	12:00:55.18	-78:20:29.4	15.6	ϵ Cha	1, 4, 18

Table B.1: Stars in young stellar kinematic groups (continued).

Star	Discoverer code ^a	α (J2000) (hh:mm:ss.ss)	δ (J2000) (dd:mm:ss.s)	G (mag)	Group ^b	Refs. ^c
2MASS J12011981-7859057	...	12:01:19.81	-78:59:05.7	15.2
UCAC4 166-081616	...	12:01:19.88	-56:49:02.6	13.3	UCL/LCC	23
HD 104467	...	12:01:39.11	-78:59:16.9	8.4	ϵ Cha	1, 4, 18
[FLG2003] ϵ Cha 11	...	12:01:43.47	-78:35:47.2	17.1	ϵ Cha	4, 18
[FLG2003] ϵ Cha 8	...	12:01:44.43	-78:19:26.6	15.2	ϵ Cha	1, 4, 18
2MASS J12015251-7818413	...	12:01:52.52	-78:18:41.4	15.0	ϵ Cha	1, 4, 18
RX J1202.1-7853	BRC 8 A	12:02:03.72	-78:53:01.3	11.5	ϵ Cha	1, 4, 18
2MASS J12025461-7718382	...	12:02:54.63	-77:18:38.1	13.4	ϵ Cha	1, 18
Gaia DR3 6075410155651501056	...	12:04:10.91	-56:43:13.2	15.2	LCC	17
Gaia DR3 5837882207728535040	...	12:04:25.16	-76:02:42.2	18.5
2MASS J12043615-7731345	...	12:04:36.14	-77:31:34.7	12.5	ϵ Cha	1, 4, 18
Gaia DR3 6075485777142123136	...	12:05:14.71	-56:13:04.6	14.9	LCC	17
Gaia DR3 5837888190620531072	...	12:05:29.29	-76:00:52.2	17.5	LCC	17
Gaia DR3 6075465543571374336	...	12:05:54.79	-56:23:16.0	15.4	LCC	17
Gaia DR3 6075685995648175872	...	12:06:18.99	-55:54:23.1	12.6	LCC	17
Gaia DR3 6075476607407381888	...	12:06:36.53	-56:12:25.4	14.7	LCC	17
EF Cha	BRC 10 A	12:07:05.52	-78:44:28.0	7.4	ϵ Cha	1, 7, 18
Gaia DR3 6072395810191887616	...	12:07:36.47	-56:46:41.1	17.7	LCC	17
[FLG2003] ϵ Cha 12	...	12:07:45.97	-78:16:06.5	14.5	ϵ Cha	18
Gaia DR3 6075501415129209984	...	12:08:06.90	-56:28:55.4	14.5	LCC	17
Gaia DR3 6075780652415957248	...	12:08:50.93	-55:43:23.0	18.8
Gaia DR3 6075520862741383808	...	12:09:01.31	-56:14:12.5	12.9	LCC	17
HD 105515	SHY 592 A, BRC 11 Aa	12:09:07.69	-78:46:52.7	6.8	ϵ Cha	1, 7, 18
Gaia DR3 5788355123065105920	BRC 11 Ab	12:09:07.93	-78:46:51.4	12.8	ϵ Cha	7, 18
HD 105785	...	12:10:42.07	-56:26:32.4	7.0	LCC	7, 19
Gaia DR3 6072502291012793472	...	12:10:49.69	-56:26:43.3	15.8	LCC	17
HD 105857	...	12:11:05.87	-56:24:04.9	7.3	LCC	17, 19, 20, 21
HD 105963B	STF1608 B	12:11:26.79	+53:25:07.4	8.0
HD 105963(A)	SHY 233 A, STF1608 A	12:11:27.77	+53:25:17.5	7.7
Gaia DR3 6052983932435878656	...	12:11:34.41	-65:30:57.2	13.0	LCC	17
Gaia DR3 6072483530595699840	...	12:11:41.46	-56:35:42.1	14.2
TYC 8986-3110-1	...	12:12:08.05	-65:54:55.0	11.1	LCC / Sco-Cen	4, 17 / 22
Gaia DR3 5860803696599969280	...	12:12:13.13	-65:54:49.2	17.0	LCC	17
UCAC4 059-012851	...	12:12:22.86	-78:22:04.0	14.4
Gaia DR3 6052999669198183168	...	12:12:26.47	-65:20:23.1	12.7	LCC	17
Gaia DR3 6075627824610577536	...	12:12:35.72	-55:23:58.9	16.8	LCC	4, 17
CD-54 4621	...	12:12:35.76	-55:20:27.3	10.2	LCC / Sco-Cen	17, 19 / 22
Gaia DR3 6075816596995760640	...	12:12:36.13	-55:20:02.8	15.5	Sco-Cen	24
Gaia DR3 6075816592695096576	...	12:12:36.21	-55:20:00.3	12.6	LCC	17
Gaia DR3 5860752431909299968	...	12:12:40.99	-66:04:18.7	15.4	LCC	17
UCAC4 054-011484	...	12:14:04.78	-79:13:51.9	14.4
Gaia DR3 5860815550755413376	...	12:14:44.85	-65:41:52.6	16.4
HD 106444	SHY 597 A, SHY 582 A, HJ 4508 A, JNN 169 A	12:14:50.72	-55:47:23.5	8.3	LCC	4, 17, 19, 20, 21
CD-55 4499	SHY 597 B, SHY 582 B, HJ 4508 B	12:14:52.31	-55:47:03.6	9.6	LCC / Sco-Cen	4, 17, 19 / 22
2MASS J12145318-5519494	...	12:14:53.19	-55:19:49.4	20.2
2MASS J12145457-5534052	...	12:14:54.58	-55:34:05.2	11.5	LCC	17
Gaia DR3 6075924830183946240	...	12:15:50.90	-55:39:54.8	15.2	LCC	17
Gaia DR3 6072916532013619712	...	12:16:04.75	-55:51:14.3	16.3	LCC	17
Gaia DR3 5860743975043966464	...	12:16:12.07	-66:01:46.0	15.1	LCC	17
2MASS J12164593-7753333	...	12:16:45.93	-77:53:33.5	12.9	ϵ Cha	1, 4, 18

Table B.1: Stars in young stellar kinematic groups (continued).

Star	Discoverer code ^a	α (J2000) (hh:mm:ss.ss)	δ (J2000) (dd:mm:ss.s)	G (mag)	Group ^b	Refs. ^c
Gaia DR3 6075939948475082880	...	12:16:45.94	-55:29:20.5	13.6	LCC	17
HD 106797	SHY 596 A	12:17:06.31	-65:41:34.7	6.1	LCC	4, 17, 19, 20, 21
HD 106906	SHY 597 C, BYV 1 A	12:17:53.19	-55:58:31.9	7.7	LCC	4, 19, 20, 21
Gaia DR3 6075933969874743680	...	12:17:54.04	-55:27:24.3	14.5	LCC	17
Gaia DR3 5860580633206845568	...	12:18:07.52	-66:00:12.0	14.5	LCC	17
Gaia DR3 6072902547600437888	...	12:18:25.13	-55:58:25.6	15.5	LCC	17
Gaia DR3 5860846745058284672	...	12:19:03.10	-65:25:46.1	19.0
MCC 645	SHY 233 C	12:19:48.06	+52:46:45.0	10.4	AB Dor	1
2MASS J12195355-7420093	...	12:19:53.60	-74:20:09.4	13.2	LCC	17
HD 107301	...	12:20:28.22	-65:50:33.6	6.2	LCC	17, 19, 20
2MASS J12203619-7353027	...	12:20:36.19	-73:53:02.8	13.1	ϵ Cha / LCC	2, 6 / 17
Gaia DR3 6072865885757810048	...	12:20:45.02	-55:57:23.9	15.2
1RXS J122053.2-653418	...	12:20:55.87	-65:34:36.5	12.2	LCC / Sco-Cen	17 / 22
Gaia DR3 5860519953903225728	...	12:21:40.79	-66:06:59.2	12.5	LCC	17
Gaia DR3 5860949137043373568	...	12:23:45.81	-65:50:28.2	11.9	LCC	17
Gaia DR3 5860897842313432576	...	12:24:21.27	-65:57:07.8	13.8	LCC	17
Gaia DR3 5860899560245289472	...	12:25:04.91	-65:59:42.0	16.0	LCC	17
Gaia DR3 5860899384145151616	...	12:25:57.04	-65:57:15.6	17.9
Gaia DR3 5860886228720919936	...	12:26:09.66	-66:01:52.8	13.3	LCC	17
NO UMa	SHY 236 E, SHY 246 F, SHY 248 G, BAG 50 A	12:31:18.92	+55:07:08.3	7.8	UMa	1, 25
RX J1231.9-7848	...	12:31:56.08	-78:48:32.5	13.1	ϵ Cha	26
DO CVn	SHY 236 B, SHY 64 B, SHY 248 H	12:35:51.29	+51:13:17.3	8.3	UMa	1, 25
Gaia DR3 5788500121160692480	...	12:37:02.46	-78:08:25.7	19.0
HD 110463	SHY 64 A, SHY 236 A	12:41:44.52	+55:43:28.8	8.0	UMa	1
RX J1241.7+5645	BWL 33 A	12:41:47.37	+56:45:13.7	12.3	UMa	1, 25
Sand 125	...	12:43:06.59	+24:15:17.2	15.1	CBer	1, 27
UCAC4 575-048616	...	12:44:30.00	+24:56:02.7	13.8	CBer	6, 27
SDSS J124431.58+254720.9	...	12:44:31.58	+25:47:20.9	18.4	CBer	6, 27
2MASS J12464254+2524004	...	12:46:42.54	+25:24:00.3	17.1	CBer	1, 27
HD 111154	SHY 612 A	12:47:06.73	+22:37:00.6	8.3	CBer	4, 27
SDSS J124722.67+244548.6	...	12:47:22.68	+24:45:48.6	19.2	CBer	6
StM 174	...	12:48:34.51	+49:33:54.1	11.3
NGP 26 151	...	12:49:00.42	+25:21:35.6	11.6	CBer	6, 27
UCAC4 586-049030	...	12:49:24.19	+27:09:58.0	12.4	CBer	6, 27
Gaia DR3 3942331514424144256	...	12:50:41.70	+20:32:13.6	17.3
BD+21 2462A	TOK 561 A, HU 640 A	12:50:41.86	+20:32:05.5	... ^d	IC2391	1
BD+21 2462B	HU 640 B	12:50:41.87	+20:32:04.9	... ^d
Gaia DR3 3954790802231914496	...	12:51:26.80	+21:32:43.6	17.4	CBer	6, 27
Sand 154	TOK 561 C	12:51:51.60	+20:22:52.1	13.4
HD 111878	SHY 612 B	12:52:11.62	+25:22:24.6	8.7	CBer	1, 27
Gaia DR3 3956537616971055360	...	12:55:55.39	+22:55:12.7	17.4	CBer	6, 27
Gaia DR3 3958585461673131520	...	12:57:48.62	+26:39:36.7	15.3	CBer	6, 27
Sand 174	...	12:57:56.56	+24:49:18.1	14.6	CBer	6, 27
Gaia DR3 3958248976756278272	...	12:59:03.09	+25:31:07.7	16.5	CBer	6, 27
78 UMa A	BU 1082 A	13:00:43.68	+56:21:59.0	4.9	UMa	1, 4
78 UMa B	BU 1082 B	13:00:43.76	+56:21:59.3	4.9	UMa	1, 4
HD 115043	SHY 246 A, MET 62 A, STTA122 A	13:13:37.01	+56:42:29.8	6.7	UMa	1, 7, 25

Table B.1: Stars in young stellar kinematic groups (continued).

Star	Discoverer code ^a	α (J2000) (hh:mm:ss.ss)	δ (J2000) (dd:mm:ss.s)	G (mag)	Group ^b	Refs. ^c
Gaia DR3 1449325173458893952	...	13:22:10.97	+27:08:31.8	16.5
HD 238224(AB)	SHY 246 E, SHY 247 F, SHY 67 A, HDS1879 Aa-Ab	13:23:23.27	+57:54:21.8	9.1	UMa	1
ζ^{01} UMa (AB)	SHY 247 A, SMR 4 A, STF1744 A, PEA 1 Aa-Ab	13:23:55.54	+54:55:31.3	2.3	UMa	1, 4
ζ^{02} UMa (AB)	STF1744 B	13:23:56.32	+54:55:18.5	3.9	UMa	1, 4
HD 116706	SHY 620 A	13:25:06.68	+23:51:15.9	5.7	CBer	27
g UMa	PSF 1 Ca, SHY 248 C, STF1744 C	13:25:13.54	+54:59:16.7	4.0	UMa	1, 4
BD+26 2461	SHY 620 B BRT 161 A	13:25:39.37	+25:40:55.9	9.0	CBer	27
Gaia DR3 1448560291323299840	...	13:33:31.80	+26:35:30.7	15.2	CBer	27
UPM J1344+5528	...	13:44:57.88	+55:28:21.9	13.9
HD 125019	SHY 645 A	14:15:17.00	+52:32:09.3	6.6	G-X	28
HD 234120A	A 1616 A	14:16:01.14	+52:47:10.7	10.0	G-X	28
HD 234120B	A 1616 B	14:16:01.32	+52:47:10.8	10.3	G-X	28
HD 125557	SHY 645 B	14:18:31.15	+52:02:00.0	6.9	G-X	28
UCAC4 709-052641	...	14:20:32.24	+51:40:11.7	13.8	G-X	28
UCAC4 709-052647	...	14:20:51.44	+51:37:52.2	12.3	G-X	28
KU Lib	CAB 1 D	14:40:31.11	-16:12:33.5	7.1	Castor	1
α^{01} Lib(AB)	ALP 30 A, BEU 19 Ba-Bb, AOT 53 B	14:50:41.17	-15:59:50.0	... ^d	Castor	1
α^{02} Lib(AB)	DSG 17 Aa-Ab, SHJ 186 A, AOT 53 A, CAB 1 A	14:50:52.71	-16:02:30.4	... ^d	Castor	1
TYC 3867-942-2	STF1898 B	14:56:29.39	+59:22:45.4	9.8	G-X	28
HD 132422	SHY 661 A, STF1898 A	14:56:29.61	+59:22:47.7	8.1	G-X	28
2MASS J14584091+5953017	...	14:58:40.94	+59:53:01.6	18.6
[EOK2015] 3 1	...	14:59:07.01	+59:31:12.9	11.9	G-X	28
HD 238423	...	15:03:16.86	+59:00:41.5	9.3	G-X	28
HD 133909	SHY 661 C	15:04:17.61	+59:32:06.2	7.4	G-X	28
Gaia DR3 1614153099017986560	...	15:04:22.64	+58:52:35.9	15.5	G-X	28
BD+60 1587	...	15:04:25.75	+59:52:50.8	9.5	G-X	28
HD 140665B	ROE 75 B	15:44:21.57	+15:18:04.2	10.1
HD 140665A	SHY 281 D, ROE 75 A	15:44:21.80	+15:17:59.0	8.0
β Ser B	STF1970 B	15:46:09.16	+15:25:15.3	9.6	UMa	1
β Ser(A)	SHY 281 A, STF1970 A	15:46:11.25	+15:25:18.6	3.7	UMa	1
AT Mic A	LDS 720 B	20:41:51.13	-32:26:06.7	9.6	β Pic	1, 2
AT Mic B	LDS 720 C	20:41:51.16	-32:26:10.2	9.6	β Pic	1, 2
AU Mic	LDS 720 A	20:45:09.53	-31:20:27.2	7.8	β Pic	1
2MASS J21163528-6005124	...	21:16:35.29	-60:05:12.4	13.1	Tuc-Hor	1, 3
2MASS J21370885-6036054	...	21:37:08.84	-60:36:05.5	12.4	Tuc-Hor	1, 3
2MASS J21380269-5744583	...	21:38:02.69	-57:44:58.4	13.9	Tuc-Hor	1, 3
Smethells 86	SHY 348 E	21:44:30.12	-60:58:38.9	10.9	Tuc-Hor	1, 3
2MASS J21490499-6413039	...	21:49:04.99	-64:13:03.9	13.6	Tuc-Hor	1, 2, 3
HD 207377(AB)	HDS3109 A-B	21:50:23.79	-58:18:18.2	7.7
2MASS J21503526-5818010	...	21:50:35.27	-58:18:01.0	16.4

Table B.1: Stars in young stellar kinematic groups (continued).

Star	Discoverer code ^a	α (J2000) (hh:mm:ss.ss)	δ (J2000) (dd:mm:ss.s)	G (mag)	Group ^b	Refs. ^c
HD 207575	SHY 347 D, CVN 31 D	21:52:09.72	-62:03:08.5	7.1	Tuc-Hor	1
HD 207964(AB)	SHY 348 A, HDO 296 A-B, CVN 31 A	21:55:11.39	-61:53:11.8	5.8	Tuc-Hor	1
HD 207964C	...	21:55:11.73	-61:53:17.8	15.2	Tuc-Hor	1
BPS CS 22956-0074	...	22:02:54.50	-64:40:44.2	11.6	Tuc-Hor	1, 3
UPM J2222-6303	...	22:22:39.69	-63:03:25.8	13.2	Tuc-Hor	1, 3
α PsA C	MAM 1 C	22:48:04.50	-24:22:07.7	11.1	Castor	1
TW PsA	SHY 106 B	22:56:24.05	-31:33:56.0	6.1	Castor	1
α PsA (AB)	SHY 106 A, MAM 1 A	22:57:39.05	-29:37:20.1	... ^d	Castor	1
UCAC4 124-178085	...	23:47:46.96	-65:17:24.8	11.5	Tuc-Hor	1, 3
2MASS J23515597-6447345	...	23:51:55.97	-64:47:34.6	13.9	Tuc-Hor	2
η Tuc	EHR 22 A	23:57:35.08	-64:17:53.6	5.0	Tuc-Hor	1

Notes. ^(a) Marked with ‘...’ are new young star candidates. ^(b) 32 Ori: 32 Orionis; AB Dor: AB Doradus; Ale13: Alessi 13; β Pic: β Pictoris; Car: Carina; Car-Near: Carina-Near; Car-Vela: Carina-Vela; γ Cas: γ Cassiopeia; Castor: Castor (α Geminorum); CBer: Coma Berenice; χ^{01} For: χ^{01} Fornacis; Col: Columba; ϵ Cha: ϵ Chamaelontis; G-X: [TPY2019] Group-X; Hya: Hyades; IC2391: IC2391 Supercluster; LCC: Lower Centarus Crux; SCO: Scorpio-Centaurus; Tuc-Hor: Tucana-Horologium; UCL: Upper Centaurus-Lupus; UMa: Ursa Major; VCA: Volans-Carina. ^(c) 1. Riedel et al. (2017); 2. Gagné et al. (2015); 3. Kraus et al. (2014); 4. Gagné et al. (2018a); 5. This work; 6. Gagné & Faherty (2018); 7. Gagné et al. (2018b); 8. Freund et al. (2020); 9. Kopytova et al. (2016); 10. Röser et al. (2011); 11. Cantat-Gaudin et al. (2018); 12. Reino et al. (2018); 13. Reid (1993); 14. Bouvier et al. (2008); 15. Guenther et al. (2005); 16. Bell et al. (2017); 17. Goldman et al. (2018); 18. Murphy et al. (2013); 19. Hoogerwerf (2000); 20. de Zeeuw et al. (1999); 21. Rizzuto et al. (2011); 22. Pecaut & Mamajek (2016); 23. Stauffer et al. (2021); 24. Bohn et al. (2022); 25. Dopcke et al. (2019); 26. Dzib et al. (2018); 27. Fürnkranz et al. (2019); 28. Tang et al. (2019). ^(d) Not available in *Gaia*.

Table B.2: Basic data of the 94 galactic field systems.

WDS	Discoverer code	Star	α (J2000) (hh:mm:ss.ss)	δ (J2000) (dd:mm:ss.s)	d (pc)	G^a (mag)
<i>Double systems</i>						
00016–0102		2MASS J00013688-0101441	00:01:36.89	−01:01:44.2	60.33±0.13	15.2
	WIS 1	SIPS J0000-0112	00:00:35.39	−01:12:46.3	65.41±0.64	17.3
01005–1923		HD 5911	01:00:28.01	−19:23:21.8	81.63±0.17	7.9
	SHY 392	HD 6103	01:02:06.90	−19:40:10.8	81.59±0.16	8.1
01066+1353		HD 6566	01:06:36.52	+13:53:04.6	58.08±0.10	7.1
	SHY 396	HD 5433 ^b	00:56:13.48	+15:39:22.2	63.44±0.43	8.5
01134–3932		HD 7382	01:13:26.52	−39:32:24.3	59.18±0.11	7.2
	SHY 397	HD 7052	01:10:16.94	−40:37:21.9	59.80±0.05	9.4
01326–4944		HD 9544	01:32:36.37	−49:43:39.8	81.15±0.13	6.2
	SHY 405	HD 9378	01:31:16.52	−49:54:14.4	81.36±0.12	7.3
02022–4550		HD 12586	02:02:10.73	−45:50:08.0	71.23±0.09	7.6
	SHY 410	HD 12808	02:04:24.58	−43:30:27.7	64.07±0.08	7.7
02025–3849		2MASS J02022892-3849021 ^c	02:02:28.94	−38:49:01.9	59.46±2.29	14.3
	WIS 48	2MASS J02004917-3848535	02:00:49.17	−38:48:53.6	66.47±0.93	19.1
02310+0823		G 4-24	02:31:03.28	+08:22:55.2	36.01±0.02	10.3
	GIC 32	G 73-59 ^c	02:27:36.67	+08:29:59.1	33.83±0.36	14.3
05444–0528		HD 38273	05:44:25.46	−05:27:53.1	86.62±0.17	7.9
	SHY 489	HD 37546	05:39:05.53	−05:53:51.1	88.57±0.19	8.2
07069+5511		HD 53075	07:06:53.34	+55:11:22.0	57.43±0.09	8.2
	TOK 508	[SLS2012] PYC J07067+5537	07:06:43.35	+55:37:47.2	66.03±0.06	13.4
07113+3307		HD 54717	07:11:19.48	+33:06:42.7	44.80±0.06	7.1
	SHY 190	HD 54718	07:11:14.72	+32:36:54.1	44.64±0.06	7.9
07160+5759		NLTT 17578 ^b	07:15:56.73	+57:59:49.4	108.6±0.2	9.9
	TOK 510	LSPM J0716+5827	07:16:39.39	+58:27:27.7	123.4±2.6	18.2
07329–5249		2MASS J07325350-5249077	07:32:53.51	−52:49:07.6	131.9±0.2	12.7
	WIS 141	2MASS J07325706-5229111	07:32:57.07	−52:29:11.2	143.5±1.4	17.4
08237–5519		HD 71257	08:23:42.41	−55:19:13.9	75.84±0.10	7.4
	SHY 526	HD 72143 ^b	08:28:39.55	−55:58:01.5	74.94±0.08	9.4
08388–1315		HD 73583	08:38:45.26	−13:15:24.1	31.59±0.02	9.3
	SHY 201	BD-09 2535	08:29:40.45	−09:58:35.1	35.21±0.02	9.8
08480–3115		HD 75514 ^{b,c}	08:49:27.20	−30:56:01.9	79.28±1.46	7.7
	SHY 529	HD 75269 ^b	08:47:59.48	−31:14:34.1	77.14±0.14	8.6
09467+1632		BD+17 2130 ^b	09:46:39.61	+16:31:54.7	68.37±0.40	10.0
	TOK 531	LP 428-36	09:45:00.18	+16:19:35.9	65.28±0.40	14.7
09568+0415		HD 86147	09:56:48.61	+04:14:31.5	45.72±0.07	6.6
	TOK 533	LSPM J0956+0441 ^c	09:56:45.72	+04:41:30.1	45.42±1.16	11.9
10532–3006		HD 94375 ^b	10:53:14.68	−30:05:47.1	82.17±0.16	7.9
	SHY 563	HD 94542 ^b	10:54:16.98	−34:57:50.0	84.57±0.14	8.5
11214+0638		HD 98697	11:21:26.79	+06:38:05.8	48.64±0.07	6.6
	TOK 544	LP 552-34	11:20:10.55	+06:38:34.1	53.75±0.16	14.4
11265+2031		HD 99419	11:26:27.19	+20:31:05.2	46.19±0.06	7.8
	TOK 546	Gaia DR3 3978588911076420736	11:28:23.30	+20:41:03.8	50.22±0.06	14.1
11455+4740		HD 102158	11:45:30.51	+47:40:00.8	51.19±0.05	7.9
	LEP 45	G 122-46	11:47:21.61	+47:45:56.5	45.79±0.03	13.2
12213–5012		HD 107440 ^b	12:21:15.07	−50:11:39.2	96.85±0.44	8.9
	TOK 556	HD 107735 ^b	12:22:59.17	−50:00:45.0	98.89±0.51	9.2
13305+2231		HD 117528	13:30:30.78	+22:30:47.1	84.22±0.12	8.5
	SHY 626	BD+22 2587	13:30:18.99	+21:30:00.9	87.44±0.13	9.8
15031–4618		CD-45 9610	15:03:03.57	−46:17:37.8	27.18±0.01	9.4
	WIS 280	L 334-33	15:04:12.46	−46:29:46.1	27.28±0.02	11.8

Table B.2: Basic data of the 94 galactic field systems (continued).

WDS	Discoverer code	Star	α (J2000) (hh:mm:ss.ss)	δ (J2000) (dd:mm:ss.s)	d (pc)	G^a (mag)
15120+0245	WIS 281	LP 562-9	15:11:58.38	+02:44:32.0	63.01 ± 0.07	13.6
		LP 562-10	15:11:59.87	+03:03:27.3	66.91 ± 0.17	15.6
15208+3129	LEP 74	HD 136654	15:20:50.08	+31:28:48.4	45.75 ± 0.03	6.8
		AX CrB	15:19:40.14	+31:50:33.0	45.52 ± 0.03	8.8
15226+3953	WIS 284	G 179-28	15:22:38.03	+39:53:14.4	115.6 ± 0.2	10.5
		LP 222-69	15:21:14.01	+39:47:06.0	110.6 ± 0.5	16.4
15356+7726	WIS 288	LSPM J1535+7725	15:35:28.14	+77:25:41.0	68.18 ± 0.05	9.9
		LP 22-358	15:31:33.41	+77:39:34.7	70.00 ± 0.05	11.1
15408-3252	SHY 278	HD 139696 ^{b,c}	15:40:45.26	-32:51:59.5	30.30 ± 0.36	8.5
		CD-32 10820	15:28:31.39	-33:08:06.3	30.94 ± 0.05	10.2
15488+4929	WIS 295	LSPM J1548+4928	15:48:48.07	+49:28:35.8	76.81 ± 0.63	17.8
		LSPM J1550+4921	15:50:31.76	+49:21:05.2	71.14 ± 0.47	18.0
15590+1820	SHY 691	HD 143292 ^b	15:59:01.82	+18:19:33.2	70.78 ± 0.11	7.7
		HD 142899	15:56:22.76	+20:25:07.5	80.97 ± 0.17	8.3
17127+3235	WIS 313	BD+32 2868	17:12:39.82	+32:35:22.8	70.36 ± 0.40	9.4
		LSPM J1711+3236	17:11:17.17	+32:36:20.1	61.00 ± 0.09	15.5
17166+0325	SHY 715	HD 156287 ^b	17:16:36.95	+03:24:30.4	82.15 ± 0.17	8.2
		HD 159243	17:33:21.55	+05:42:02.6	73.29 ± 0.11	8.5
18496+1313	SHY 309	HD 229635	18:49:38.34	+13:13:07.0	37.76 ± 0.02	8.4
		HD 229830	18:52:29.36	+11:12:36.5	38.39 ± 0.02	9.8
18571+5143	SHY 749	HD 176341	18:57:04.94	+51:43:15.5	83.71 ± 0.12	7.8
		BD+49 2879	18:50:39.84	+49:46:03.1	87.39 ± 0.09	8.6
18597+1615	TOK 622	HD 176441 ^b	18:59:42.53	+16:15:09.3	45.24 ± 0.05	7.0
		LSPM J1858+1613 ^c	18:58:14.90	+16:13:54.8	44.65 ± 0.52	11.7
19290-4952	SHY 319	HD 182857	19:29:02.85	-49:52:31.5	41.43 ± 0.03	8.7
		HD 185112 ^b	19:39:45.84	-48:11:36.0	45.21 ± 0.08	8.8
20080-0041	SHY 325	64 Aql	20:08:01.82	-00:40:41.5	46.43 ± 0.09	5.7
		HD 190873	20:07:09.17	-00:52:27.3	46.65 ± 0.05	8.1
20124-1237	TDT2085	ξ Cap	20:12:25.87	-12:37:03.0	28.23 ± 0.03	5.7
		LP 754-50	20:12:09.45	-12:53:35.4	28.22 ± 0.01	10.6
20371+6122	SHY 780	HD 196903	20:37:07.93	+61:21:52.5	57.19 ± 0.05	6.9
		HD 198662	20:48:57.32	+61:07:07.5	65.06 ± 0.07	7.8
20404-3251	SHY 781	HD 196746 ^b	20:40:25.75	-32:51:06.1	87.46 ± 0.40	8.3
		HD 196189	20:36:45.00	-32:12:25.7	91.83 ± 0.17	8.9
21009-4132	WIS 346	L 424-30	21:00:54.94	-41:31:44.0	18.74 ± 0.01	12.4
		APMPM J2101-4125	21:01:03.82	-41:14:33.3	18.77 ± 0.01	13.0
21066+8048	TOK 632	G 261-37	21:06:38.34	+80:47:36.8	34.61 ± 0.02	10.4
		G 261-40	21:13:48.18	+81:00:25.0	34.46 ± 0.02	12.1
21105+2227	SHY 793	HD 201670 ^d	21:10:30.94	+22:27:25.6	113.8 ± 1.0	7.7
		HD 198759	20:51:49.87	+21:52:07.2	107.9 ± 0.2	8.1
21190+2614	TOK 634	HD 203030	21:18:58.22	+26:13:50.0	39.28 ± 0.03	8.3
		Gaia DR3 1846992067932879744	21:20:02.85	+26:37:04.7	44.52 ± 0.05	14.7
22175+2335	GIC 179	G 127-13 ^c	22:17:25.87	+23:35:04.6	44.63 ± 0.37	12.7
		G 127-14	22:17:59.54	+24:09:20.2	47.26 ± 0.06	12.9
22378-0414	TOK 640	κ Aqr	22:37:45.38	-04:13:41.0	67.96 ± 0.46	4.7
		Gaia DR3 2624935581540867200	22:36:30.00	-04:21:34.7	75.46 ± 0.30	16.1
<i>Triple systems</i>						
02062-4726	NSN 219 WIS 52	CD-48 554(A)	02:06:14.44	-47:25:30.7	90.12 ± 0.14	10.9
		CD-48 554B	02:06:14.37	-47:25:32.5	91.16 ± 0.30	13.6
		LEHPM 2187	02:06:37.55	-47:06:59.7	80.81 ± 0.47	15.4

Table B.2: Basic data of the 94 galactic field systems (continued).

WDS	Discoverer code	Star	α (J2000) (hh:mm:ss.ss)	δ (J2000) (dd:mm:ss.s)	d (pc)	G^a (mag)
04346–3539	TOK 488	HD 29231	04:34:38.50	−35:39:29.0	28.13±0.01	7.4
	WIS 108	L 447-2	04:36:28.87	−35:54:52.8	30.31±0.01	12.2
		UCAC3 109-11370 ^c	04:35:41.32	−35:54:54.1	31.17±0.37	13.4
06536–3956		L 454-11 ^c	06:58:18.90	−39:32:15.5	24.96±0.11	12.0
	SUB 2	WT 202	06:53:35.34	−39:55:33.3	24.84±0.01	15.4
	SUB 2	WT 201	06:53:30.21	−39:54:29.1	24.79±0.02	15.9
07166–2319		HD 56578 ^b	07:16:38.36	−23:18:39.4	106.3±0.5	5.9
	SHY 508	HD 57527 ^b	07:20:32.54	−26:42:01.0	90.85±0.28	6.7
	...	Gaia DR3 5613164850183516544	07:23:41.97	−26:09:27.4	90.35±0.20	15.0
08211+4021		BD+40 2030 ^b	08:21:08.34	+40:20:52.7	60.62±0.08	8.9
	TOK 516	G 111-70	08:19:16.81	+40:37:39.5	52.59±0.05	10.8
	...	Gaia DR3 914608342177083648	08:21:08.20	+40:20:51.0	61.83±0.60	13.8
09150+3837		HD 79392 ^b	09:14:57.85	+38:36:33.5	54.20±0.07	6.7
	TOK 525	Gaia DR3 812086579467748736	09:13:39.31	+38:28:14.5	54.03±0.05	13.6
	DAM1575	Gaia DR3 812109085097488768	09:14:58.95	+38:36:58.3	54.52±0.14	16.2
09487–2625		HD 85043A ^b	09:48:42.84	−26:24:52.0	41.40±0.04	6.6
	I 205	HD 85043B ^b	09:48:42.72	−26:24:51.2	41.28±0.07	10.0 ^f
	TOK 532	PM J09486-2644	09:48:41.42	−26:44:08.5	41.32±0.03	11.2
10289+3453		HD 90681	10:28:51.39	+34:53:08.4	49.13±0.06	7.7
	SHY 215	HD 92194	10:39:07.82	+32:49:59.6	50.64±0.06	8.5
	...	Gaia DR3 749786356557791744	10:28:50.90	+34:52:56.2	45.69±1.08	19.6
11513+4516		Ross 916A	11:51:18.97	+45:16:12.9	29.66±0.03	12.3
	KPP3247	Ross 916B	11:51:18.83	+45:16:13.1	29.63±0.03	12.4
	WIS 193	G 176-59	11:50:48.98	+45:34:02.6	29.60±0.02	14.0
12416+1026		27 Vir	12:41:34.39	+10:25:34.6	71.65±0.18	6.2
	SHY 610	HD 111069 ^b	12:46:34.18	+11:22:42.6	65.33±0.10	8.5
	...	Gaia DR3 3927438805519604352	12:41:37.10	+10:25:43.6	71.36±0.36	16.1
13470+3833		HD 120164	13:46:59.77	+38:32:33.7	91.69±0.43	5.2
	SHY 633	HD 119767	13:44:20.30	+38:47:51.8	94.73±0.15	8.7
	S 654	BD+39 2679	13:46:54.65	+38:31:55.1	91.51±0.12	8.9
13496+1301	...	HD 120510(Aab)	13:49:36.06	+13:00:37.1	56.44±0.08	6.6
	SHY 635	HD 120865	13:51:51.00	+11:56:13.9	58.35±0.09	6.8
14153+0308		HD 124757A ^b	14:15:19.39	+03:07:52.9	41.27±0.13	7.6
	STF1819	HD 124757B	14:15:19.36	+03:07:52.2	41.27±0.13	7.7
	SHY 261	HD 126961	14:28:31.14	+02:47:19.8	39.70±0.04	6.9
14190–0636		ι Vir ^b	14:16:00.87	−06:00:02.0	22.03±0.14	3.9
	SHY 71/HDS2016	HD 125354(Aab) ^b	14:18:58.27	−06:36:19.9	22.53±0.39	8.6
14396–6050		α Cen A ^g	14:39:36.49	−60:50:02.4	1.346±0.002 ^h	−0.2 ⁱ
	RHD 1	α Cen B ^g	14:39:35.06	−60:50:15.1	1.346±0.002 ^h	0.8 ⁱ
	LDS 494	Proxima Centauri	14:29:42.95	−62:40:46.2	~1.30	9.0
15318–0204		HD 138370	15:31:48.92	−02:03:59.2	76.03±0.11	8.3
	SHY 677	HD 138159	15:30:25.18	−01:19:07.7	67.38±0.07	9.0
	...	Gaia DR3 4416092627948054400	15:30:41.60	−01:20:03.6	67.47±0.30	16.3
17415+4924		Wolf 1378 ^c	17:41:27.96	+49:24:05.6	127.0±2.0	11.4
	WIS 321	LSPM J1741+4941	17:41:02.02	+49:41:34.2	123.5±0.5	16.2
	...	Gaia DR3 1367008242580377216	17:41:27.65	+49:24:08.7	127.8±1.6	17.8
19235–6924		HD 180808(A) ^b	19:23:31.21	−69:24:26.7	59.07±0.07	7.7
	DON 957	HD 180808B	19:23:30.70	−69:24:27.7	59.21±0.10	11.7
	SHY 755	HD 181958 ^b	19:28:06.43	−69:37:54.6	58.59±0.31	6.6
19476+0105	ENG 67	HD 187003(Aab) ^b	19:47:33.32	+01:05:20.0	46.79±0.05	6.6
	SHY 322	BD+00 4221	19:29:26.34	+00:31:41.3	43.95±0.03	10.2
20084+1503		G 143-33	20:08:22.02	+15:02:34.2	324.4±2.1	11.4

Table B.2: Basic data of the 94 galactic field systems (continued).

WDS	Discoverer code	Star	α (J2000) (hh:mm:ss.ss)	δ (J2000) (dd:mm:ss.s)	d (pc)	G^a (mag)
21096–1122	LDS1033	G 143-27(Aab)	20:05:51.02	+15:01:59.3	333.9±2.8	12.8
		ν Aqr	21:09:35.65	-11:22:18.1	49.79±0.28	4.3
	TOK 633	Gaia DR3 6895305771635806208	21:08:43.51	-11:10:15.7	49.59±0.06	13.0
	...	Gaia DR3 6895305771635806464 ^d	21:08:43.59	-11:10:12.4	49.52±0.08	15.1
22596–1246	...	HD 217250(Aab)	22:59:34.08	-12:45:38.1	64.12±0.07	9.5
	TOK 642	Gaia DR3 2603671950077707776	22:58:01.65	-12:48:45.7	70.50±0.63	17.9
23328–1651		HD 221503	23:32:49.40	-16:50:44.3	14.55±0.01	8.1
23506+5412	SHY 110/...	G 273-59(Aab) ^b	23:30:13.44	-20:23:27.5	15.91±0.02	9.9
		HD 223582 ^b	23:50:37.98	+54:11:53.6	54.80±0.06	7.1
	SHY 840	HD 223788	23:52:39.67	+54:16:07.8	54.65±0.05	7.5
	ES 700	BD+53 3238B	23:50:38.93	+54:12:05.6	54.94±0.04	11.0
<i>Quadruple systems</i>						
01024+0504		HD 6101A ^b	01:02:24.56	+05:03:41.2	22.49±0.07	8.5 ⁱ
	HDS 135	HD 6101B ^b	01:02:24.59	+05:03:41.5	22.49±0.07	10.1 ⁱ
	WNO 50	EGGR 7(Cab)	01:03:49.92	+05:04:30.6	22.02±0.04	13.9
02462+0536		HD 17250	02:46:14.61	+05:35:33.3	57.04±0.08	7.8
	TOK 651	HD 17163	02:45:20.91	+04:42:41.9	49.09±0.15	6.0
	RAO 9	HD 17250B	02:46:14.49	+05:35:32.7	57.37±0.30	12.8
	TOK 651	ATO J041.4695+05.4898	02:45:52.61	+05:29:24.2	59.68±0.08	12.6
05222+0524	...	HD 35066(Aab) ^{b,e}	05:22:11.20	+05:23:43.1	61.80±0.44	6.9
	TOK 497	TYC 109-530-1	05:23:28.98	+05:13:02.9	61.09±0.06	10.3
	STT 106	HD 35066B ^b	05:22:11.61	+05:23:50.3	61.05±0.07	10.3
06384+3945		BD+39 1687	06:38:26.85	+39:44:32.4	61.85±0.07	10.2
	TOK 502	LP 205-19	06:40:08.62	+39:52:14.7	57.93±0.10	14.8
	...	LP 205-22 ^d	06:41:27.63	+39:57:33.2	70.09±0.18	15.7
	...	Gaia DR3 945027740109972224	06:37:21.98	+39:01:33.4	63.26±0.52	17.7
08447–5443	KEL 1/I 10/...	δ Vel (Aabc) ^h	08:44:42.23	-54:42:31.7	24.70±0.24	2.0 ⁱ
	SHY 49	HD 76653	08:55:11.78	-54:57:56.8	24.34±0.02	5.6
11486+1417	BU 603	HD 102590(Aab) ^b	11:48:38.71	+14:17:03.1	67.41±0.46	5.9
	TOK 552	Gaia DR3 3923967883532679168	11:46:59.18	+14:34:17.2	68.40±0.13	12.6
	...	Gaia DR3 3923191426460144896	11:48:39.39	+14:17:05.4	69.08±0.80	15.9
12317+1208		HD 109032	12:31:39.36	+12:07:40.3	106.3±0.4	8.0
	SHY 607	BD+13 2551	12:35:06.65	+12:56:20.3	105.8±0.2	9.1
	...	Gaia DR3 3907691061288324992	12:31:29.12	+12:12:49.7	106.1±0.7	16.4
	...	Gaia DR3 3904562400951238144	12:33:26.14	+12:25:17.5	95.02±0.60	16.6
15330–0111		11 Ser	15:32:57.94	-01:11:11.0	83.61±0.42	5.2
	SHY 678	HD 142011	15:52:12.51	-02:16:42.6	88.31±0.15	8.4
	...	Gaia DR3 4403070145373483392	15:52:12.65	-02:16:50.1	88.96±0.36	14.1
	...	Gaia DR3 4403070149671286272 ^d	15:30:41.60	-01:20:03.6	89.28±0.43	14.4
18143–4309		HD 166793	18:14:19.51	-43:09:15.4	103.5±0.3	7.7
	SHY 740	HD 166533	18:13:01.82	-42:17:17.9	110.4±0.3	8.0
	...	Gaia DR3 6721465492884350080	18:14:29.91	-43:07:09.8	104.3±1.1	14.1
	...	Gaia DR3 6724532477492271104	18:12:48.44	-42:30:04.2	101.8±0.2	14.1
20154+6412	MLR 60	HD 193215(Aab)	20:15:21.95	+64:11:59.3	63.62±2.79	8.3
	SHY 772	BD+63 1588	20:01:46.09	+63:32:42.7	66.34±0.05	9.8
	...	G 262-11	20:24:35.87	+65:53:13.8	65.04±0.06	13.7
22220–3431	B 557	HD 210111(Aab)	22:08:42.64	-33:07:32.5	78.66±0.22	6.3
	SHY 805	HD 212025 ^c	22:21:57.61	-34:31:12.7	86.57±2.63	7.3
	SHY 802	HD 212035	22:22:04.58	-34:29:20.1	86.34±0.17	7.4
22455+1112	...	HD 215243(Aab) ^{b,c}	22:43:42.71	+10:56:21.7	36.95±0.52	6.4
	SHY 358	BD+10 4812A ^b	22:45:27.87	+11:11:31.0	43.43±0.04	9.7
	BU 711	BD+10 4812B ^b	22:45:27.85	+11:11:33.5	43.48±0.04	10.7

Table B.2: Basic data of the 94 galactic field systems (continued).

WDS	Discoverer code	Star	α (J2000) (hh:mm:ss.ss)	δ (J2000) (dd:mm:ss.s)	d (pc)	G^a (mag)
22497+6612		ι Cep	22:49:40.82	+66:12:01.5	36.65 ± 0.18	3.2
	SHY 359	HD 215588	22:45:03.63	+58:08:49.4	35.28 ± 0.02	6.3
	...	UCAC3 297-187960	22:45:03.65	+58:08:34.9	35.18 ± 0.02	13.0
	...	SDSS J230056.41+640815.5	23:00:56.46	+64:08:16.0	36.50 ± 0.12	17.9
23309-5807		HD 221738 ^b	23:35:02.13	-56:49:31.3	97.66 ± 0.21	6.6
	SHY 833	HD 221252(AB)	23:30:56.45	-58:06:44.2	97.75 ± 0.25	9.1
	I 145	TYC 8838-832-2	23:30:56.60	-58:06:44.8	98.89 ± 0.34	9.7
<i>Quintuple systems</i>						
07294-1500		HD 59438A ^b	07:29:21.86	-14:59:55.2	36.48 ± 0.03	6.2
	STF1104	HD 59438B ^b	07:29:21.92	-14:59:53.4	36.52 ± 0.06	7.5
	TOK 391	LP 722-24	07:29:00.43	-14:42:48.1	36.78 ± 0.02	11.1
	STF1104/TOK 391	HD 59438C(ab) ^c	07:29:21.75	-15:00:15.6	38.65 ± 0.51	11.6
16278-0822	RST3949/...	ν Oph(Aabc) ^b	16:27:48.19	-08:22:18.2	42.95 ± 1.74	4.5
	TOK 603	HD 148300	16:27:28.91	-08:34:19.2	40.77 ± 0.04	8.6
	SHY 287	HD 144660	16:07:21.23	-08:10:10.9	39.55 ± 0.03	9.0
<i>Sextuple systems</i>						
02315+0106		HD 15695	02:31:29.87	+01:05:39.2	105.5 ± 0.3	7.5
	STF 274	BD+00 415B	02:31:29.29	+01:05:28.9	105.4 ± 0.3	7.6
	SHY 422	HD 17000	02:43:36.98	-00:20:40.3	89.89 ± 0.16	8.8
	...	HD 16985	02:43:33.96	+03:15:46.8	121.0 ± 0.3	9.7
	...	Gaia DR3 2497835645142616192 ^d	02:54:18.64	-00:51:20.7	90.95 ± 0.28	15.4
	...	Gaia DR3 2514005200579732608	02:21:42.89	+02:40:11.5	117.3 ± 1.3	17.0
03503-0131		HD 24098A	03:50:16.16	-01:31:21.3	44.27 ± 0.05	6.4
	SHY 164	HD 22584 ^b	03:37:54.39	-02:30:42.0	46.04 ± 0.09	9.4
	BU 401	HD 24098B	03:50:15.87	-01:31:22.6	44.21 ± 0.03	10.1
	...	UCAC4 438-004875	03:37:54.01	-02:30:54.2	45.68 ± 0.07	11.9
	...	Gaia DR3 3250466403920143488	03:50:38.91	-01:21:12.9	44.62 ± 0.30	17.6
	...	Gaia DR3 3250466403923273088	03:50:38.79	-01:21:12.7	44.28 ± 0.07	15.2
20489-6847		HD 197569	20:48:56.52	-68:47:28.5	86.47 ± 0.14	7.0
	SHY 782	HD 199760	21:03:18.14	-69:10:16.5	87.60 ± 0.14	8.2
	...	Gaia DR3 6376446646807117312	20:48:56.93	-68:47:26.9	87.23 ± 1.11	14.2
	...	Gaia DR3 6374759136976638336	20:35:18.54	-70:12:48.0	81.37 ± 0.17	15.2
	...	Gaia DR3 6375565697474377088	21:20:55.99	-69:41:48.3	97.40 ± 0.25	15.4
	...	Gaia DR3 6376941667557429888	20:53:56.24	-67:33:41.4	86.77 ± 0.47	17.0
<i>Septuple systems</i>						
19507-5912		HD 188162	19:57:06.31	-58:54:04.9	90.32 ± 0.93	5.2
	SHY 761/I 121	HD 186957(Aab)	19:50:44.80	-59:11:37.2	92.39 ± 0.69	5.6
	SHY 759	HD 186810	19:50:03.31	-59:15:50.5	90.76 ± 0.26	7.0
	...	Gaia DR3 6447086042643463936	19:57:54.06	-59:02:08.3	88.38 ± 0.15	14.2
	...	Gaia DR3 6447030135053741952 ^d	19:50:02.19	-59:15:52.4	90.77 ± 0.28	14.9
	...	Gaia DR3 6447128820517666944	19:54:08.05	-58:54:13.7	95.60 ± 0.43	15.8
20599+4016	COU2431/LSC 1	HD 200077(Aa1a2b)	20:59:55.28	+40:15:31.8	40.53 ± 0.22	6.5
	LEP 98/HDS2989	G 210-44(Aab) ^{b,c}	20:58:11.46	+40:11:29.0	38.67 ± 0.75	10.2

Notes. ^(a) The maximum error in G provided by *Gaia* DR3 is less than 0.005 mag; ^(b) Proper motion anomaly measured by Kervella et al. (2019), Brandt (2021) or both; ^(c) RUWE > 10; ^(d) Large σ_{V_r} for its G magnitude; ^(e) HD 35066(Aab) was recently resolved at SOAR with $\rho = 0.14$ arcsec (anonymous reviewer, priv.comm); ^(f) Value from *Gaia* DR2; ^(g) Very shiny star, not resolved by *Gaia* DR3. Astrometric data from *Hipparcos*; ^(h) Pourbaix & Boffin (2016); ⁽ⁱ⁾ Pecaut & Mamajek (2013).

Table B.3: Masses, ρ , θ , separations and gravitational binding energy of the systems identified in the sample of work.

WDS	Discoverer code	Star	M (M_{\odot})	ρ (arcsec)	θ (deg)	s (10^3 au)	$ U_g^* $ (10^{33} J)
<i>Double systems</i>							
00016–0102	WIS 1	2MASS J00013688-0101441	0.22±0.02	1135	234	68.4±0.2	0.74±0.10
		SIPS J0000-0112	0.13±0.01				
01005–1923	SHY 392	HD 5911	1.32±0.13	1725	126	140.8±0.3	20.6±2.9
		HD 6103	1.24±0.12				
01066+1353	SHY 396	HD 6566	1.32±0.10	11089	305	643.7±1.2	3.69±0.52
		HD 5433 ^a	1.02±0.10				
01134–3932	SHY 397	HD 7382	1.32±0.13	4472	209	264.6±0.5	7.82±1.11
		HD 7052	0.89±0.09				
01326–4944	SHY 405	HD 9544	1.89±0.19	1001	231	81.2±0.1	61.1±8.6
		HD 9378	1.49±0.15				
02022–4550	SHY 410	HD 12586	1.31±0.13	8496	10	605.0±0.8	4.63±0.66
		HD 12808	1.21±0.12				
02025–3849	WIS 48	2MASS J02022892-3849021 ^b	0.32±0.03	1166	270	69.3±2.7	0.72±0.11
		2MASS J02004917-3848535	0.09±0.01				
02310+0823	GIC 32	G 4-24	0.64±0.06	3096	278	111.5±0.1	2.09±0.30
		G 73-59 ^b	0.21±0.02				
05444–0528	SHY 489	HD 38273	1.35±0.13	5025	252	435.2±0.9	6.97±0.99
		HD 37546	1.27±0.13				
07069+5511	TOK 508	HD 53075	1.04±0.10	1587	357	91.2±0.1	8.87±1.25
		[SLS2012] PYC J07067+5537	0.44±0.04				
07113+3307	SHY 190	HD 54717	1.19±0.12	1790	182	80.2±0.1	26.2±3.7
		HD 54718	1.00±0.10				
07160+5759	TOK 510	NLTT 17578 ^a	0.99±0.10	1693	11	183.9±0.4	1.43±0.20
		LSPM J0716+5827	0.15±0.01				
07329–5249	WIS 141	2MASS J07325350-5249077	0.68±0.07	1197	1.6	157.9±0.2	1.58±0.22
		2MASS J07325706-5229111	0.21±0.02				
08237–5519	SHY 526	HD 71257	1.41±0.14	3442	133	261.0±0.3	9.04±1.28
		HD 72143 ^a	0.95±0.09				
08388–1315	SHY 201	HD 73583	0.71±0.07	14236	326	449.3±0.2	1.90±0.27
		BD-09 2535	0.69±0.07				
08480–3115	SHY 529	HD 75514 ^{a,b}	1.33±0.13	1585	225	125.6±2.3	20.3±2.9
		HD 75269 ^a	1.08±0.11				
09467+1632	TOK 531	BD+17 2130 ^a	0.82±0.08	1610	243	110.1±0.7	3.84±0.54
		LP 428-36	0.29±0.03				
09568+0415	TOK 533	HD 86147	1.32±0.13	1619	359	74.0±0.2	16.4±2.3
		LSPM J0956+0441 ^b	0.52±0.05				
10532–3006	SHY 563	HD 94375 ^a	1.32±0.13	17541	178	1439±3	1.91±0.27
		HD 94542 ^a	1.19±0.12				
11214+0638	TOK 544	HD 98697	1.37±0.14	1136	271	55.3±0.1	12.2±1.7
		LP 552-34	0.28±0.03				
11265+2031	TOK 546	HD 99419	1.03±0.10	1737	70	80.2±0.1	6.95±0.98
		Gaia DR3 3978588911076420736	0.31±0.03				
11455+4740	LEP 45	HD 102158	1.05±0.11	1178	72	60.3±0.1	11.9±1.7
		G 122-46	0.38±0.04				
12213–5012	TOK 556	HD 107440 ^a	1.16±0.12	1195	57	115.7±0.5	19.0±2.7
		HD 107735 ^a	1.08±0.11				
13305+2231	SHY 626	HD 117528	1.19±0.12	3650	183	307.4±0.4	6.40±0.90
		BD+22 2587	0.94±0.09				
15031–4618	WIS 280	CD-45 9610	0.67±0.07	1020	136	27.73±0.01	17.4±2.5
		L 334-33	0.41±0.04				

Table B.3: Masses, ρ , θ , separations, and gravitational binding energy of the systems identified in the sample of work (continued).

WDS	Discoverer code	Star	M (M_{\odot})	ρ (arcsec)	θ (deg)	s (10^3 au)	$ U_g^* $ (10^{33} J)
15120+0245	WIS 281	LP 562-9	0.41±0.04	1136	1.1	71.56±0.08	2.17±0.31
		LP 562-10	0.22±0.02				
15208+3129	LEP 74	HD 136654	1.27±0.13	1582	326	72.37±0.05	27.3±3.9
		AX CrB	0.88±0.09				
15226+3953	WIS 284	G 179-28	0.93±0.09	1035	249	119.7±0.2	3.23±0.46
		LP 222-69	0.24±0.02				
15356+7726	WIS 288	LSPM J1535+7725	0.84±0.08	1133	318	77.2±0.1	13.4±1.9
		LP 22-358	0.70±0.07				
15408-3252	SHY 278	HD 139696 ^{a,b}	0.79±0.08	9296	264	281.6±3.3	3.04±0.43
		CD-32 10820	0.62±0.06				
15488+4929	WIS 295	LSPM J1548+4928	0.12±0.01	1106	114	85.0±0.7	0.29±0.04
		LSPM J1550+4921	0.11±0.01				
15590+1820	SHY 691	HD 143292 ^a	1.29±0.13	7867	344	556.7±0.8	4.87±0.69
		HD 142899	1.19±0.12				
17127+3235	WIS 313	BD+32 2868	0.93±0.09	1046	273	73.6±0.4	4.69±0.66
		LSPM J1711+3236	0.21±0.02				
17166+0325	SHY 715	HD 156287 ^a	1.24±0.12	17154	61	1407±3	1.68±0.24
		HD 159243	1.08±0.11				
18496+1313	SHY 309	HD 229635	0.89±0.09	7650	161	288.8±0.2	3.77±0.53
		HD 229830	0.70±0.07				
18571+5143	SHY 749	HD 176341	1.35±0.14	7890	208	660.3±1.0	4.24±0.60
		BD+49 2879	1.17±0.12				
18597+1615	TOK 622	HD 176441 ^a	1.21±0.12	1264	267	57.2±0.1	20.2±2.9
		LSPM J1858+1613 ^b	0.54±0.05				
19290-4952	SHY 319	HD 182857	0.88±0.09	8677	47	359.4±0.2	3.81±0.54
		HD 185112 ^a	0.89±0.09				
20080-0041	SHY 325	64 Aql	1.00±0.27	1059	228	49.2±0.1	35.4±5.0
		HD 190873	0.99±0.10				
20124-1237	TDT2085	ξ Cap	1.27±0.13	1021	194	28.83±0.03	42.9±6.1
		LP 754-50	0.55±0.06				
20371+6122	SHY 780	HD 196903	1.37±0.14	5176	100	296.0±0.3	9.76±1.38
		HD 198662	1.20±0.12				
20404-3251	SHY 781	HD 196746 ^a	1.23±0.12	3623	310	316.8±1.4	7.82±1.11
		HD 196189	1.15±0.11				
21009-4132	WIS 346	L 424-30	0.25±0.02	1036	5.5	19.41±0.01	4.69±0.66
		APMPM J2101-4125	0.21±0.02				
21066+8048	TOK 632	G 261-37	0.62±0.06	1286	53	44.52±0.03	10.5±1.5
		G 261-40	0.43±0.04				
21105+2227	SHY 793	HD 201670 ^c	1.74±0.17	15684	262	1783±15	2.49±0.35
		HD 198759	1.45±0.15				
21190+2614	TOK 634	HD 203030	0.91±0.09	1701	34	66.8±0.1	5.20±0.74
		Gaia DR3 1846992067932879744 ^d	0.22±0.02				
22175+2335	GIC 179	G 127-13 ^b	0.42±0.04	2107	13	94.0±0.8	3.32±0.47
		G 127-14	0.42±0.04				
22378-0414	TOK 640	κ Aqr	2.55±0.13	1223	247	83.1±0.6	10.8±1.5
		Gaia DR3 2624935581540867200	0.20±0.02				
<i>Triple systems</i>							
02062-4726	NSN 219	CD-48 554(A)	0.79±0.08	1.9	200	0.1702±0.0003	6.00±0.72
		CD-48 554B	0.50±0.05				
		LEHPM 2187	0.27±0.03				

Table B.3: Masses, ρ , θ , separations, and gravitational binding energy of the systems identified in the sample of work (continued).

WDS	Discoverer code	Star	M (M_{\odot})	ρ (arcsec)	θ (deg)	s (10^3 au)	$ U^* $ (10^{33} J)
04346–3539	TOK 488	HD 29231	0.93±0.09				...
	WIS 108	L 447-2	0.39±0.04	1632	125	45.89±0.02	
		UCAC3 109-11370 ^b	0.27±0.03	1201	140	33.77±0.01	
06536–3956		L 454-11 ^b	0.37±0.04				9.43±0.99
	SUB 2	WT 202	0.64±0.02	3565	247	89.0±0.4	
	SUB 2	WT 201	0.64±0.02	3596	248	89.8±0.4	
07166–2319		HD 56578 ^a	2.42±0.24				...
	SHY 508	HD 57527 ^a	1.92±0.19	12620	166	1340±6	
	...	Gaia DR3 5613164850183516544	0.35±0.03	11792	151	1253±6	
08211+4021		BD+40 2030 ^a	0.96±0.10				16.3±1.7
	TOK 516	G 111-70	0.68±0.07	1624	308	98.5±0.1	
	...	Gaia DR3 914608342177083648	0.38±0.04	2.2	222	0.1343±0.0002	
09150+3837		HD 79392 ^a	1.44±0.14				19.0±3.3
	TOK 525	Gaia DR3 812086579467748736	0.38±0.04	1047	242	56.76±0.07	
	DAM1575	Gaia DR3 812109085097488768	0.16±0.02	28	27	1.510±0.002	
09487–2625		HD 85043A ^a	1.27±0.13				42.1±7.3
	I 205	HD 85043B ^a	0.69±0.07	1.8	281	0.0756±0.0001	
	TOK 532	PM J09486-2644	0.58±0.06	1157	181	47.9±0.1	
10289+3453		HD 90681	1.07±0.11				3.77±0.65
	SHY 215	HD 92194	0.97±0.10	10588	134	52.0±0.6	
	...	Gaia DR3 749786356557791744	0.08±0.01	14	207	0.674±0.001	
11513+4516		Ross 916A	0.38±0.04				8.14±1.415
	KPP3247	Ross 916B	0.37±0.04	1.4	281	0.0405±0.0001	
	WIS 193	G 176-59	0.20±0.02	1116	344	33.08±0.04	
12416+1026		27 Vir	1.93±0.19				9.67±1.67
	SHY 610	HD 111069 ^a	1.04±0.10	5595	52	400.9±1.0	
	...	Gaia DR3 3927438805519604352	0.19±0.02	41	77	2.93±0.01	
13470+3833		HD 120164	2.42±0.29 ^e				39.2±6.8
	SHY 633	HD 119767	1.19±0.12	2084	296	191.1±0.9	
	S 654	BD+39 2679	1.14±0.11	71	237	6.55±0.03	
13496+1301	...	HD 120510(Aab)	2.66±0.27 ^f				27.7±3.9
	SHY 635	HD 120865	1.44±0.14	4337	153	244.8±0.3	
14153+0308		HD 124757A ^a	} 1.92±1.08 ^g				8.13±4.64
	STF1819	HD 124757B		0.9	166	0.03729±0.0001	
	SHY 261	HD 126961		11923	96	491.7±1.6	
14190–0636		ι Vir ^a	1.810±0.001 ^h				50.8±5.1
	SHY 71/HDS016	HD 125354(Aab) ^a	1.20±0.12 ⁱ	3423	129	75.4±0.5	
14396–6050		α Cen A	1.11±0.01 ^j				41.1±4.1
	RHD 1	α Cen B	0.93±0.01 ^j	15	222	0.0207±0.0001	
	LDS 494	Proxima Centauri	0.12±0.01	7960	212	10.71±0.02	
15318–0204		HD 138370	1.18±0.12				...
	SHY 677	HD 138159	0.98±0.10	2970	335	225.8±0.3	
	...	Gaia DR3 4416092627948054400	0.18±0.02	2822	339	214.6±0.3	
17415+4924		Wolf 1378 ^b	0.82±0.08				3.58±0.62
	WIS 321	LSPM J1741+4941	0.28±0.03	1079	346	137.0±2.1	
	...	Gaia DR3 1367008242580377216	0.17±0.02	4.4	314	0.56±0.01	
19235–6924		HD 180808(A) ^a	1.18±0.12				47.9±8.3
	DON 957	HD 180808B	0.61±0.06	2.8	249	0.1668±0.0002	
	SHY 755	HD 181958 ^a	1.49±0.15	1662	119	98.2±0.1	
19476+0105	ENG 67	HD 187003(Aab) ^a	2.40±0.24				3.81±0.54
	SHY 322	BD+00 4221	0.69±0.07	16426	263	767.7±0.8	
20084+1503		G 143-33	1.18±0.12				3.40±0.98
	LDS1033	G 143-27(Aab)	1.16±0.12	2188	269	709.7±4.6	

Table B.3: Masses, ρ , θ , separations, and gravitational binding energy of the systems identified in the sample of work (continued).

WDS	Discoverer code	Star	M (M_{\odot})	ρ (arcsec)	θ (deg)	s (10^3 au)	$ U_g^* $ (10^{33} J)
21096–1122		ν Aqr	2.01 ± 0.11				42.3 ± 6.4
TOK 633		Gaia DR3 6895305771635806208	0.42 ± 0.04	1053	313	52.5 ± 0.3	
...		Gaia DR3 6895305771635806464 ^c	0.21 ± 0.02	1055	313	52.5 ± 0.3	
22596–1246	...	HD 217250(Aab)	0.90 ± 0.09^k				2.10 ± 0.30
TOK 642		Gaia DR3 2603671950077707776	0.12 ± 0.01	1365	262	87.5 ± 0.1	
23328–1651		HD 221503	0.67 ± 0.07				3.00 ± 0.42
SHY 110/...		G 273-59(Aab) ^a	0.48 ± 0.05	12958	190	188.4 ± 0.1	
23506+5412		HD 223582 ^a	1.30 ± 0.13				69.0 ± 12.0
SHY 840		HD 223788	1.20 ± 0.12	1098	77	60.1 ± 0.1	
ES 700		BD+53 3238B	0.67 ± 0.07	15	35	0.804 ± 0.001	
<i>Quadruple systems</i>							
01024+0504		HD 6101A ^a	$\} 1.13 \pm 0.11^g$				53.5 ± 5.4
HDS 135		HD 6101B ^a		0.5	53	0.01083 ± 0.00003	
WNO 50		EGGR 7(Cab)		0.77 ± 0.08	1276	88	28.7 ± 0.1
02462+0536		HD 17250	1.16 ± 0.12				...
TOK 651		HD 17163	1.60 ± 0.16	3271	194	186.6 ± 0.3	
RAO 9		HD 17250B	0.47 ± 0.05	1.9	254	0.108 ± 0.002	
TOK 651		ATO J041.4695+05.4898	0.51 ± 0.05	494	222	28.18 ± 0.04	
05222+0524	...	HD 35066(Aab) ^a	1.45 ± 0.15				36.0 ± 6.2
TOK 497		TYC 109-530-1	0.76 ± 0.08	1326	119	82.0 ± 0.6	
STT 106		HD 35066B ^a	0.76 ± 0.08	9.5	40	0.584 ± 0.004	
06384+3945		BD+39 1687	0.78 ± 0.08				...
TOK 502		LP 205-19	0.26 ± 0.03	1261	68	78.0 ± 0.1	
...		LP 205-22 ^c	0.22 ± 0.02	2227	69	137.7 ± 0.2	
...		Gaia DR3 945027740109972224	0.11 ± 0.01	2685	196	166.1 ± 0.2	
08447–5443	KEL 1/I 10/...	δ Vel (Aabc)	6.18 ± 0.04^l				96.6 ± 9.7
SHY 49		HD 76653	1.21 ± 0.12	5534	100	136.7 ± 1.4	
11486+1417	BU 603	HD 102590(Aab) ^a	1.88 ± 0.19				16.5 ± 2.9
TOK 552		Gaia DR3 3923967883532679168	0.54 ± 0.05	1778	306	119.9 ± 0.8	
...		Gaia DR3 3923191426460144896	0.20 ± 0.02	10	77	0.680 ± 0.005	
12317+1208		HD 109032	1.46 ± 0.15				...
SHY 607		BD+13 2551	1.17 ± 0.12	4215	46	448.1 ± 1.5	
...		Gaia DR3 3907691061288324992	0.23 ± 0.02	344	334	36.6 ± 0.1	
...		Gaia DR3 3904562400951238144	0.20 ± 0.02	2986	148	317.5 ± 1.0	
15330–0111		11 Ser	1.27 ± 0.35^m				3.08 ± 0.62
SHY 678		HD 142011	1.21 ± 0.12	17755	103	1483 ± 7	
...		Gaia DR3 4403070145373483392	0.43 ± 0.04	17758	103	1483 ± 7	
...		Gaia DR3 4403070149671286272 ^c	0.40 ± 0.04	17758	103	1483 ± 7	
18143–4309		HD 166793	1.54 ± 0.15				...
SHY 740		HD 166533	1.49 ± 0.15	3231	345	334.3 ± 1.1	
...		Gaia DR3 6721465492884350080	0.46 ± 0.05	169	42	17.5 ± 0.1	
...		Gaia DR3 6724532477492271104	0.46 ± 0.05	2554	337	264.2 ± 0.8	
20154+6412	MLR 60	HD 193215(Aab)	1.07 ± 0.11				...
SHY 772		BD+63 1588	0.85 ± 0.09	5820	247	370.3 ± 16.2	
...		G 262-11	0.41 ± 0.04	7074	29	450.0 ± 19.7	
22220–3431	B 557	HD 210111(Aab)	1.90 ± 0.19				11.5 ± 2.3
SHY 805		HD 212025 ^b	1.52 ± 0.15	11176	117	878.7 ± 2.4	
SHY 802		HD 212035	1.50 ± 0.15	11205	116	880.9 ± 2.5	
22455+1112	...	HD 215243(Aab) ^{a,b}	1.37 ± 0.14^f				50.0 ± 8.7
SHY 358		BD+10 4812A ^a	0.73 ± 0.07	1796	60	66.4 ± 0.9	
BU 711		BD+10 4812B ^a	0.64 ± 0.06	1797	59	66.4 ± 0.9	
22497+6612		ι Cep	1.55 ± 0.20				...

Table B.3: Masses, ρ , θ , separations, and gravitational binding energy of the systems identified in the sample of work (continued).

WDS	Discoverer code	Star	M (M_{\odot})	ρ (arcsec)	θ (deg)	s (10^3 au)	$ U_g^* $ (10^{33} J)
23309–5807	SHY 359	HD 215588	1.23±0.12	29040	184	1061±5	
	...	UCAC3 297-187960	0.35±0.03	29055	184	1061±5	
	...	SDSS J230056.41+640815.5	0.50±0.10	8477	149	310.6±1.5	
		HD 221738 ^a	1.86±0.19				14.0±2.4
	SHY 833	HD 221252(AB)	1.12±0.11	5053	203	493.4±1.1	
	I 145	TYC 8838-832-2	0.99±0.10	5053	203	493.4±1.1	
<i>Quintuple systems</i>							
07294–1500		HD 59438A ^a	1.29±0.13				71.2±1.4
	STF1104	HD 59438B ^a	1.00±0.10	1.8	37	0.0654±0.0001	
	TOK 391	LP 722-24	0.56±0.06	1073	343	39.14±0.03	
	STF1104/TOK 391	HD 59438C(ab) ^b	0.52±0.05	21	185	0.749±0.001	
16278–0822	RST3949/...	ν Oph(Aabc) ^a	2.28±0.12 ^k				...
	TOK 603	HD 148300	0.88±0.09	775	202	33.3±1.3	
	SHY 287	HD 144660	0.80±0.08	18223	272	781.6±31.6	
<i>Sextuple systems</i>							
02315+0106		HD 15695	1.75±0.18				...
	STF 274	BD+00 415B	1.63±0.16	13	220	1.422±0.005	
	SHY 422	HD 17000	1.14±0.11	12071	115	1273±4	
	...	HD 16985	1.07±0.11	13373	234	1410±4	
	...	Gaia DR3 2497835645142616192 ^c	0.30±0.03	21691	109	2285±7	
	...	Gaia DR3 2514005200579732608	0.20±0.02	10471	303	1104±3	
03503–0131		HD 24098A	1.36±0.14				...
	SHY 164	HD 22584 ^a	0.80±0.08	11678	252	516.7±0.6	
	BU 401	HD 24098B	0.70±0.07	4.6	73	0.2031±0.0002	
	...	UCAC4 438-004875	0.52±0.05	11687	252	517.1±0.6	
	...	Gaia DR3 3250466403920143488	0.10±0.01	697	29	30.87±0.03	
	...	Gaia DR3 3250466403923273088	0.19±0.02	696	29	30.84±0.03	
20489–6847		HD 197569	1.81±0.18				...
	SHY 782	HD 199760	1.27±0.13	4872	107	421.2±0.7	
	...	Gaia DR3 6376446646807117312	0.41±0.04	2.7	232	0.2344±0.0004	
	...	Gaia DR3 6374759136976638336	0.30±0.03	6776	219	585.8±0.9	
	...	Gaia DR3 6375565697474377088	0.32±0.03	10914	108	943.3±1.5	
	...	Gaia DR3 6376941667557429888	0.17±0.02	4716	21	407.8±0.7	
<i>Septuple systems</i>							
19507–5912		HD 188162	2.82±0.28				...
	SHY 761/I 121	HD 186957(Aab)	2.52±0.25 ^k	3138	250	283.4±2.9	
	SHY 759	HD 186810	1.79±0.18	3528	248	318.6±3.3	
	...	Gaia DR3 6447086042643463936	0.43±0.04	609	143	55.0±0.6	
	...	Gaia DR3 6447030135053741952 ^c	0.36±0.04	3536	248	319.4±3.3	
	...	Gaia DR3 6447128820517666944	0.26±0.03	1381	270	124.8±1.3	
20599+4016	COU2431/LSC 1	HD 200077(Aa1a2bBab)	4.14±0.23 ^{n,o}				99.7±23.5
	LEP 98/HDS2989	G 210-44(Aab) ^{a,b}	0.67±0.07	1213	258	49.2±0.3	

Notes. ^(a) Proper motion anomaly measured by Kervella et al. (2019), Brandt (2021) or both. ^(b) RUWE > 10; ^(c) Large σ_V , for its G magnitude; ^(d) Classified as a white dwarf candidate by Gentile Fusillo et al. (2019), it has instead absolute magnitudes and colours of an intermediate M dwarf; ^(e) da Silva et al. (2015); ^(f) Tokovinin (2014); ^(g) Dynamical mass (Malkov et al. 2012); ^(h) Gontcharov & Kiyaeva (2010); ⁽ⁱ⁾ Mitrofanova et al. (2021); ^(j) Pourbaix & Boffin (2016); ^(k) Kervella et al. (2019); ^(l) Eker et al. (2018); ^(m) Feuillet et al. (2016); ⁽ⁿ⁾ Tokovinin (2018); ^(o) Montes et al. (2018).

Table B.4: Candidate stars to be part of the γ Cas association, in order of the distance to the central star γ Cas.

Star	α (J2000) (hh:mm:ss.ss)	δ (J2000) (dd:mm:ss.s)	SpT	M (M_\odot)	G^a (mag)	J^b (mag)	$\rho_{\gamma\text{Cas}}$ (deg)
γ Cas	00:56:42.53	+60:43:00.3	B0.5IV	$\sim 13^c$	2.3	2.0	0.000
Gaia DR3 426558563962119808	00:56:26.00	+60:41:55.5		0.80 ± 0.08	12.3	10.8	0.038
Gaia DR3 426559693524626816	00:55:55.21	+60:45:44.5		0.16 ± 0.02	18.7	15.0	0.107
UCAC4 752-011208	00:56:44.80	+60:22:46.3	M4Ve	0.46 ± 0.05	15.4	12.4	0.337
HD 5408(Aa)			B7V	3.40 ± 0.10^d			
HD 5408(Ab)	} 00:56:46.97	+60:21:46.2	B9V	4.10 ± 0.10^d	} 6.0	5.6	0.354
HD 5408(B)			A1V	3.40 ± 0.10^d			
Gaia DR3 426494169508443520	00:59:29.59	+60:28:43.0		0.14 ± 0.01	19.4	15.4	0.417
Gaia DR3 426656106950424960	00:58:49.75	+61:07:34.5		0.19 ± 0.02	18.3	14.7	0.484
Gaia DR3 426907040426100352	00:52:12.81	+60:28:25.5		0.45 ± 0.05	15.3	12.9	0.603
Gaia DR3 426117827290256896	00:53:27.10	+60:01:58.1		0.75 ± 0.08	12.7	11.1	0.794
Gaia DR3 426696758828470144	00:59:12.34	+61:38:10.3		0.28 ± 0.03	17.3	14.2	0.967
Gaia DR3 426391055933615872	01:05:01.74	+60:30:11.1		0.11 ± 0.01	20.4	16.3	1.04
Gaia DR3 427444254930463744	00:52:19.64	+61:37:04.8		0.24 ± 0.02	17.4	13.9	1.04
Gaia DR3 426937483155345280	00:48:27.00	+60:20:51.1		0.43 ± 0.04	15.7	12.9	1.08
Gaia DR3 427465454889829248	00:55:51.79	+61:52:51.7		0.35 ± 0.03	16.5	13.4	1.17
Gaia DR3 426833373147610240	00:48:42.59	+60:03:34.6		0.39 ± 0.04	15.9	12.7	1.19
Gaia DR3 426416177204072448	01:06:29.72	+60:53:50.6		0.40 ± 0.04	16.0	12.9	1.21
Gaia DR3 426831375980796800	00:48:27.33	+59:58:28.6		0.11 ± 0.01	20.1	16.2	1.26
Gaia DR3 522715116413884416	01:04:25.80	+61:38:25.1		0.38 ± 0.04	16.3	13.3	1.31
Gaia DR3 426835125494086144	00:47:19.08	+60:00:51.0		0.14 ± 0.01	19.2	15.8	1.36
Gaia DR3 426326116027684480	01:07:11.44	+60:15:44.2		0.25 ± 0.03	17.6	14.4	1.37
Gaia DR3 425868517332283776	01:01:36.89	+59:29:25.4		0.41 ± 0.04	15.9	12.9	1.37
TYC 4021-505-1	01:02:27.29	+62:01:55.3	G5V	0.91 ± 0.09	11.4	10.0	1.48
Gaia DR3 522555034397334912	01:06:20.90	+61:43:55.1		0.78 ± 0.08	12.4	10.9	1.54
Gaia DR3 522765865748123648	01:02:51.30	+62:07:44.7		0.34 ± 0.03	16.6	13.4	1.59
Gaia DR3 427035030443328000	00:44:21.55	+60:11:20.1		0.18 ± 0.02	18.7	15.6	1.61
Gaia DR3 522537644061868544	01:08:10.45	+61:35:06.6		0.21 ± 0.02	18.2	14.9	1.63
Gaia DR3 427202843412335104	00:43:54.51	+61:23:23.2		0.32 ± 0.03	16.9	13.8	1.69
HD 236617	01:05:43.02	+59:23:26.8	G5	1.28 ± 0.13	9.9	8.6	1.74
Gaia DR3 427169445745848832	00:41:53.36	+60:57:58.8		0.23 ± 0.02	17.7	14.2	1.82
Gaia DR3 523592384950148992	00:57:02.17	+62:39:28.4		0.22 ± 0.02	17.7	14.7	1.94
Gaia DR3 426197133869019520	01:09:50.64	+59:30:48.7		0.27 ± 0.03	17.4	14.7	2.03
Gaia DR3 523605720834117632	00:56:04.78	+62:46:10.7		0.34 ± 0.03	16.6	13.7	2.05
Gaia DR3 523606820345403520	00:55:29.74	+62:49:28.9		0.48 ± 0.05	15.6	13.1	2.11
TYC 4021-815-1	00:59:20.89	+62:48:42.6		0.99 ± 0.10	11.0	9.9	2.12
Gaia DR3 427108354134806784	00:39:17.10	+60:36:55.3		0.56 ± 0.06	14.5	11.4	2.14
V761 Cas	01:13:09.85	+61:42:22.3	B9V	3.22 ± 0.32	6.5	6.2	2.21
Gaia DR3 522574580780909440	01:13:19.43	+61:40:00.1		0.19 ± 0.02	18.4	14.8	2.22
Gaia DR3 425198223255334400	00:48:24.65	+58:45:19.6		0.16 ± 0.02	19.1	15.8	2.22
Gaia DR3 427777647475959680	00:41:34.65	+62:31:42.5		0.28 ± 0.03	17.3	14.2	2.55
Gaia DR3 430106477517090560	00:35:44.63	+60:49:57.6		0.79 ± 0.08	12.5	10.9	2.56
Gaia DR3 510588362155056384	01:16:30.81	+61:41:01.5		0.19 ± 0.02	18.4	14.9	2.57
Gaia DR3 425164005257167232	00:43:17.19	+58:42:44.3		0.27 ± 0.03	17.5	14.4	2.62
Gaia DR3 430133793510727040	00:35:08.90	+60:59:03.0		0.17 ± 0.02	18.8	15.5	2.64
Gaia DR3 510353788221523584	01:18:57.90	+60:10:51.9		0.31 ± 0.03	16.8	13.7	2.80
Gaia DR3 425348547108352768	00:41:07.58	+58:40:29.8		0.24 ± 0.02	17.6	14.6	2.83
Gaia DR3 428588949621015296	00:33:48.86	+60:21:42.7		0.15 ± 0.01	19.4	15.8	2.84
Gaia DR3 523346541025484160	01:03:22.37	+63:28:35.3		0.12 ± 0.01	19.9	16.2	2.87
Gaia DR3 430258798542242176	00:33:41.47	+61:36:28.7		0.26 ± 0.03	17.6	14.5	2.91
Gaia DR3 428608599088304512	00:32:59.63	+60:30:54.1		0.13 ± 0.01	19.6	15.0	2.92
Cl* NGC 129 SS 525	00:32:36.63	+60:41:19.2		0.96 ± 0.10	11.2	10.1	2.95
BD+62 170	00:55:40.97	+63:40:51.8	F8	1.24 ± 0.12	9.7	8.8	2.97
Gaia DR3 430199734155452160	00:32:04.70	+61:14:49.8		0.29 ± 0.03	16.9	14.1	3.03
Gaia DR3 523899664093745408	00:43:41.06	+63:20:19.7		0.17 ± 0.02	18.8	15.6	3.03
Gaia DR3 414097283284109952	01:16:18.96	+58:55:15.9		0.44 ± 0.04	15.7	12.7	3.05
Gaia DR3 523114788890667776	01:11:43.52	+63:12:14.3		0.39 ± 0.04	16.1	13.2	3.05
Gaia DR3 428606507444503552	00:31:41.43	+60:32:29.1		0.32 ± 0.03	16.8	13.7	3.07

Table B.4: (Continued): Candidates to be part of the moving group, in order of the distance to γ Cas.

Star	α (J2000) (hh:mm:ss.ss)	δ (J2000) (dd:mm:ss.s)	SpT	M (M_\odot)	G^a (mag)	J^b (mag)	$\rho_{\gamma\text{Cas}}$ (deg)
Gaia DR3 428651789276927872	00:31:28.31	+60:30:36.4		0.18 ± 0.02	18.8	15.1	3.10
Gaia DR3 430206674822463744	00:31:16.38	+61:27:47.3		0.26 ± 0.03	17.3	13.9	3.16
Gaia DR3 424138538865527168	00:57:44.28	+57:31:32.6		0.76 ± 0.08	12.8	11.1	3.19
Gaia DR3 523891933149775616	00:46:04.81	+63:39:46.4		0.23 ± 0.02	17.8	14.8	3.20
Gaia DR3 430351707277551616	00:33:23.98	+62:18:00.1		0.44 ± 0.04	15.7	12.9	3.20
Gaia DR3 413591954612999296	01:06:23.15	+57:44:02.9		0.28 ± 0.03	17.2	14.0	3.23
NGC 129 48	00:30:33.45	+60:17:27.3	F6V	1.27 ± 0.13	9.5	8.8	3.25
Gaia DR3 424242404052127872	00:54:06.70	+57:27:25.2		0.22 ± 0.02	17.7	14.7	3.28
Gaia DR3 523918424511630208	00:40:28.49	+63:26:04.7		0.10 ± 0.01	20.4	16.6	3.32
Gaia DR3 424738421233795072	00:42:39.06	+57:52:50.3		0.20 ± 0.02	17.9	14.7	3.36
BD+61 258	01:23:33.25	+61:46:05.2	F2	1.44 ± 0.14	9.6	8.9	3.39
Gaia DR3 523413271935393280	01:09:59.65	+63:45:58.1		0.39 ± 0.04	16.1	13.1	3.42
Gaia DR3 524005221511877120	00:49:59.25	+64:05:45.1		0.32 ± 0.03	16.9	13.8	3.47
Gaia DR3 523228549680118656	01:14:29.82	+63:34:44.6		0.22 ± 0.02	17.6	14.4	3.54
Gaia DR3 428677391586484480	00:27:30.80	+60:57:36.1		0.42 ± 0.04	16.0	12.7	3.56
Gaia DR3 424897712980359296	00:41:06.06	+57:45:14.0		0.20 ± 0.02	18.0	14.6	3.57
Gaia DR3 424073525939801984	01:01:54.61	+57:11:58.5		0.19 ± 0.02	18.4	15.1	3.58
Gaia DR3 424031851879846912	00:57:35.08	+57:07:43.0		0.52 ± 0.05	15.1	12.9	3.59
Gaia DR3 430861399634552448	00:37:36.63	+63:35:12.6		0.59 ± 0.06	14.3	12.0	3.63
Gaia DR3 428484045032883456	00:28:38.41	+59:39:27.0		0.15 ± 0.02	19.2	15.9	3.64
Gaia DR3 430518764324231040	00:28:32.52	+62:06:39.1		0.52 ± 0.05	14.8	12.0	3.64
HD 4810	00:51:11.44	+64:19:29.7	A2	1.87 ± 0.19	8.4	8.1	3.66
TYC 4024-250-1	00:51:04.61	+64:20:17.9		1.07 ± 0.11	10.7	9.7	3.68
Gaia DR3 413481488050839424	01:16:18.59	+57:58:51.2		0.80 ± 0.08	12.7	10.5	3.70
Gaia DR3 510825478709127424	01:26:26.82	+61:49:43.0		0.33 ± 0.03	17.0	14.1	3.74
Gaia DR3 423826513780557952	00:53:28.82	+56:54:47.2		0.11 ± 0.01	20.5	16.9	3.83
Gaia DR3 424630050620861312	00:45:16.82	+57:06:56.8		0.23 ± 0.02	17.4	14.4	3.89
Gaia DR3 524282706455103744	01:02:14.82	+64:37:47.9		0.23 ± 0.02	17.6	14.3	3.96
Gaia DR3 423823494422951040	00:53:26.81	+56:44:57.9		0.57 ± 0.06	14.3	12.2	3.99
Gaia DR3 524957222478303616	01:10:05.51	+64:25:50.8		0.19 ± 0.02	18.1	14.7	4.02
TYC 4015-1647-1	00:23:32.15	+60:38:28.4		0.97 ± 0.10	11.2	10.0	4.06
Gaia DR3 427905706211506560	00:30:32.34	+58:20:28.2		0.14 ± 0.01	19.5	16.2	4.08
Gaia DR3 512646373042841984	01:24:00.84	+63:21:27.8		0.79 ± 0.08	12.5	11.1	4.15
Gaia DR3 524328581007238656	00:57:51.06	+64:52:55.5		0.40 ± 0.04	16.2	13.4	4.17
Gaia DR3 423947460059430912	01:03:02.76	+56:37:16.3		0.10 ± 0.01	20.5	16.2	4.18
Gaia DR3 524704236026503552	01:17:29.40	+64:09:57.5		0.26 ± 0.03	17.5	14.4	4.20
Gaia DR3 526998195239910656	00:34:15.41	+64:02:07.1		0.39 ± 0.04	16.3	13.5	4.21
Gaia DR3 526998195239908736	00:34:13.63	+64:02:13.1		0.79 ± 0.08	12.6	11.2	4.22
HD 6822	01:10:16.31	+64:38:45.2	A0	1.89 ± 0.19	8.2	7.8	4.22
Gaia DR3 431081851713650944	00:30:03.36	+63:38:14.5		0.51 ± 0.05	15.2	12.8	4.26
TYC 4031-2224-1	01:31:39.03	+60:30:44.6	F5	0.99 ± 0.10	11.0	9.9	4.29
Gaia DR3 512575969937525376	01:27:42.20	+62:58:26.6		0.25 ± 0.03	17.3	14.2	4.29
Gaia DR3 510790844092027008	01:31:20.08	+61:52:29.1		0.20 ± 0.02	18.4	15.7	4.31
Gaia DR3 424842569903670656	00:34:37.72	+57:24:57.8		0.32 ± 0.03	16.8	13.9	4.35
Gaia DR3 428283418521147392	00:23:09.47	+59:12:54.8		0.29 ± 0.03	17.1	14.0	4.45
Gaia DR3 428172299125461120	00:24:08.03	+58:53:49.3		0.25 ± 0.03	17.4	14.1	4.48
BD+59 37	00:20:47.67	+60:03:39.4		1.26 ± 0.13	9.8	6.8	4.48
Gaia DR3 423769102956471680	00:53:28.68	+56:12:18.6		0.44 ± 0.04	15.6	12.7	4.53
Gaia DR3 430603907757603584	00:22:05.36	+62:52:09.2		0.46 ± 0.05	15.4	12.7	4.62
Gaia DR3 428342762091655168	00:19:49.86	+59:36:50.2		0.53 ± 0.05	14.7	11.9	4.71
Gaia DR3 527493250347583872	00:42:12.63	+65:10:36.1		0.32 ± 0.03	16.8	13.6	4.75
Gaia DR3 423535250579327488	00:59:56.20	+55:51:15.4		0.27 ± 0.03	17.5	14.8	4.88
Gaia DR3 411948871922993024	01:10:06.75	+56:09:03.8		0.47 ± 0.05	15.5	13.1	4.89
Gaia DR3 512501989120374144	01:32:08.47	+63:18:56.2		0.19 ± 0.02	18.4	14.8	4.90
Gaia DR3 512789034676716032	01:27:08.42	+64:13:28.1		0.22 ± 0.02	17.6	14.2	4.96
Gaia DR3 509912226919850880	01:37:26.63	+60:48:22.2		0.19 ± 0.02	18.4	14.9	4.97
Gaia DR3 524616854909023488	00:45:39.31	+65:32:40.3		0.22 ± 0.02	17.8	14.5	4.99
Gaia DR3 527148725254317312	00:35:20.74	+65:04:29.5		0.62 ± 0.06	14.3	12.1	4.99

Table B.4: (Continued): Candidates to be part of the moving group, in order of the distance to γ Cas.

Star	α (J2000) (hh:mm:ss.ss)	δ (J2000) (dd:mm:ss.s)	SpT	M (M_\odot)	G^a (mag)	J^b (mag)	$\rho_{\gamma\text{Cas}}$ (deg)
Gaia DR3 421818053931122176	00:29:34.63	+57:07:03.5		0.74 ± 0.07	12.8	11.2	5.02
Gaia DR3 524934716850804992	01:16:26.04	+65:13:51.0		0.82 ± 0.08	12.3	10.9	5.04
Gaia DR3 418461897767667456	00:45:39.92	+55:52:59.2		0.22 ± 0.02	17.9	14.7	5.05
Gaia DR3 421811697379570688	00:29:48.73	+57:01:45.2		0.13 ± 0.01	19.2	12.8	5.06
Gaia DR3 524938084107230720	01:16:01.32	+65:18:17.2		0.10 ± 0.01	20.6	16.7	5.08
Gaia DR3 429704571660226176	00:15:13.72	+61:46:23.3		0.18 ± 0.02	18.3	15.0	5.09
Gaia DR3 512451931283034112	01:35:47.24	+63:06:48.3		0.53 ± 0.05	15.0	12.0	5.18
HD 4948	00:52:36.09	+65:53:30.3	A2	1.89 ± 0.19	8.3	8.1	5.20
Gaia DR3 527534653834163072	00:41:10.00	+65:46:21.3		0.21 ± 0.02	18.0	14.8	5.35
Gaia DR3 411492437156666368	01:05:30.07	+55:27:14.2		0.60 ± 0.06	14.3	12.3	5.39
Gaia DR3 422967112302952192	00:15:35.09	+58:59:21.4		0.55 ± 0.06	14.9	12.7	5.44
Gaia DR3 421980919092603392	00:22:46.22	+57:25:23.3		0.49 ± 0.05	15.2	12.6	5.46
Gaia DR3 431392360672275584	00:15:18.31	+63:14:19.4		0.22 ± 0.02	17.9	14.9	5.47
TYC 4028-969-1	00:48:42.53	+66:07:10.6		0.86 ± 0.09	11.9	10.6	5.48
Gaia DR3 421990608538759808	00:21:17.48	+57:27:37.2		0.30 ± 0.03	17.2	14.3	5.59
Gaia DR3 512489211600057600	01:37:48.00	+63:36:33.3		0.53 ± 0.05	15.0	12.6	5.59
Gaia DR3 422982677264653440	00:13:53.86	+59:04:25.8		0.36 ± 0.04	16.5	13.6	5.61
Gaia DR3 508974691392427776	01:37:12.24	+58:23:19.4		0.39 ± 0.04	16.3	13.2	5.63
TYC 3673-1289-1	01:18:51.10	+55:49:08.2		1.28 ± 0.13	9.7	8.8	5.69
Gaia DR3 429623693140336512	00:09:54.06	+61:10:34.9		0.21 ± 0.02	18.2	12.2	5.69
Gaia DR3 421959169377531264	00:21:46.47	+57:08:46.7		0.15 ± 0.02	18.9	15.7	5.74
Gaia DR3 421945356762784640	00:22:33.71	+56:59:31.6		0.34 ± 0.03	16.9	13.7	5.77
Gaia DR3 526042891426149888	01:01:11.94	+66:32:38.6		0.11 ± 0.01	20.4	16.2	5.85
Gaia DR3 421933021616821504	00:23:06.48	+56:47:52.9		0.64 ± 0.06	14.0	11.9	5.85
Gaia DR3 526137930469180288	00:51:34.57	+66:35:09.8		0.71 ± 0.07	13.2	11.4	5.90
Gaia DR3 509511974622906496	01:43:21.47	+59:34:09.2		0.21 ± 0.02	18.2	14.5	5.91
Gaia DR3 509092884599480704	01:41:43.57	+58:49:22.1		0.14 ± 0.01	19.6	16.4	5.97
Gaia DR3 431890542519116928	00:15:25.61	+64:20:23.2		0.53 ± 0.05	14.9	12.3	5.97
Gaia DR3 422021291786053120	00:18:16.50	+57:20:46.3		0.47 ± 0.05	15.4	12.6	5.97

Notes. ^(a) The maximum error in G provided by *Gaia* DR3 is less than 0.005 mag; ^(b) The maximum error in J provided by 2MASS is less than 0.2 mag; ^(c) Nemravová et al. (2012); ^(d) Tokovinin (2021).